Supergen Offshore Renewable Energy

Early Career Researcher Posters 2025

Abel Arredondo-Galeana, University of Strathclyde A hybrid wind and wave floating platform to provide a minimum power baseload for offshore applications.
Abigail Bateman, University of Southampton Using elastic foam tests to investigate an interpretation method of the ROCOCONE p-y module
Scott Brown, University of Plymouth Development of High-Fidelity Models for Extreme Loading Events on ORE Devices
Xiaosheng Chen, University of Oxford WaveTide: Wave Effects on a Benchmark Tidal Energy Device
Jamie Crispin, University of Southampton Predicting the response of monopile foundations to storm loading from laboratory test data
Federico Della Santa, University of Strathclyde Fatigue in Offshore Wind Foundations
Yadong Han, University of Oxford Tidal Turbine Benchmarking Project: Stage II – Experiments on Unsteady Loading in Waves
Fei He, University of Oxford Tidal Resource Assessment for the Co-Tide Project
Madhubhashitha Herath, University of Hull Distributed Optical Fibre Sensing for Monitoring of Large Bending Deformations of Subsea Power Cables
Ioannis Kamas, University of Oxford Data-Driven 1D Design Model for Monopile Foundations in Layered Soils
Xuemei Lin, University of Dundee Adapting Building-Structure Bolt Design Practices for Offshore Wind Applications
Shuyue Lin, University of Exeter Intelligent Fault-Tolerant Control of Offshore Wind Turbines via Deep Reinforcement Learning
Zaibin Lin, University of Aberdeen Advancing Floating Offshore Wind Turbine (FOWT) Stability and Performance through Coupled Aero-Hydro-Mooring Analysis
Yabin Liu, University of Cambridge Controlling Tip Vortices with a Grooved-tip Design
Chenying Liu, University of Oxford Origami-Enhanced Dielectric Fluid Generator for Wave Energy Conversion
Sebastian Neira Castillo, The University of Edinburgh Wide-Bandgap Power Electronics Topologies for Wave Energy Dielectric Elastomer/Fluid Generators
Duc Nguyen, University of Bristol Applied Bifurcation Methods For Efficient Airborne Wind Energy Generation

Supergen Offshore Renewable Energy

Early Career Researcher Posters 2025

Charikleia Oikonomou, Hellenic Centre for Marine Research (HCMR), Institute of Oceanography Multi-axis motion analysis of TALOS Wave Energy Converter under realistic sea states
Claudio Alexis Rodriguez Castillo University of Strathclyde Assessing Operational Profiles for Offshore Renewable Energy: A Data-Driven Approach for Hydrogen Production Feasibility
Miad Saberi, University of Oxford Numerical Simulation of Laterally Loaded Monopiles for Offshore Wind Turbines using an Advanced Hyperplasticity Model
Isha Saxena, Durham University Reducing Uncertainty for Bayesian Analysis in Wind Energy Systems
Zhenyi Yan, University of Plymouth Enhancing Marine Concrete Performance: Fatigue Mechanics of Polymer-Modified Concrete
Markella Zormpa, University of Oxford Impact of support structure modelling methods in actuator line method large eddy simulations of wind turbine wakes

A hybrid wind and wave floating platform to provide a minimum power baseload for offshore applications.

Dr Abel Arredondo-Galeana[a], Dr Gabriel Scarlett[b], Professor Maurizio Collu[a], Professor Feargal Brennan[a]

[a] Department of Naval Architecture, Ocean & Marine Engineering, University of Strathclyde

b Mocean Energy Ltd, King's Buildings, Edinburgh, UK

Hybrid platform

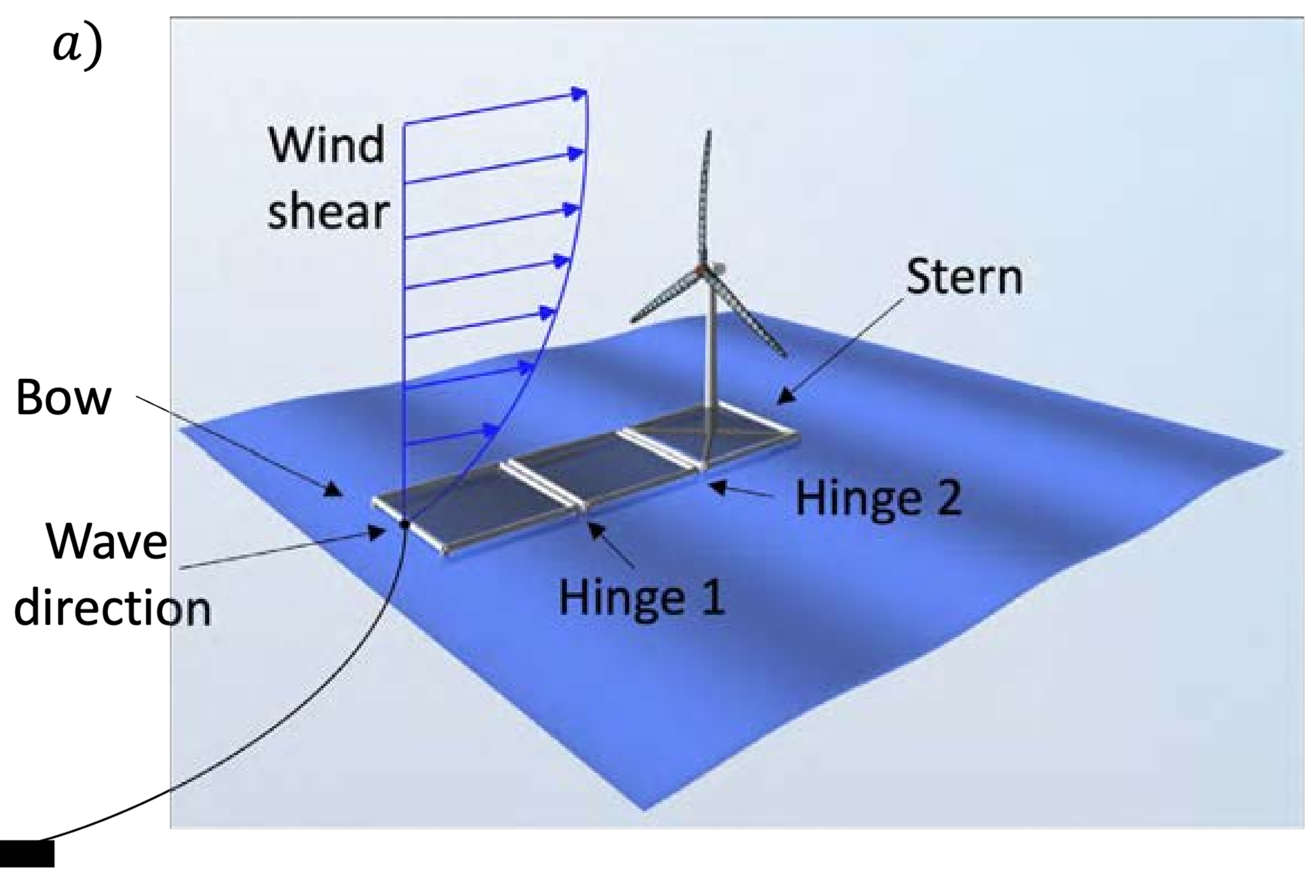

Figure 1– Hinged very large floating structure (VLFS) with 5MW NREL wind turbine

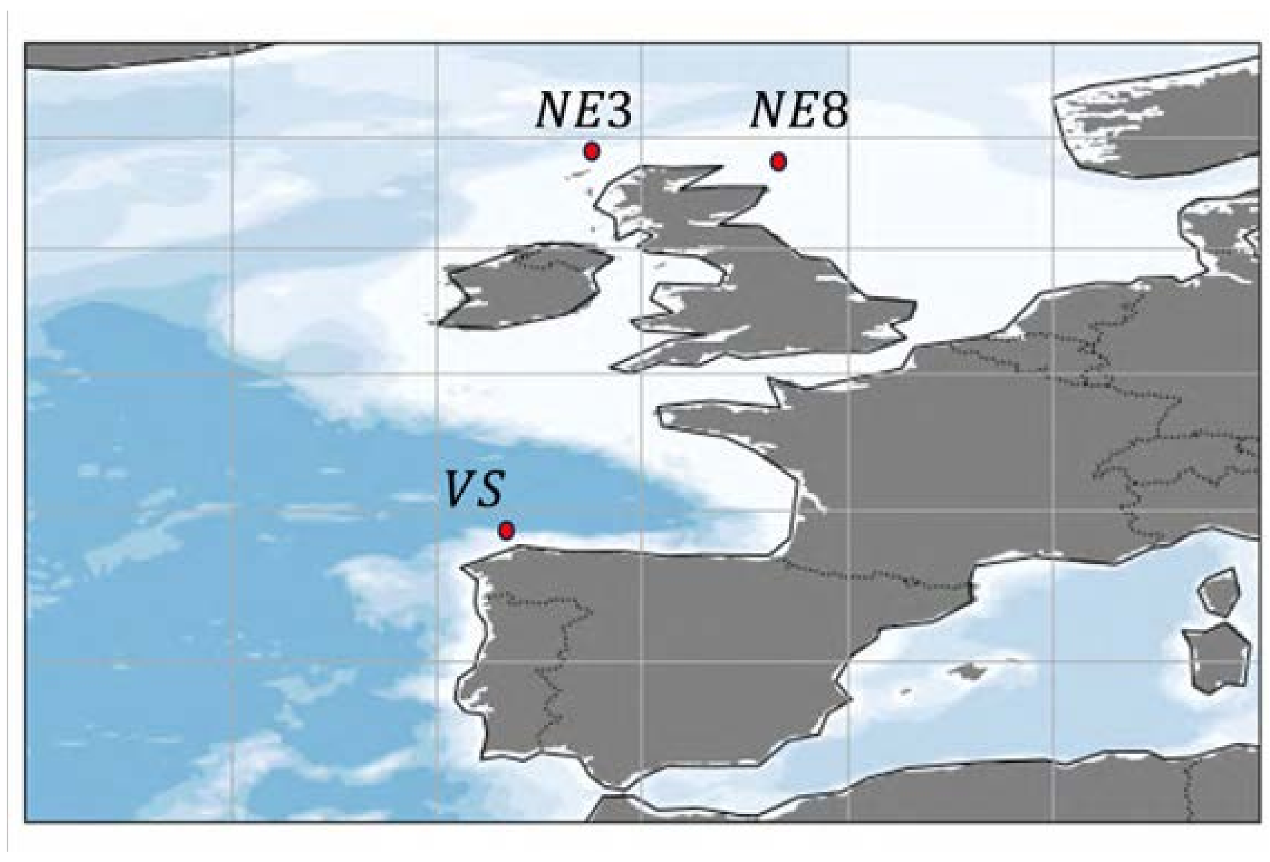

Figure 2– Locations selected to analyse the performance of the hybrid platform

References

Power performance

10 s < Ts

< 12 s

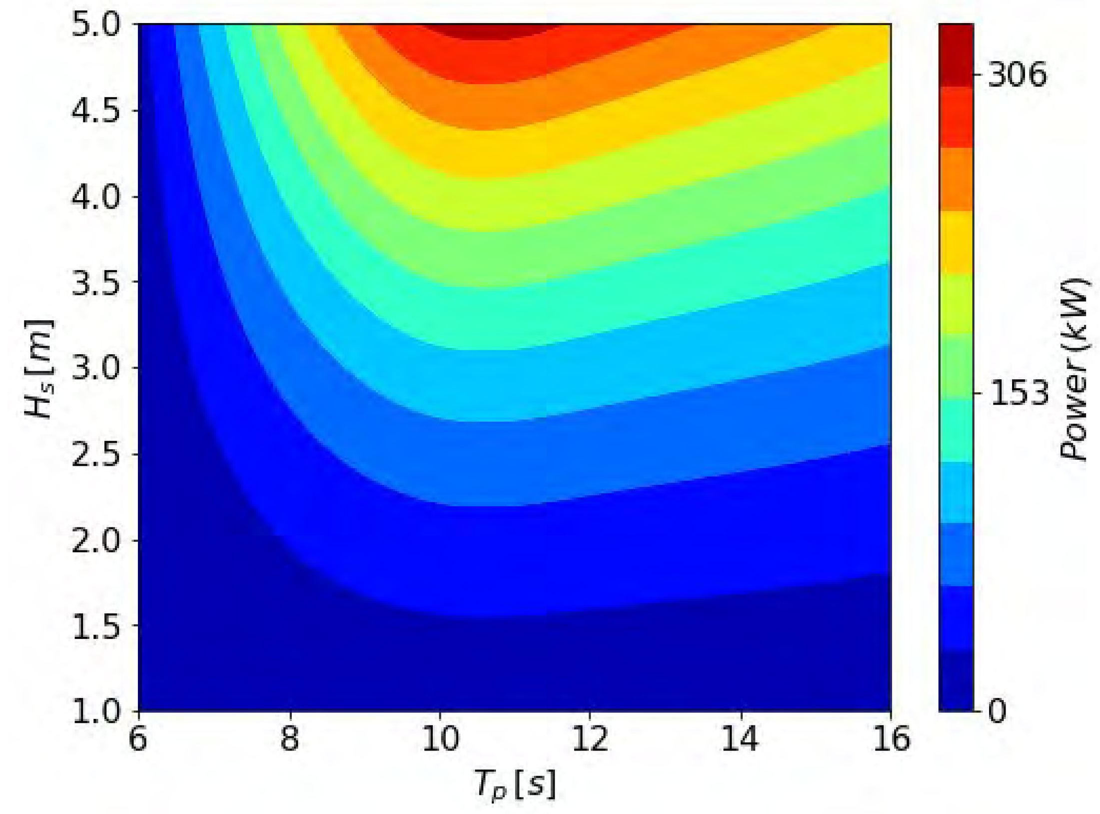

Figure 3 – Power matrix of hinged platform assuming irregular waves

Results

reduction in power downtime

: 8.2% to 3.6%, 6.1% to 3.1% and 4.7% to 4.3% for VS, NE3 and NE3, respectively

Location (correlation index)	% Power downtime Wind	% Power downtime Hybrid
VS (low)	8.2%	3.6%
NE3 (med)	6.1%	3.1%
NE8 (high)	4.7%	4.3%

Table 1– Power downtime considering only wind and hybrid power generation.

Long term analysis

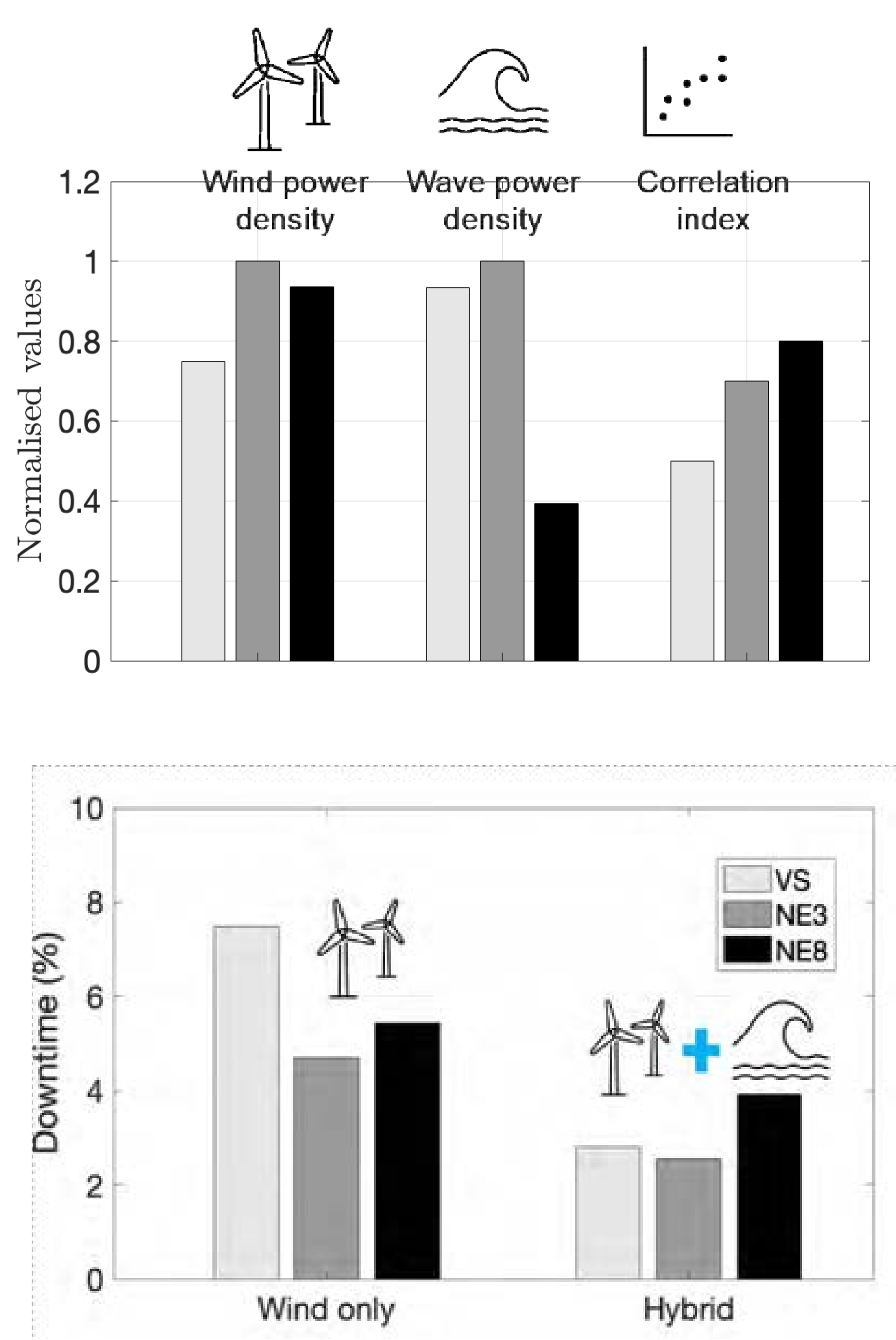

Figure 5– a) Wind, wave power density, and correlation indices of VS, NE3 and NE8, b) power downtime due to wind and hybrid platform during 2000-2019

University of Strathclyde
Supergen Offshore Renewable Energy
UKRI Engineering and Physical Sciences Research Council
RE
ashes

Using elastic foam tests to investigate an interpretation method of the ROCOCONE p-y module

Abigail H. Bateman
a.bateman@soton.ac.uk

University of Southampton

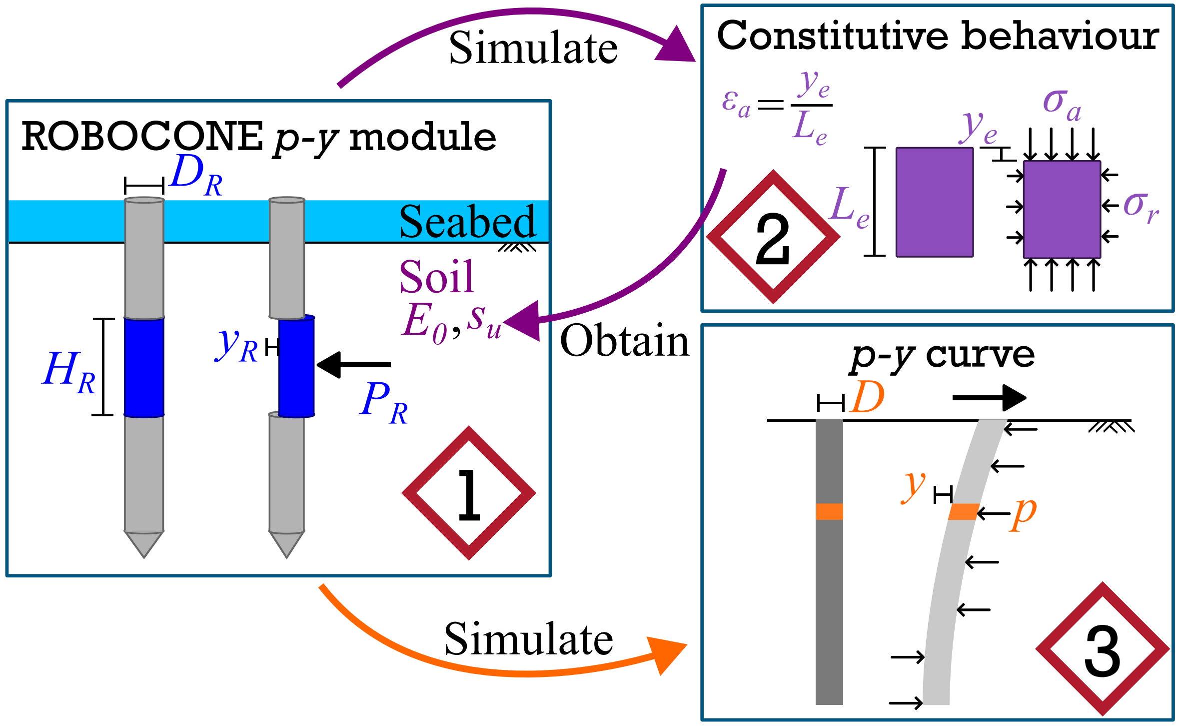

Fig 1. Schematic of the ROBOCONE p-y module to obtain soil properties and simulate p-y curves

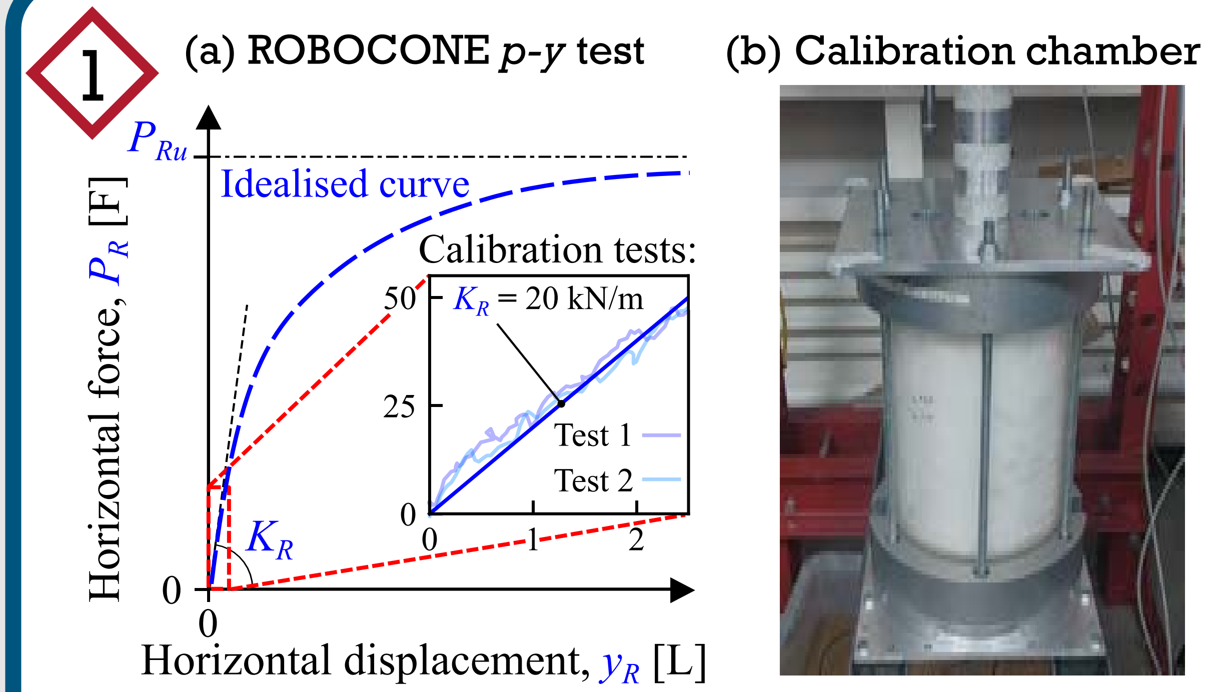

Fig 2. Idealised load-displacement curve of the ROBOCONE *p-y* module and measured response of elastic foam in (b) the calibration chamber

Development of High-Fidelity Models for Extreme Loading Events on ORE Devices

Scott Brown[1*], Vivek Francis[1], Abel Arredondo Galeana[2], Tom Tosdevin[1], Deborah Greaves[1]

1 University of Plymouth, Plymouth, UK; 2 University of Strathclyde, Glasgow, UK

**Corresponding email: scott.brown@plymouth.ac.uk*

UNIVERSITY OF PLYMOUTH

Aims and Objectives

- Develop high-fidelity numerical tools in OpenFOAM to assess the survivability of floating offshore renewable energy (ORE) devices.
- Integrate response-conditioned short design wave (SDW) techniques into the models, developed through Supergen ORE Hub, for more efficient ultimate load estimation.

Design Waves and High-Fidelity Modelling

- SDW techniques efficiently predict ultimate loads for given metocean conditions.
- Unlike traditional 3-hr irregular sea states, SDWs are typically short wave groups that target extreme events.
- Response-conditioned methods are being developed through Supergen, using the response RAOs.
- The short duration of SDWs enables high-fidelity simulations of extreme responses to be more practical.
- This makes computational fluid dynamics (CFD) a more viable tool in the design process for floating ORE devices.

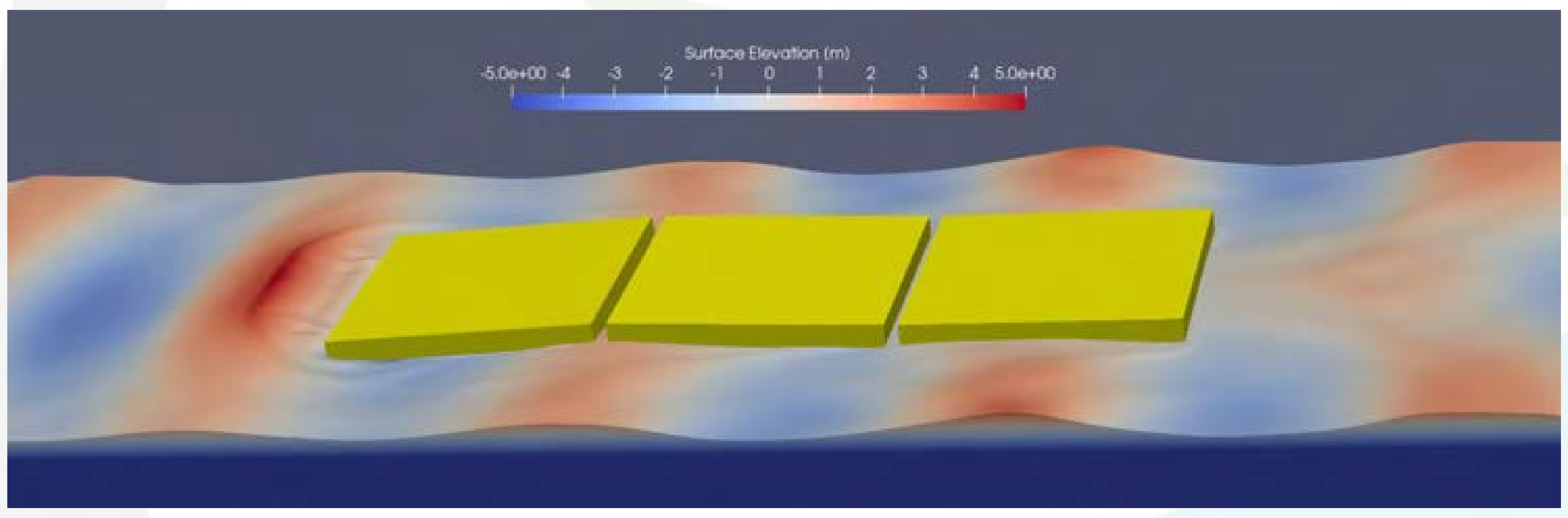

Figure 1: CFD model of the VLFS. The model is being validated against regular wave data collected in the COAST Lab.

Very Large Floating Structures (VLFS)

- Developed a numerical model of a floating VLFS, the basis of a hybrid wind-wave platform being considered in Supergen[1].
- The platform consists of three interconnected pontoons with mechanical hinges.
- A potential flow model was developed to estimate the motion of the platform in regular and irregular wave loading.
- A three-way validation between experiments, high fidelity and low order numerical approaches is currently under way.
- The CFD model enables assessment of green water impact, extreme hinge/mooring loads, and pressure distributions.

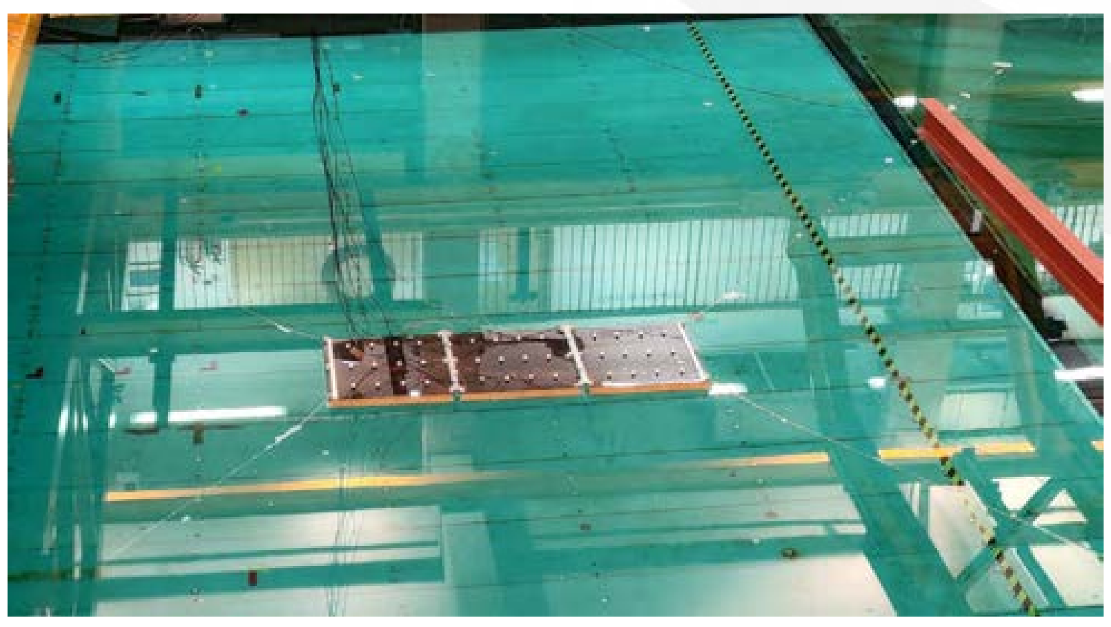

University of Strathclyde Glasgow

Figure 2: Physical model of the VLFS being tested in the COAST Laboratory.

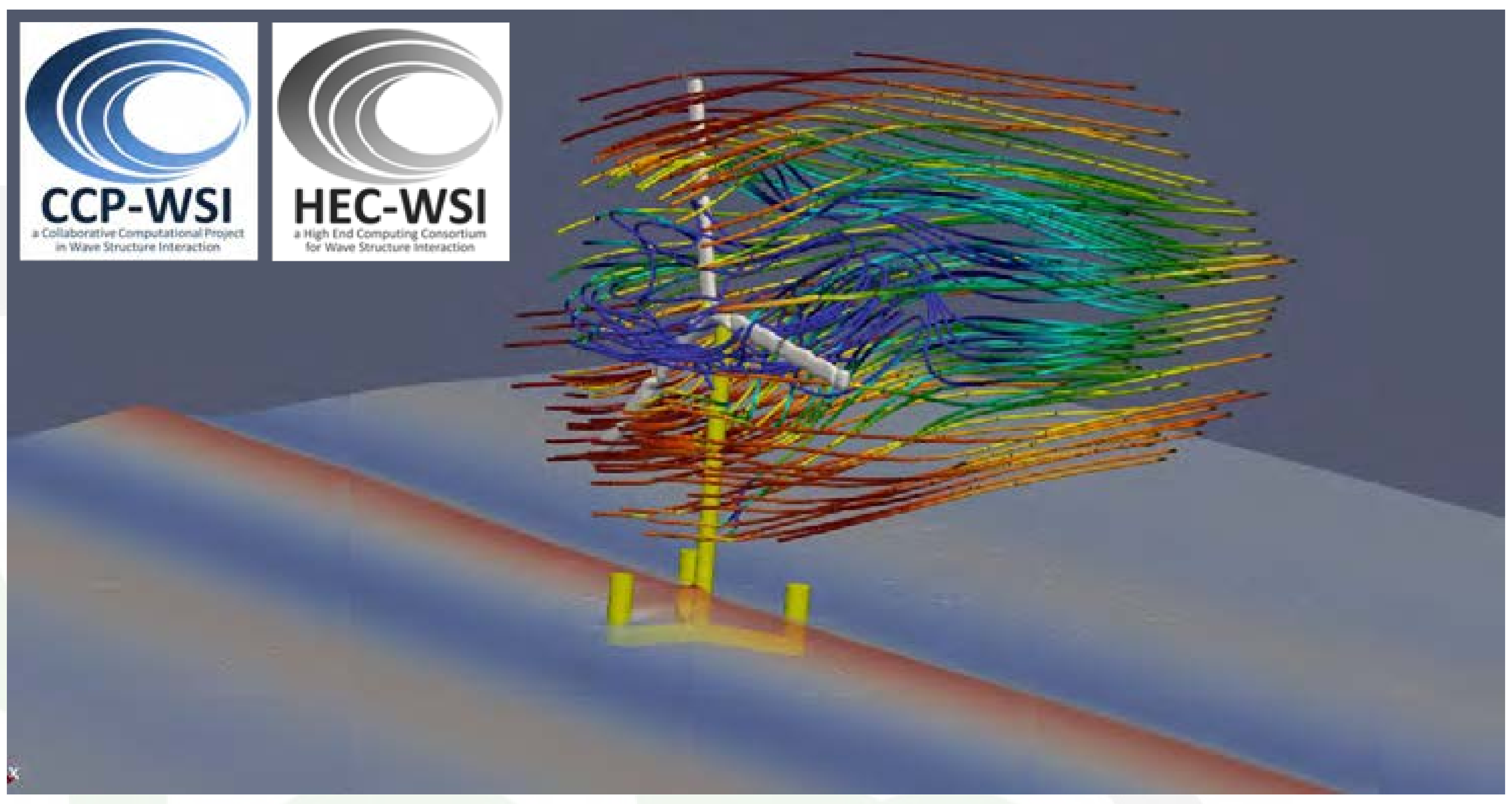

Figure 3: CFD model of a pitch response-conditioned SDW (most likely extreme response) interaction with a FOWT.

Floating Offshore Wind

- Developing a numerical replica (Fig. 3) of the COAST Lab's 1:70 scale VolturnUS-S (Fig. 4).
- The model enables:
  - Insight on fluid flow.
  - Increased flexibility to vary device characteristics.
  - Expansion of databases on ORE ultimate loads.
  - Consideration of flow-related responses.
- Test case being developed of pitch response-conditioned SDW interactions with a FOWT (Fig. 3).

Figure 4: Photograph of the COAST Lab's 1:70 scale model of the VolturnUS-S[3].

Future Work

- Extend the FOWT model to include combined wind-wave short design events, building on a recent Impact Acceleration Project[4].
- Publicly release the FOWT model for broader research and industry use.
- Validate both CFD models against physical modelling data.
- Utilise models to expand databases on ultimate loads for ORE structures[5].

References

[1] Arredondo-Galeana et al. (2023). Understanding the force motion trade off of rigid and hinged floating platforms for marine renewables. Proceedings of 15th EWTEC Conference.

[2] Allen et al. (2020). Definition of the Umaine VolturnUS-S reference platform developed for the IEA Wind 15-Megawatt Offshore Reference Wind Turbine. Technical Report, NREL/TP-5000-76773.

[3] Brown et al. (2023). On the selection of design waves for predicting extreme motions of a floating offshore wind turbine. Ocean Eng., 290, 116400.

[4] Tosdevin et al. (2025). On the development and application of short design events for the prediction of extreme responses of floating offshore wind turbines, Ocean Eng., 327, 120929.

[5] Brown et al. (2025). On the sensitivity of short design waves for semi-submersible wind platforms. Ocean Eng., 328, 121054.

Supergen Offshore Renewable Energy | UKRI Engineering and Physical Sciences Research Council | CoSeC Computational Science Centre for Research Communities

This work was supported by the Engineering and Physical Research Council (EPSRC) through funding from Supergen ORE Hub [EP/Y016297/1], including an Early Career Researcher (ECR) fund for SB and AAG, and the Collaborative Computational Project in Wave Structure Interaction (CCP-WSI) [EP/T026782/1], including additional bridging funds from the Computational Science Centre for Research Communities. Further support was provided by the High-End Computing Consortium for Wave-Structure Interaction (HEC-WSI) [EP/X035751/1] in the form of computational resource on the UK supercomputing service (Archer2).

WaveTide: Wave Effects on a Benchmark Tidal Energy Device

X. Chen[1], F. Zilic de Arcos[1], G. Pinon[2], R.H.J. Willden[1]

[1] Department of Engineering Science, University of Oxford, Oxford, UK.

[2] Laboratoire Ondes et Milieux Complexes, UMR 6294 CNRS, France.

Introduction

- The tidal turbine benchmark exercise **Stage II experiments with steady wave** has finished in **March 2025**.
- Workshops to be held for the **blind prediction campaign with Stage II measurements** during **summer 2025**, in order to:
  - improve accuracy and confidence of wave-rotor modelling techniques
  - quantify modelling errors for different techniques under different wave scenarios

This project aims to **develop and evaluate** the current CFD modelling technologies for **tidal turbine under waves on a current** through collaboration with research partners, and is published in **AWTEC 2024 Conference**.

This project is funded by the EPSRC SupergenORE HUB EP/S000747/1 ECR research fund, simulations are supported by the HEC-WSI EP/X035751/1 code development fund.

Motivation

The complex flow environment of a tidal turbine. [1]

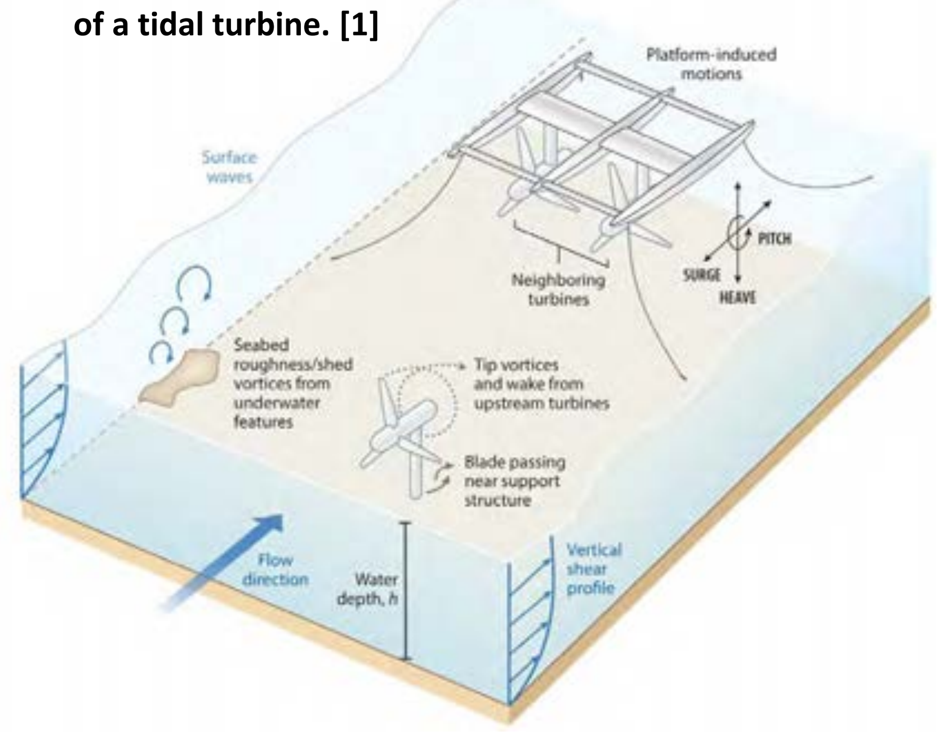

The **complex flow environment under water** leads to **highly unsteady loadings** on the tidal turbine.

Unsteady loading and the **inability to confidently predict unsteady loading** leads to **huge performance uncertainty** and drives **unnecessary overdesign**, which all contribute to the **high costs in tidal energy**.

One of the **most challenging** aspects for all ORE systems is to design, develop and optimise devices **passively or actively interacting with waves**.

Wave Simulation Method Development & Validation

Simulation Methodologies

- Solver tools are using OpenFOAM-v2106, waves2foam [2] and stabRAS_v1712 [3].
- Water-air interface is modelled by a volume of fluid (VoF) method.
- Turbulence model is stabilised k-ω SST model.
- Wave is generated and modelled by the Fenton's stream wave theory and absorbed by the GABC method.
- Simulation methodologies are utilised in another CFD study on a small-scale experimental scale rotor [4].
- Constant resolution in wave height direction (10 cells per wave-height or 976 cells per wave-length, non-dimensional resolution of 0.1).
- Wave standing frequency of $0.4\,Hz$, encounter frequency of $0.502\,Hz$.

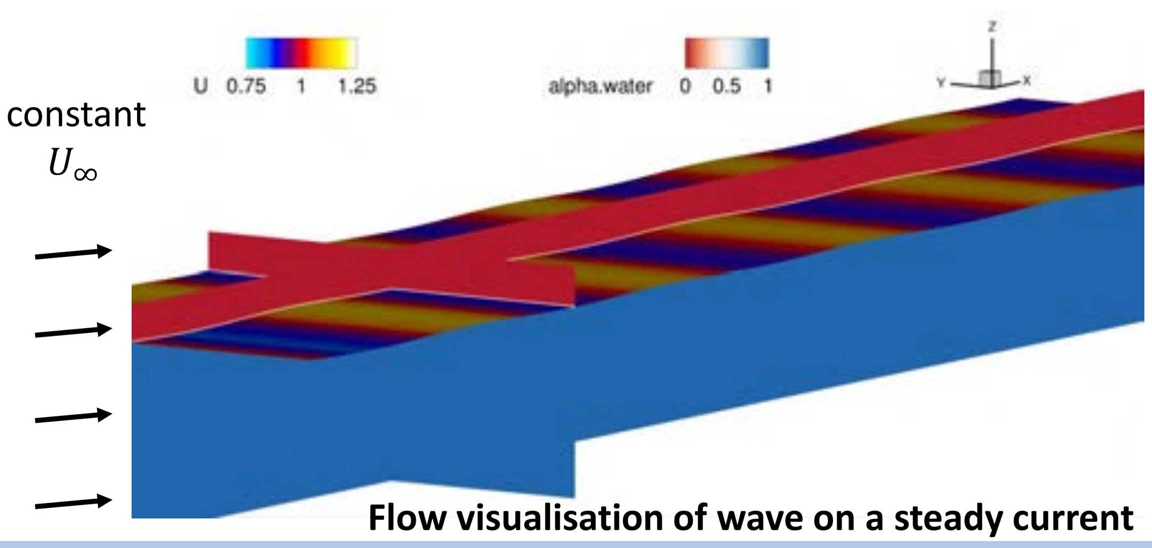

Flow visualisation of wave on a steady current

Wave Energy Grid Dissipation Study

- Different span and stream resolutions studied:
  - Spanwise resolution from 0.1 to 1.0.
  - Streamwise resolution from 0.1 to 0.8.
- Results show that:
  - Spanwise resolution (and cell aspect ratio) influences the stability of the simulation.
  - Streamwise resolution shows close relationship with numerical dissipation in wave energy.
  - 90% of wave energy is maintained with >360 cells per wave-length.

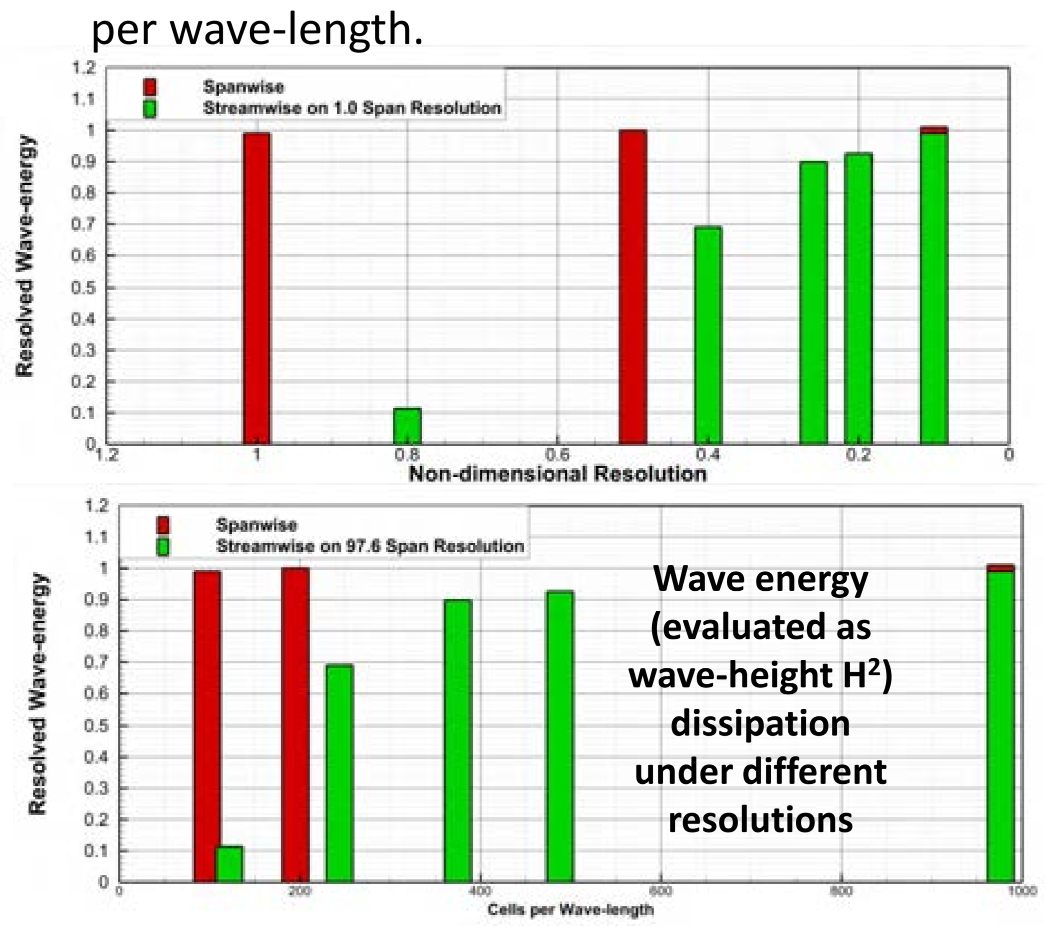

HPC Scaling Tests

- Based on non-dimensional wave resolution of 1/10, and non-dimensional rotor resolution of 1/160.
- Total cell count 155 million, with 91.6% spent in wave interface, and 8.4% in rotor and wake.
- Scaling test performed on ARCHER2 UK National Supercomputing facility.
- Results shows that:
  - Simulation speed scale well up to 1536 cores (100,000 cells per core).
  - Simulation efficiency drops when <100,000 cells per core.

HPC speed scaling results

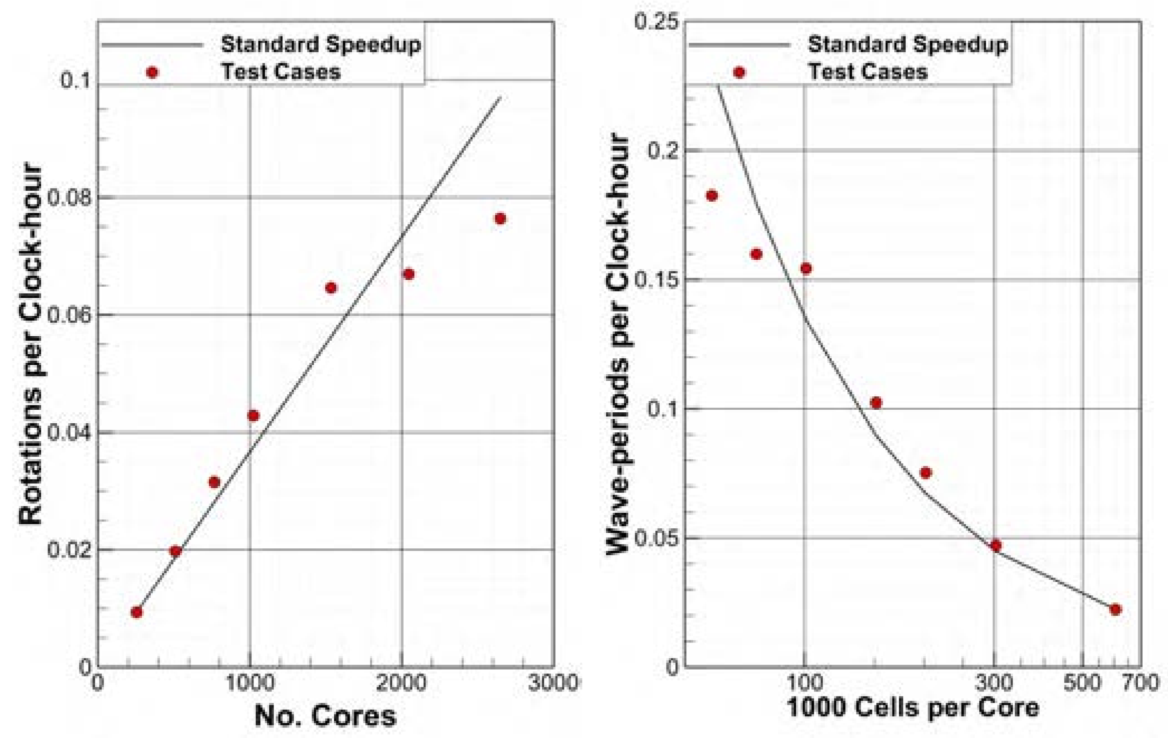

Wave-rotor Interaction Study

- Configurations [5]:
  - The 1.6m-diameter benchmark tidal turbine.
  - Tip clearance $0.354\,m$.
  - Current $U_\infty = 1.0\,m/s$
  - Wave conditions: frequency $f = 0.4\,Hz$, height $H = 0.10\,m$
  - Turbine operation conditions: $RPM = 72$, $TSR \sim 5.0$ to 7.20
- Experiment and CFD configurations available from https://supergen-ore.net/projects/tidal-turbine-benchmarking

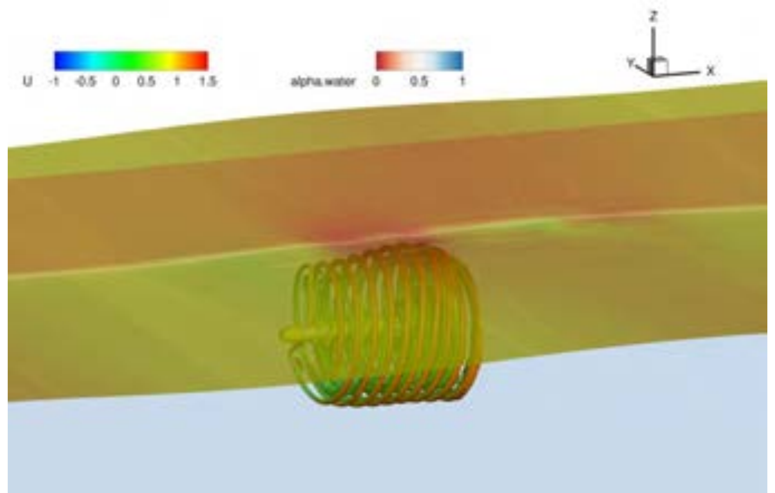

Flow visualisation of the benchmark tidal turbine with wave on steady and uniform current

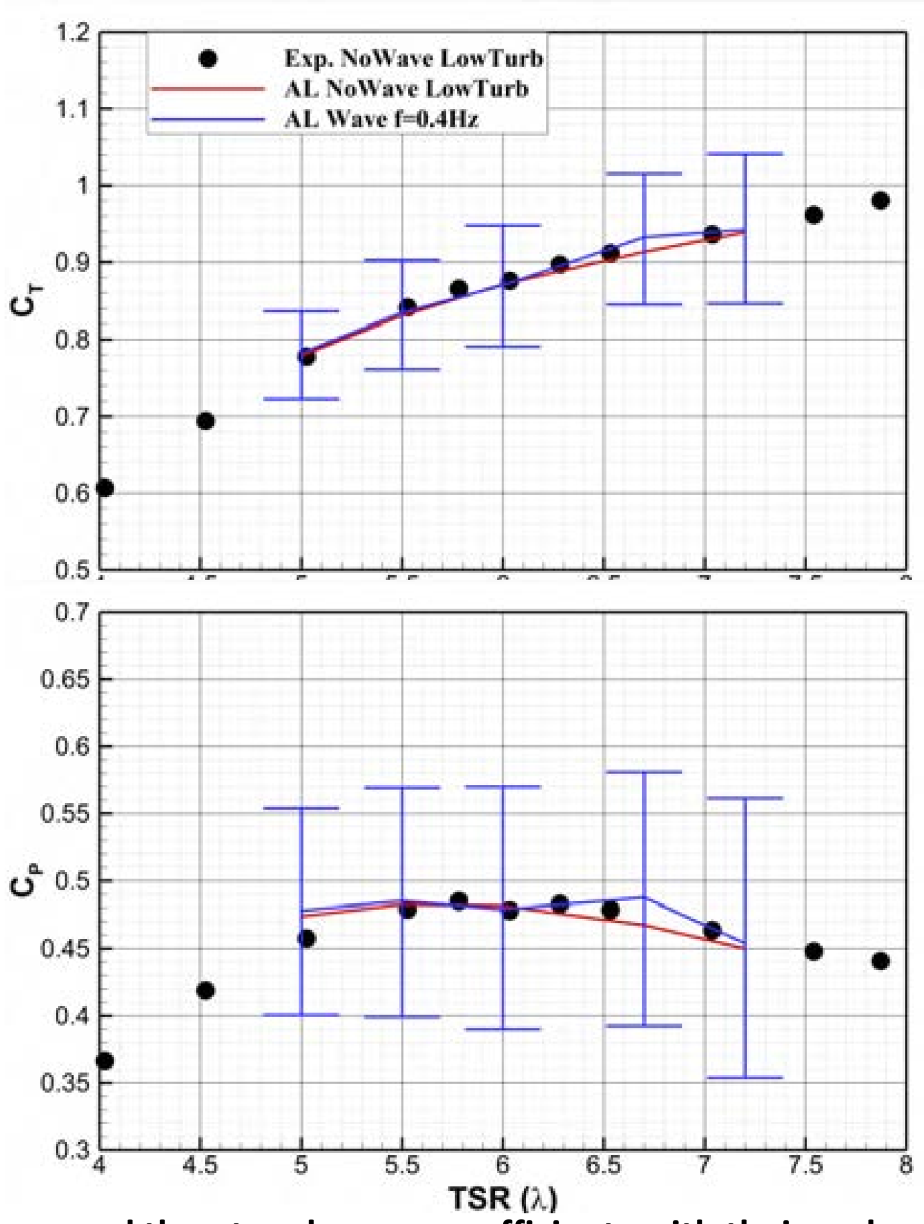

Time-averaged thrust and power coefficients with their cycle variations

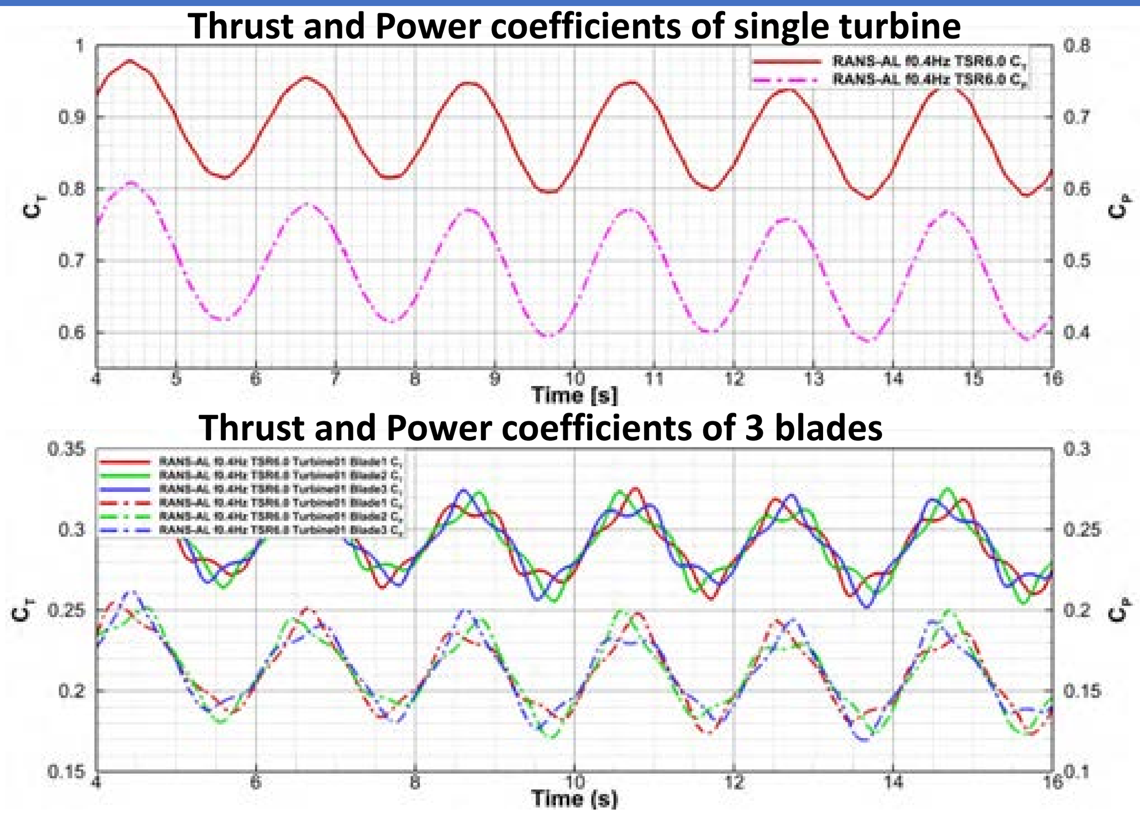

Rotor performance cycle follow **wave encounter periods**, while blade performance cycle shows **mixed frequencies of both wave and rotation**.

Time-averaged rotor performance under wave condition similar to that without wave.

Large fluctuations in performance and blade forces found during wave cycles.

References

[1] Adcock T.A.A. et al., The fluid mechanics of tidal stream energy conversion. *Annu. Rev. Fluid Mech.*, 53: 287-310, 2021.

[2] Jacobsen et al., A wave generation toolbox for the open-source cfd library: OpenFoam. *Int. J. Numer. Meth. Fluids*, 70: 1073-1088, 2012.

[3] Larsen B.E. and Fuhrman D.R., On the over-production of turbulence beneath surface waves in Reynolds-averaged Navier-Stokes models. *J. Fluid Mech.*, 853: 419-460, 2018.

[4] Zilic de Arcos, F. et al., A study on a tidal rotor under the combined effects of currents and regular waves using Actuator-Line CFD simulations, *Proc. EWTEC*, vol. 15, 367:1-9, Sep. 2023.

[5] Willden R.H.J. et al., Tidal turbine benchmarking project: stage I – steady flow experiments, *Proc. EWTEC*, vol. 15, Sep. 2023.

Predicting the response of monopile foundations to storm loading from laboratory test data

Supergen Offshore Renewable Energy

Jamie J. Crispin University of Southampton

j.j.crispin@soton.ac.uk
Department of Civil, Maritime and Environmental Engineering, University of Southampton (Formerly University of Oxford)

1 Storm loading on monopiles

Wind and waves loading is highly variable, with loading concentrated in high intensity storm events.

Predicting the accumulated rotations and cyclic secant stiffness changes due to these storm events is critical to designing monopiles for serviceability.

An ideal modelling approach would be calibrated with routinely obtained cyclic laboratory testing but allow predictions of the response to realistic storm loading.

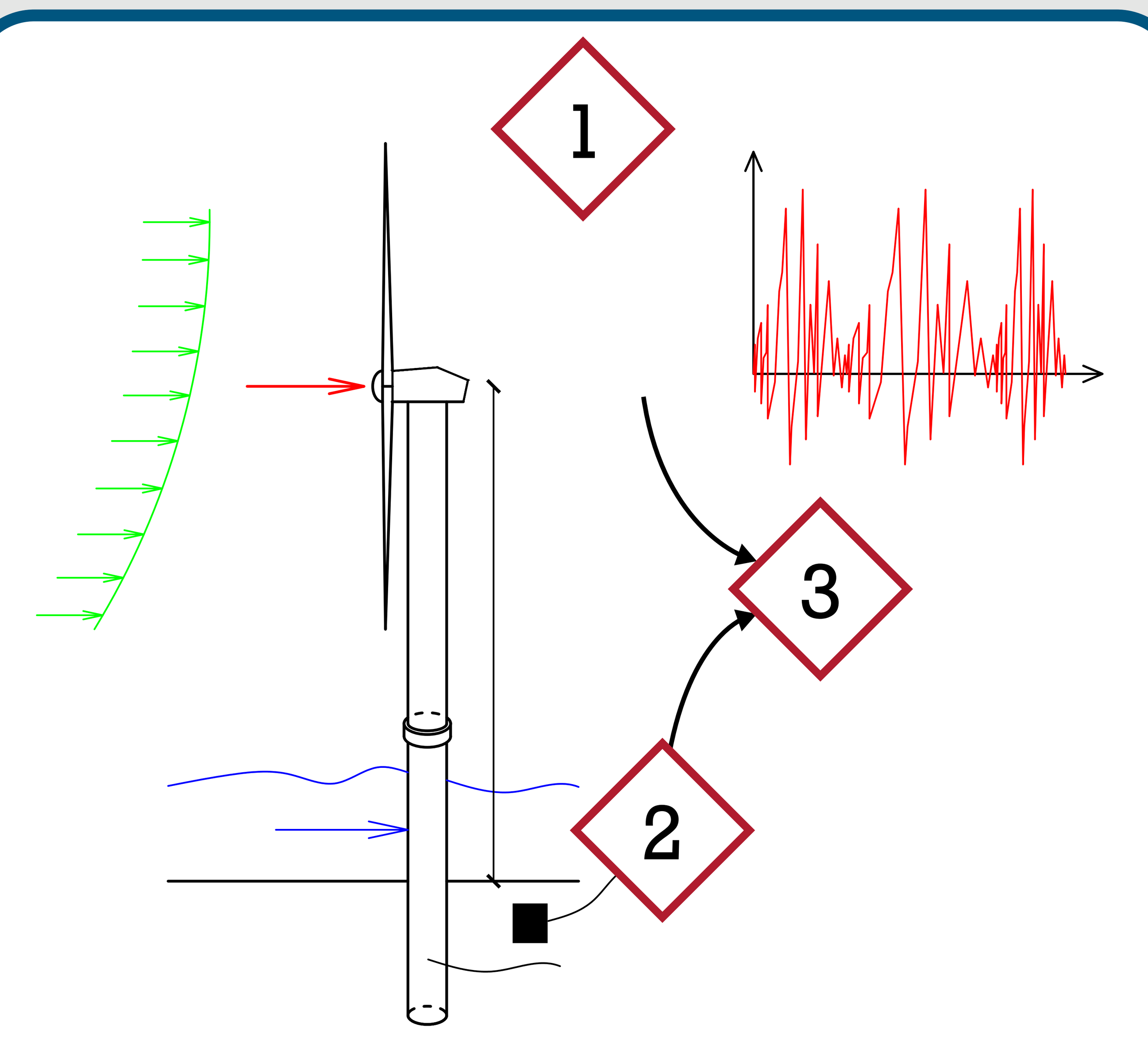

Fig. 1: The problem

2 UDCAM-S

NGI

The Simplified UnDrained Cyclic Accumulation Model (UDCAM-S [1]) was developed at NGI.

Calibrated using routinely obtained cyclic laboratory testing (e.g. DSS), so can be applied to a new material relatively inexpensively through generation of cyclic contour diagrams.

However, UDCAM-S is limited to sinusoidal cycles, so realistic storms must be idealised to packets of increasing amplitude (see Fig. 2).

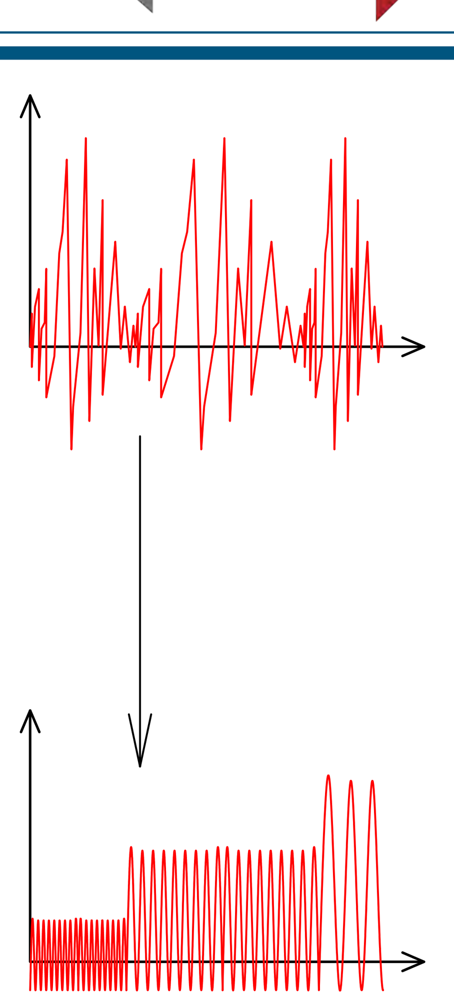
Fig. 2: Idealised loading

3 HARM

University of Oxford

The Hyperplastic Accelerated Ratcheting Model (HARM [2]) was developed at University of Oxford (Fig. 3).

The response to realistic storm loading is modelled directly with a ratchet attached to an Iwan model.

However, HARM is calibrated via higher cost model, laboratory and/or field tests on monopile foundations.

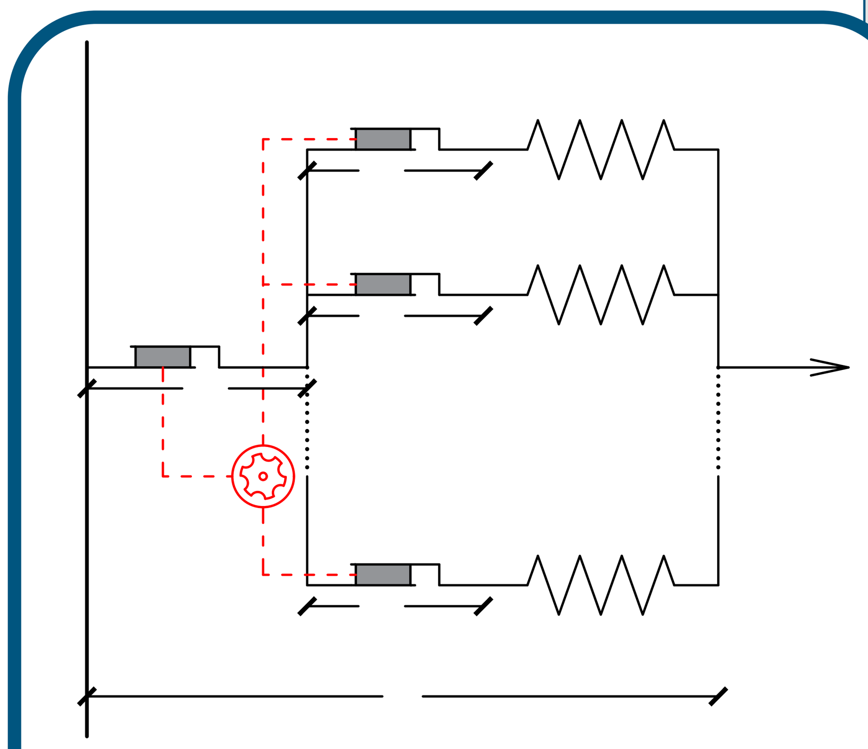

$$R = R_{ref}\left(\frac{\beta}{\beta_{ref}}\right)^{-m_r}\left(\frac{|\sigma|}{\sigma_{ref}}\right)^{m_s}$$

Fig. 3: HARM

4 Proposed model

In this work, two existing models are combined:

1. Cyclic contour diagrams are calibrated against routine element tests.
2. Use UDCAM-S to predict monopile response during sinusoidal loading with different amplitude and asymmetry.
3. Calibrate HARM against the obtained UDCAM-S results.

The resulting model allows improved prediction of the monopile response during realistic storm loading from only laboratory test data.

1

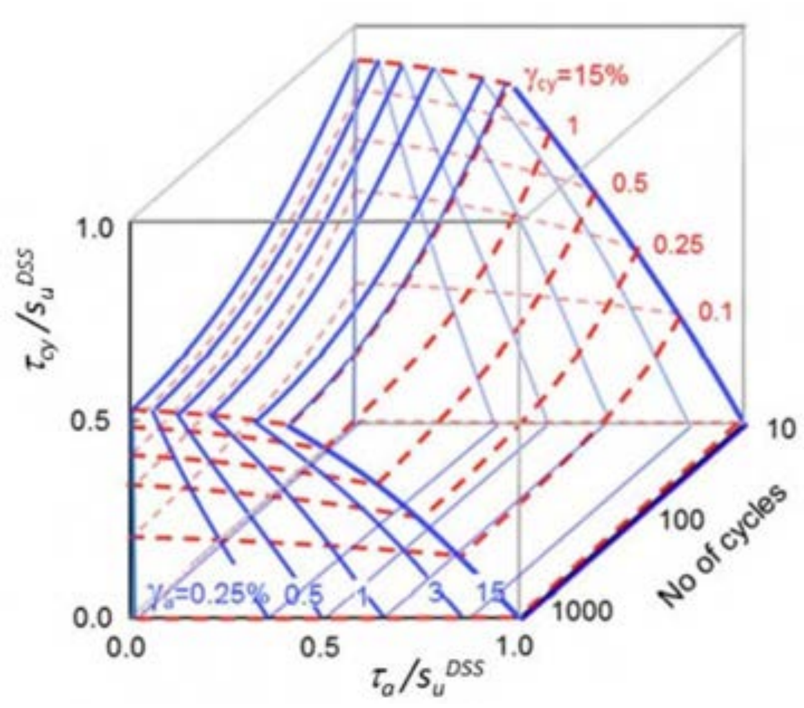

Example 3D cyclic contour diagram for OCR=1 Drammen Clay (reproduced from [1])

2

$$\zeta_b = \frac{H_p}{H_{ref}} \qquad \zeta_c = \frac{H_m}{H_p}$$

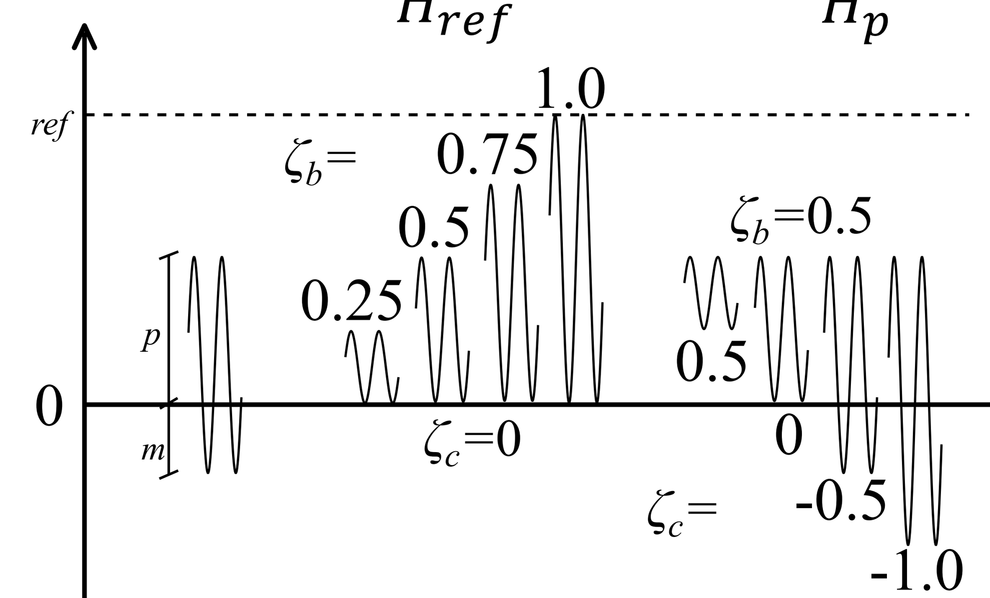

Different amplitude and asymmetry sinusoidal loading used as input to UDCAM-S model

3

HARM parameters calibrated to results of UDCAM-S analyses:

R_{ref} m_s m_r

Fig. 4: Proposed combined model

Acknowledgements
The author would like to acknowledge Prof. Byron Byrne from the University of Oxford for his support developing this project, as well as both Dr. Hans-Petter Jostad and Dr. Nallathamby Sivasithamparam from NGI for hosting a placement at NGI and sharing their knowledge of UDCAM-S.
The author was supported by a ECR fund made available by the Offshore Renewable Energy Supergen Hub project, Engineering and Physical Sciences Research Council grant no EP/Y016297/1.

References:
[1] Jostad, H.P., Liu, H., and Sivasithamparam, N. (2023). Accounting for effects of cyclic loading in design of offshore wind turbine foundations. In: (Zdravkovic L, Kontoe S, Taborda DMG, Tsiampousi A (eds.)) *Proceedings 10th European Conference on Numerical Methods in Geotechnical Engineering*. London, UK. doi:10.53243/NUMGE2023-438.
[2] Houlsby, G.T., Abadie, C.N., W.J.A.P. Beuckelaers & Byrne, B.W. (2017) A model for nonlinear ratcheting behaviour. *International Journal of Solids and Structures*, 120, 68-80. doi:10.1016/j.ijsolstr.2017.04.031.

Fatigue in Offshore Wind Foundations

Comparison of S-N curves from various standards, new regression analyses, and parameters influencing the size effect in welds

Federico Della Santa, Ali Mehmanparast

e-mail: federico.della-santa@strath.ac.uk

Background

The most common type of offshore wind turbine foundation is the monopile [1]:

- They are continuously subjected to cyclic loadings (i.e. fatigue) given as stress ranges ($\Delta\sigma$)
- They are increasing in size: up to 150 mm in wall thickness (T) and 10 m in diameter (D) [2]
- They are designed to operate for 20 to 30 years (i.e. they have to withstand more than 10^7 cycles)
- They contain double-V groove welds that can be ground flush (GF) or in as welded condition (AW)

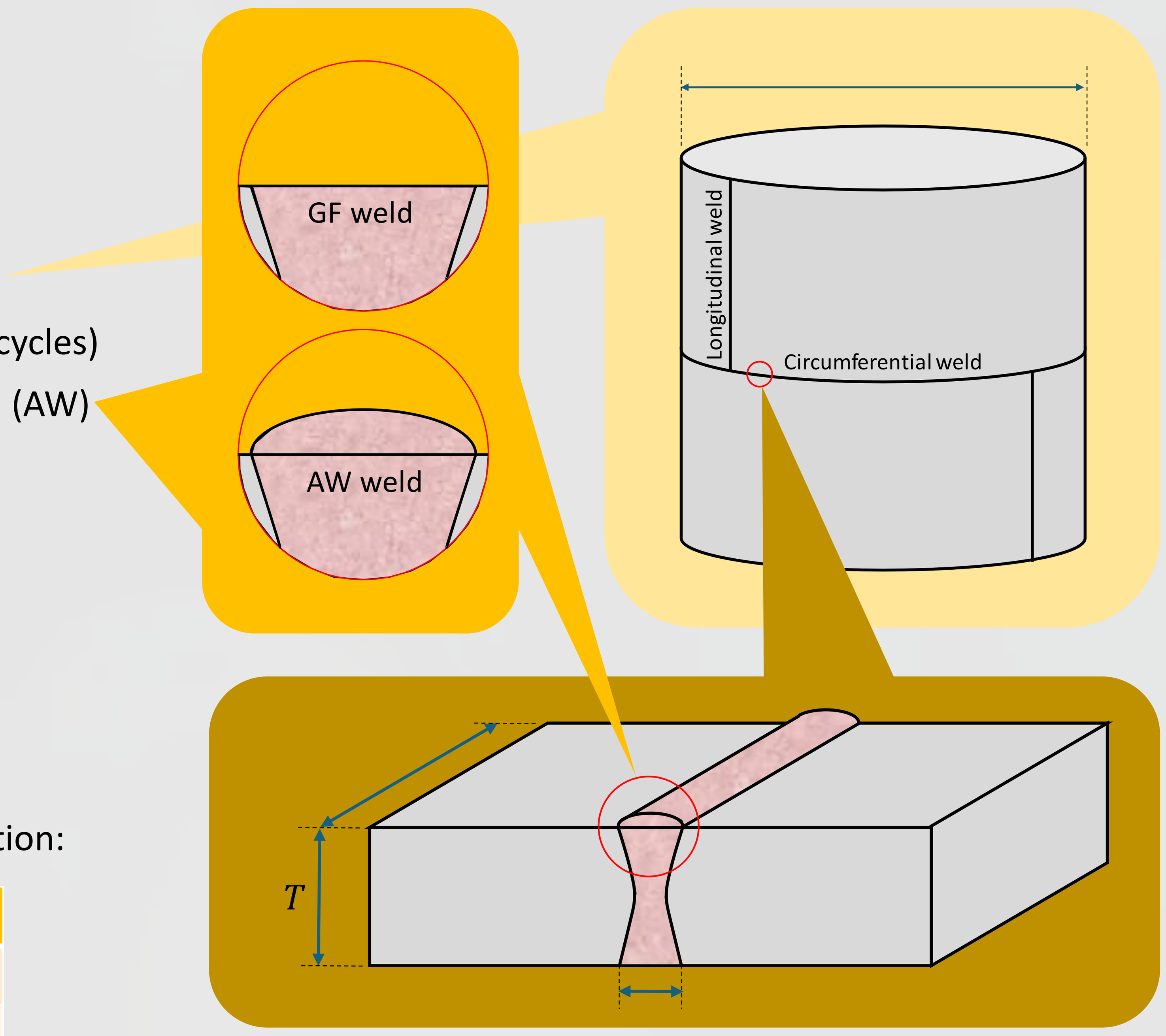

S-N curve

A power law relates the number of cycles to failure (N_f) to the stress range ($\Delta\sigma$):

$$\log N_f = q - m \log \Delta\sigma$$

In log-log coordinates this is a straight line (with slope m and intercept q) called S-N curve.

Conditions of interest

Three standards were analysed in air, and seawater with (CP) and without (FC) cathodic protection:

- DNV-RP-C203-2021 (DNV 2021)
- DNV-RP-C203-2024 (DNV 2024)
- BS 7608:2014+A1:2015 (BS)
- EN 1993-1-9:2005:E (EC)

Class	DNV 2021	DNV 2024	BS	EC
GF	C1	C1	C	112
AW	D	Monopile	D	90

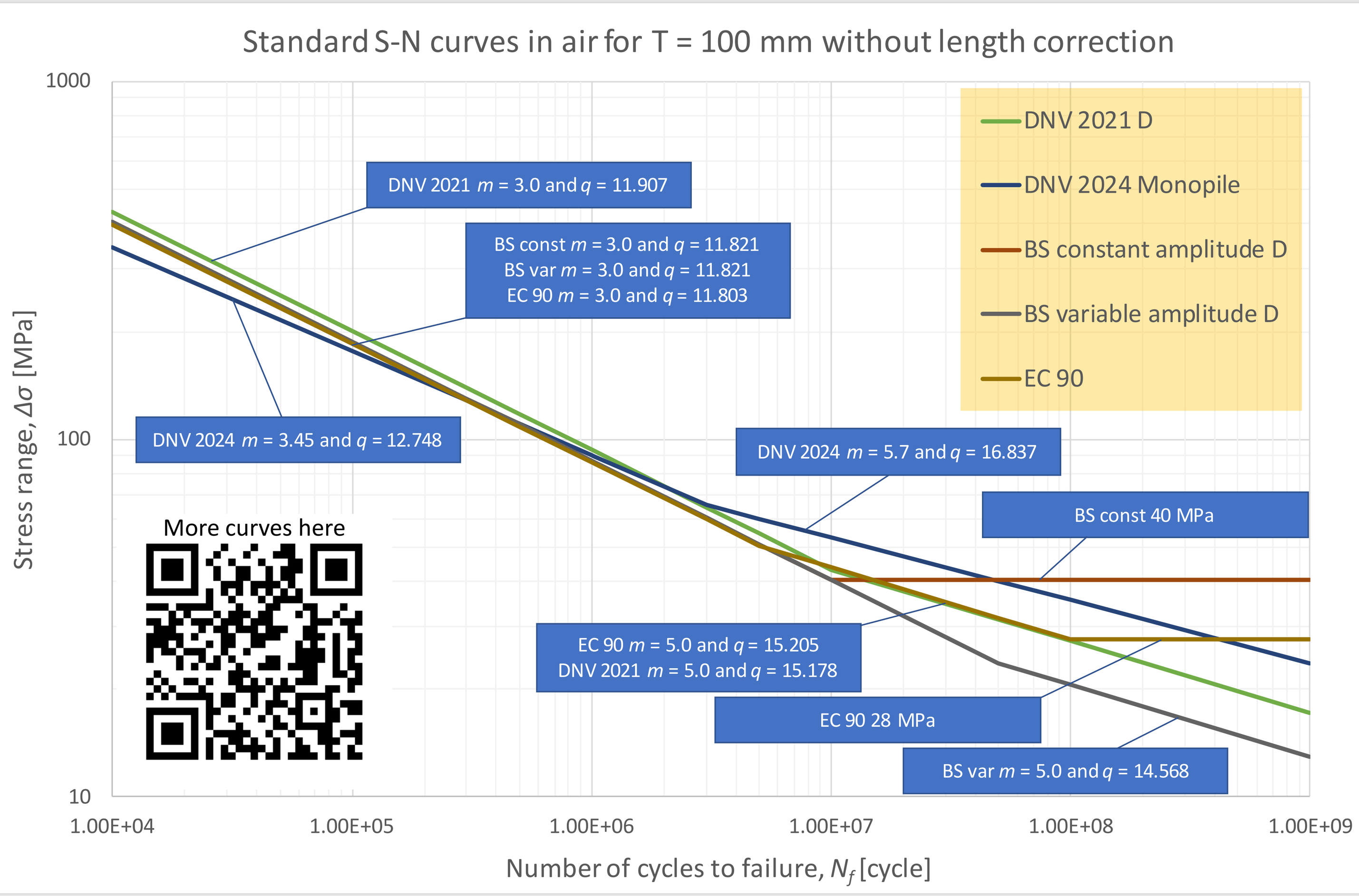

c	Air			Cathodic Protection			Free corrosion		
	DNV	BS	EC	DNV	BS	EC	DNV	BS	EC
GF	0.10	0	0.20	0.10	0	-	0.15	0	-
AW	0.20	0.20	0.20	0.20	0.20	-	0.20	0.20	-

Thickness reduction

All standards reduce fatigue life with the following formula when $T > 25\ mm$ ($t = T$ apart for DNV):

$$\log N_f = q - m \log \Delta\sigma - mc \log \frac{t}{25}$$

Weld width reduction

DNV suggests $t = \min(T, 14 + 0.66 L_t)$ to weaken the thickness reduction at high T values.

For an asymmetric double V groove, the weld width L_t can be estimated as:

$$= 2(L_{t1} + L_{t2}) \sin\frac{\alpha}{2} = b + \frac{4}{3} T \tan\frac{\alpha}{2}$$

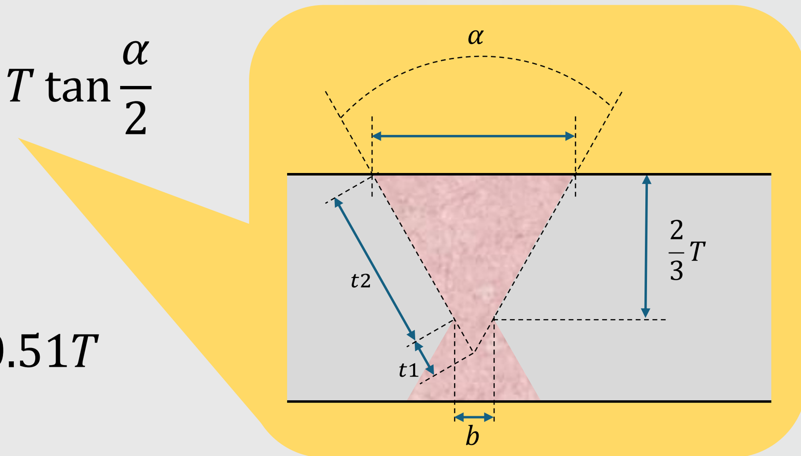

Using $\alpha = 60°$ and $b = 3\ mm$:

$$\text{For } T < 32.5, \quad t = T$$

$$\text{For } T < 32.5, \quad t = 15.98 + 0.51T$$

Weld length reduction

DNV standard suggests a further reduction for long welds (if $D = 8.0\ m$ the q is reduced by 0.24):

$$\log N_f = q - m \log \Delta\sigma - mc \log \frac{t}{25} - 0.1 \log\left(\frac{}{100}\right)$$

S-N curve comparison

- Standards suggest that in the ultrahigh-cycle fatigue (UHCF) regime (N_f after the change in slope), thick joints may encounter a further reduction in fatigue life due to the product between m and c.
- The most conservative standard in the UHCF is DNV 2021 for GF classes (regardless of thickness and environment) and thin AW joints in FC, and BS (with variable amplitude loads) for the others.
- For thin joints, disregarding the curves that display a horizontal asymptote in the UHCF regime, DNV 2024 is the least conservative in all environment apart from AW joints in free corrosion.
- For thick joints, disregarding the curves that display a horizontal asymptote in the UHCF regime, DNV 2024 is the least conservative for AW classes, while BS variable amplitude for the GF ones.
- The highest reduction in the allowable fatigue life is for AW joints in the UHCF: comparing plates 25 and 100 mm thick, a reduction up to 75% is obtained [3].

New regression analyses

- The regression line is lowered by 2 standard deviation (SD) to get 2.3% probability of failure
- SLIC data brings to $m = 3.37$ for $T = 50\ mm$ AW joints (leading up to 30% increase in N_f) [4]
- Preliminary results using literature data: stresses were normalised to 25 mm, the slope was fixed (LF) or not (L) to 3, and the regression line (mean) was lowered by two SD and using $t = 50\ mm$.
- Due to experimental difficulties there is a lack of data at $N_f > 10^7$ especially for high T values.
- Future Bayesian regression will tell more about slopes and intercepts distributions, and allow the inclusion of runouts (suspended tests without failure) in the analyses.

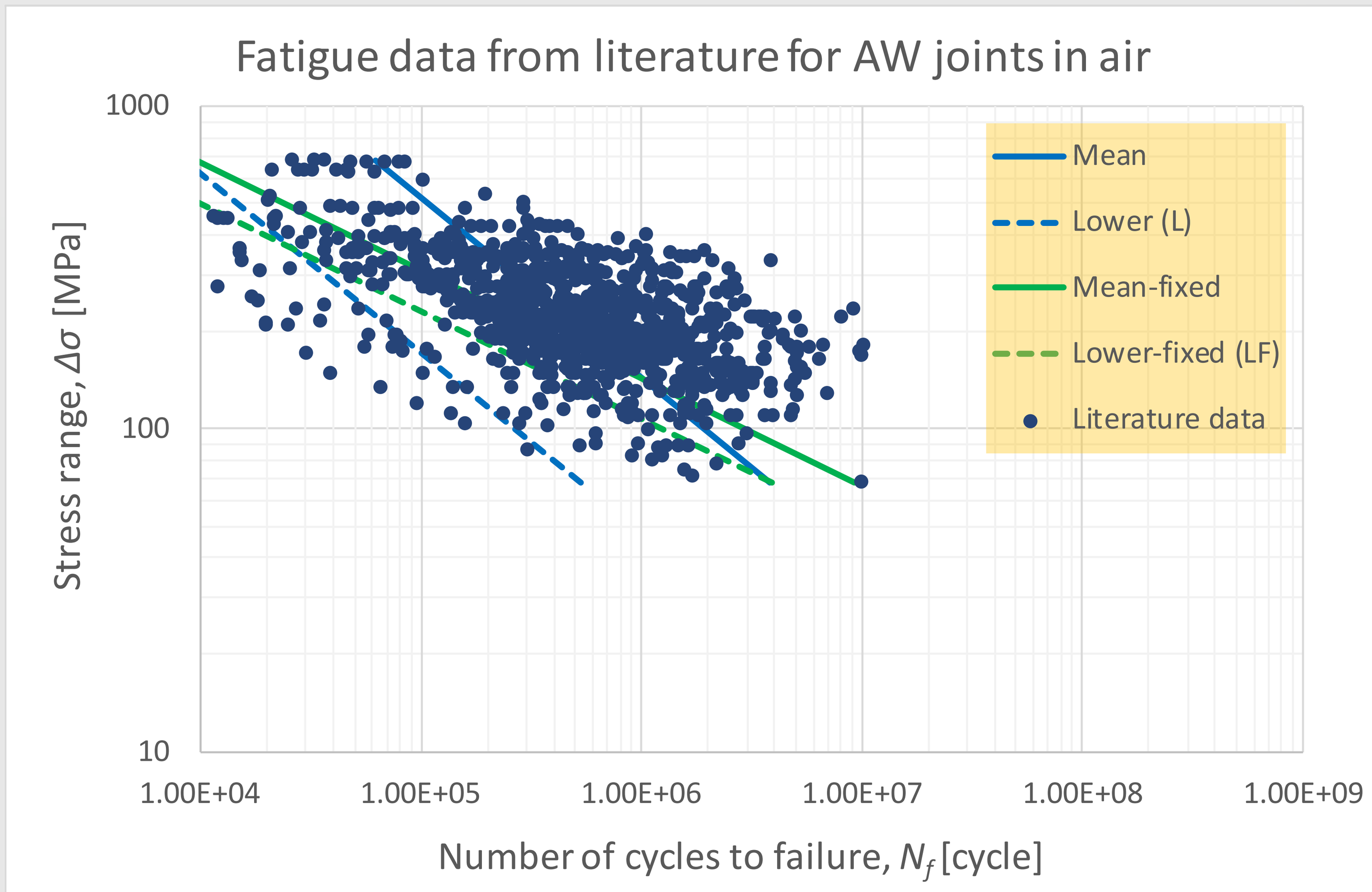

AW air 50mm	DNV 2021	DNV 2024	BS	EC	SLIC	L	LF
m	3.00	3.45	3.00	3.00	3.37	1.79	3.00
q	12.033	12.891	12.001	11.983	12.786	8.906	11.909
SD	0.20	0.20	0.21	-	0.21	0.43	0.19

References: [1] Leite, O.B: "Review of Design Procedures for Monopile Offshore Wind Structures". [2] Nordenham, S. Steelwind Nordenham Company Brochure. [3] Della Santa, F.: "Comparison of S-N Curves from International Fatigue Design Standards for a Better Understanding of the Long-Term Operation of Offshore Wind Turbine Welded Foundations". [4] Mehmanparast, A.: "Re-evaluation of fatigue design curves for offshore wind monopile foundations using thick as-welded test specimens".

UKRI Engineering and Physical Sciences Research Council

Wind & Marine Energy Systems & Structures CDT

University of Strathclyde Glasgow

Tidal Turbine Benchmarking Project: Stage II – Experiments on Unsteady Loading in Waves

Yadong Han, Nijmeh Marouf, Ian Campbell, Ross Calvert, Christopher Vogel, Richard Willden
Department of Engineering Science, University of Oxford

Introduction

- **Motivation**
  Unsteady loading and the instability to confidently predict unsteady loading and / or quantify errors drives unnecessary redundancy and design conservatism.
  Open access benchmarking datasets are available for the wind energy sector, but little is available for the tidal energy sector.
- **Objectives**
  Improve accuracy of modelling techniques.
  Improve confidence in the use of modelling techniques.
  Quantify modelling errors for different techniques under different loading scenarios.
  Development of novel measurement techniques.
- **Approaches**
  Conduct large laboratory tests of a highly instrumented tidal turbine in turbulent flow and waves to provide underlying data.
  Conduct a series of community wide (academia and industry) blind prediction exercises with staged data release, leading to an open access dataset.

Experimental Campaigns

- **Stage I: Steady Flow Experiments, July 2021 – January 2023**
  Turbulence Grid and wave characterization experiments
  Steady and turbulent flow experiments
  Preliminary wave experiments
  Blind prediction campaigns
- **Stage II: Experiments on Unsteady Loading in Waves, March 2025 – 2026**
  Wave characterization
  Wave experiments covering **20 wave conditions**
  Frequency (Hz): 0.225, 0.25, 0.3, 0.35, 0.4, 0.45, 0.5
  Amplitude (m): 0.025, 0.035, 0.05, 0.075, 0.1
  Additional steady flow **experiments with yawed turbine**
  Total of **175 tests** performed
  Blind prediction campaigns and data dissemination

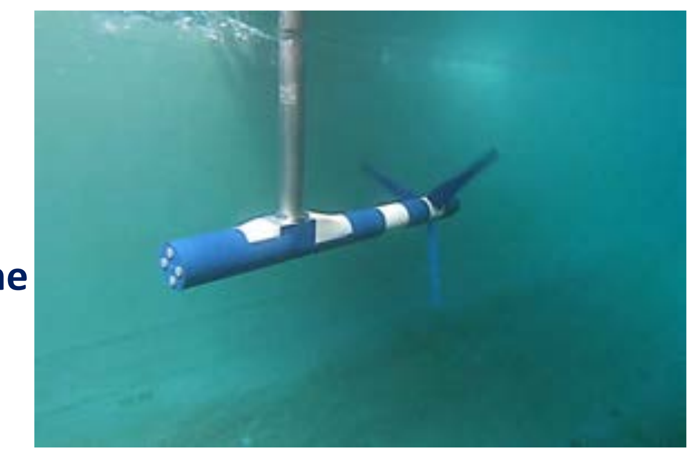

Turbine Instrumentation and Experimental Facilities

- **Turbine Instrumentation**
  1.6m diameter rotor / 0.2m diameter nacelle
  Instrumented blades with strain gauges, integrated **root bending sensors** (100 strain gauges)
  Torque and Thrust transducers, **Shaft rotary encoder** for speed and position
- **QinetiQ Towing Tank Facility (270m (L) x 12.2m (W) x 5.4m (D))**
  Rake of 5-hole **Barnacle Probes** developed by Bath.
  Solid Wave Gauges and **Ultrasonic Probes** are mounted on the carriage.
  Tow speed 1m/s, Tow length approx. 150m, Settling time ~15mins

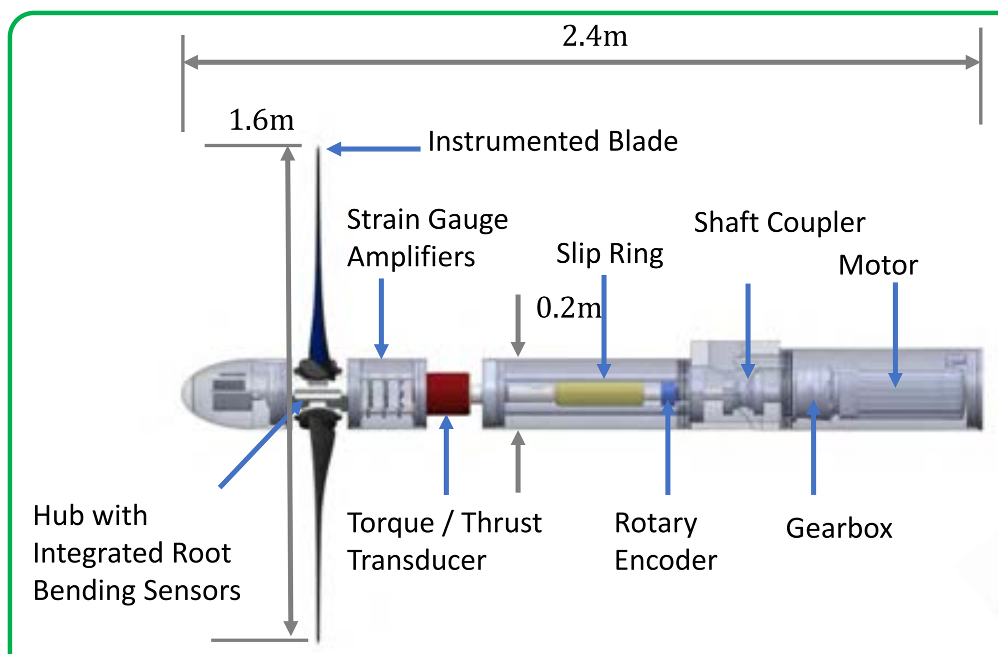

Highly Instrumented Turbine

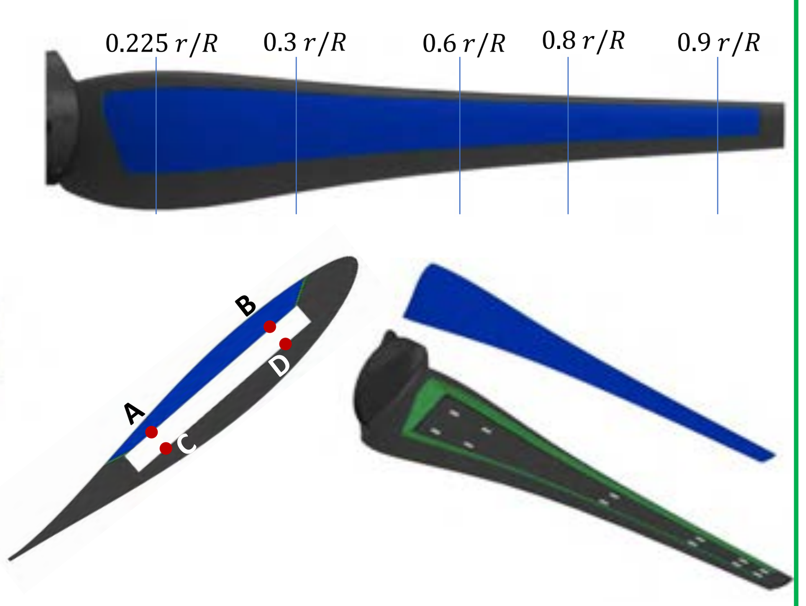

Baldes Instrumented with Strain Gauges

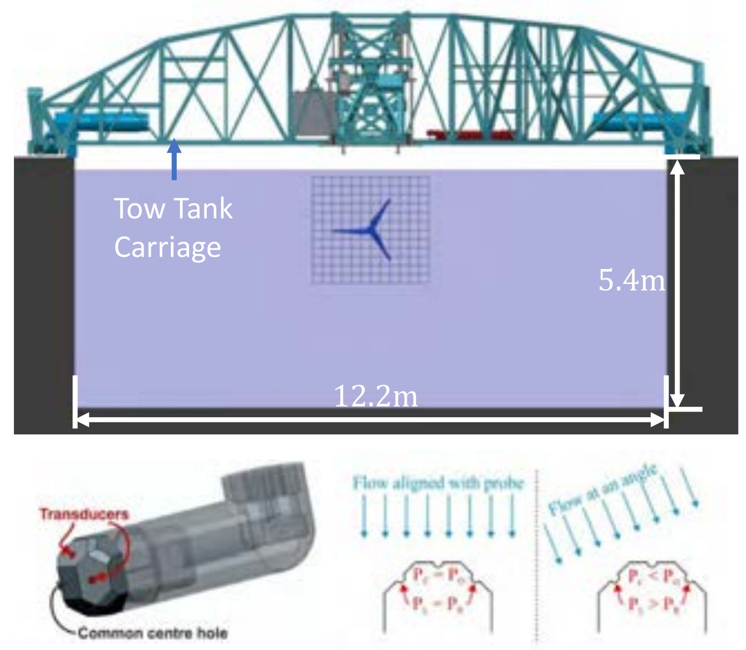

5-Hole Unsteady Barnacle Probe

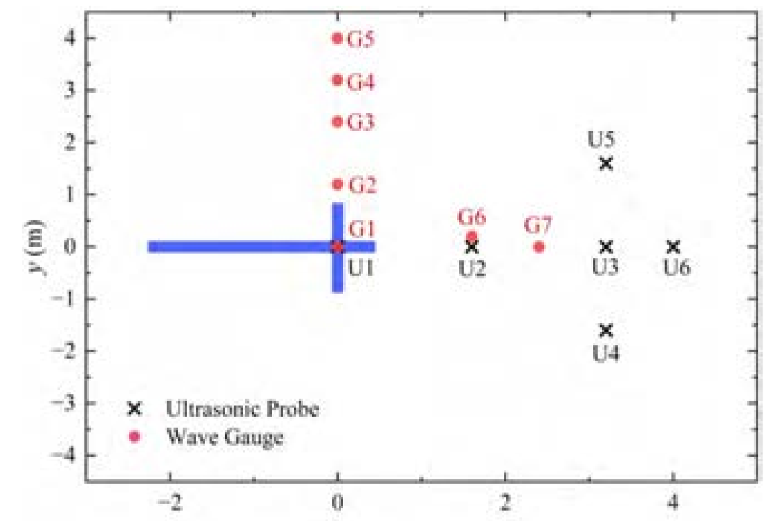

Wave Gauge and Ultrasonic Probe Locations

Wave Data Analysis

- **Wave Elevation Comparison: With and Without Turbine**
  Wave amplitudes remain consistent in clean wave cycles. The dominant wave frequencies are highly stable, with minimal variation observed between tests.
  The installed turbine has negligible influence on the energy content of both the incident and reflected wave components, but it introduces a slight increase in energy at higher frequencies, due to flow disturbances or turbulence induced by the rotating turbine.

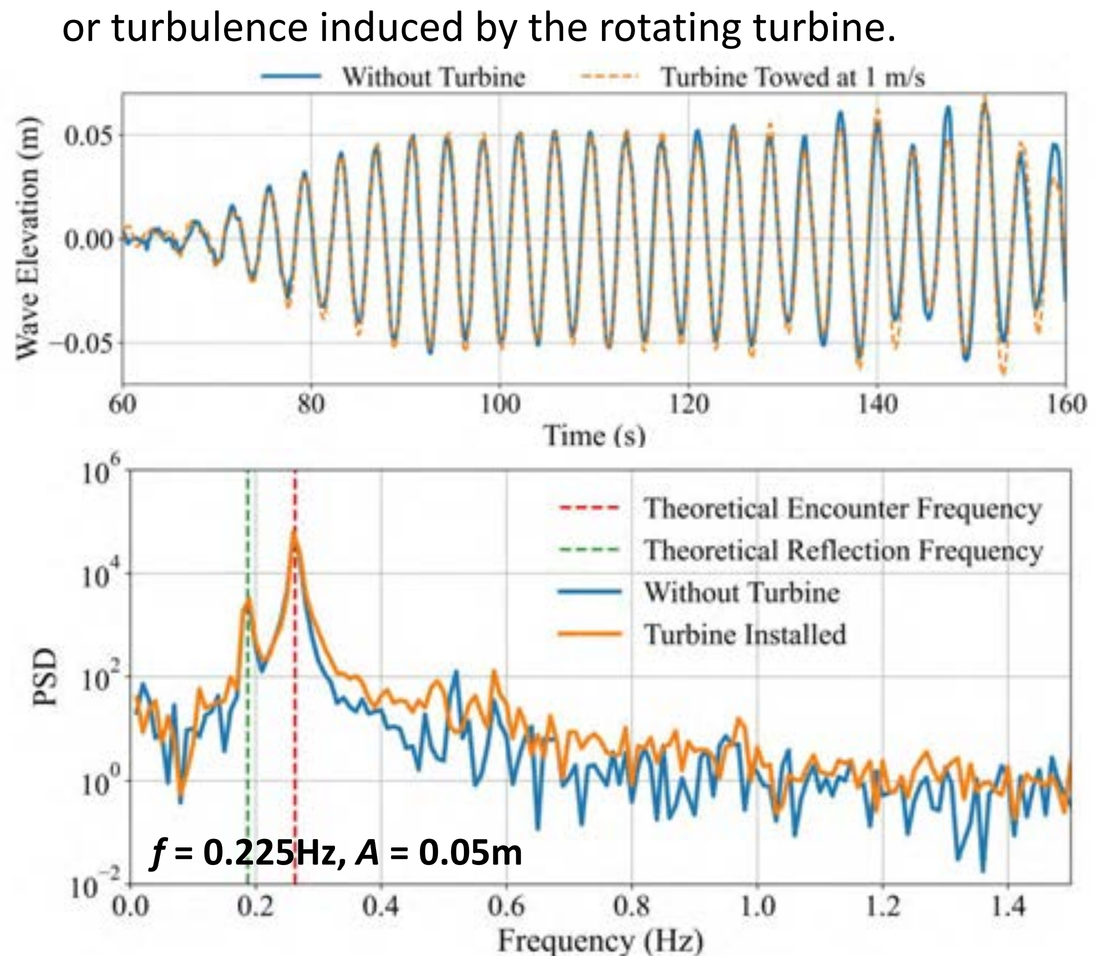

Impact of the Turbine on Wave Field

- **Reliability of Wave Elevation Measurements**
  Wave Gauge (WG) and the Ultrasonic Probe (UP) show excellent agreement in both amplitude and phase.
  The overall spectral shape is consistent, and UP signal shows slightly more noise at higher frequencies.
  These results confirm the reliability and consistency of wave elevation measurements.
  The energy of the reflected waves is significantly lower than that of the incident waves in this case.

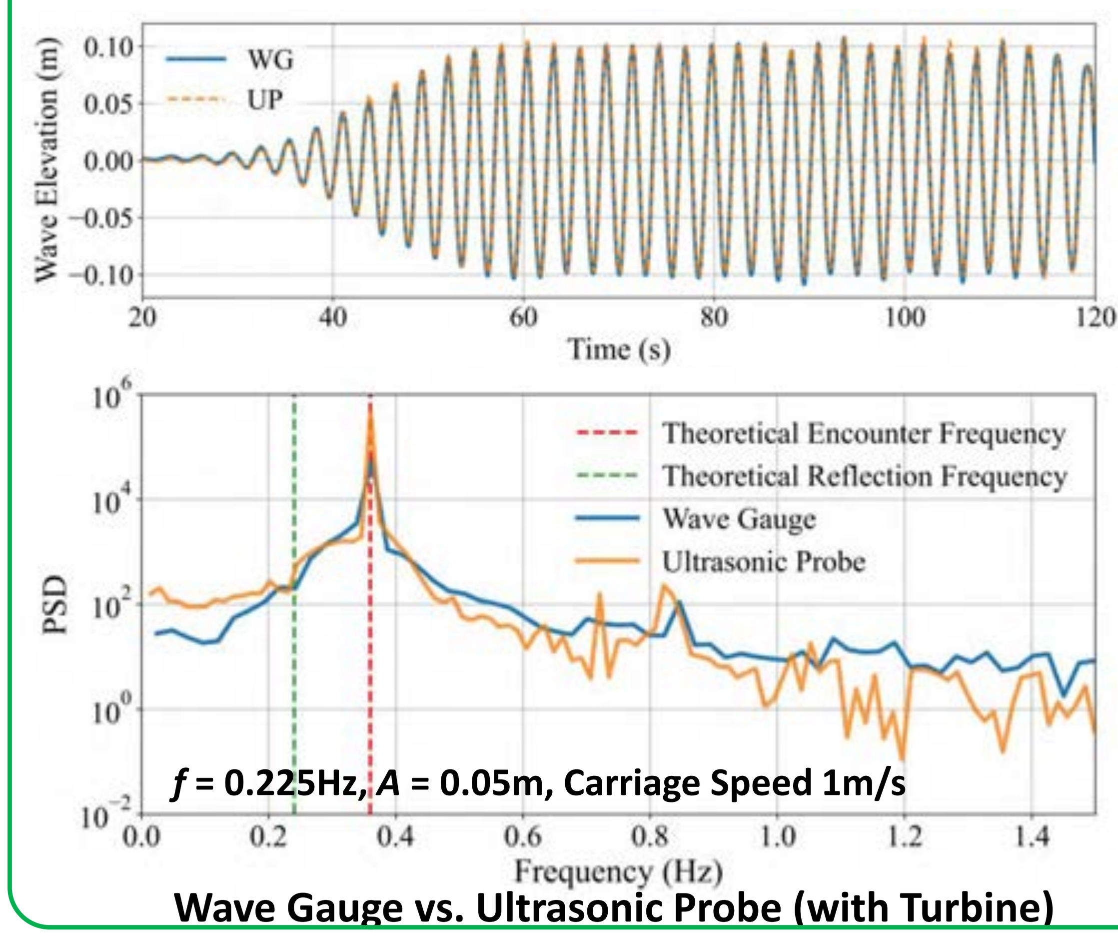

Wave Gauge vs. Ultrasonic Probe (with Turbine)

- **Wave Repeatability in Turbine Experiments**
  Multiple test repeats show nearly identical waveforms.
  The amplitude envelopes of all four tests are very closely aligned over the entire test duration. Slight variations may be observed, but they remain within a small range (~mm scale).
  These results confirm excellent repeatability in wave generation and measurement, even with the turbine installed.

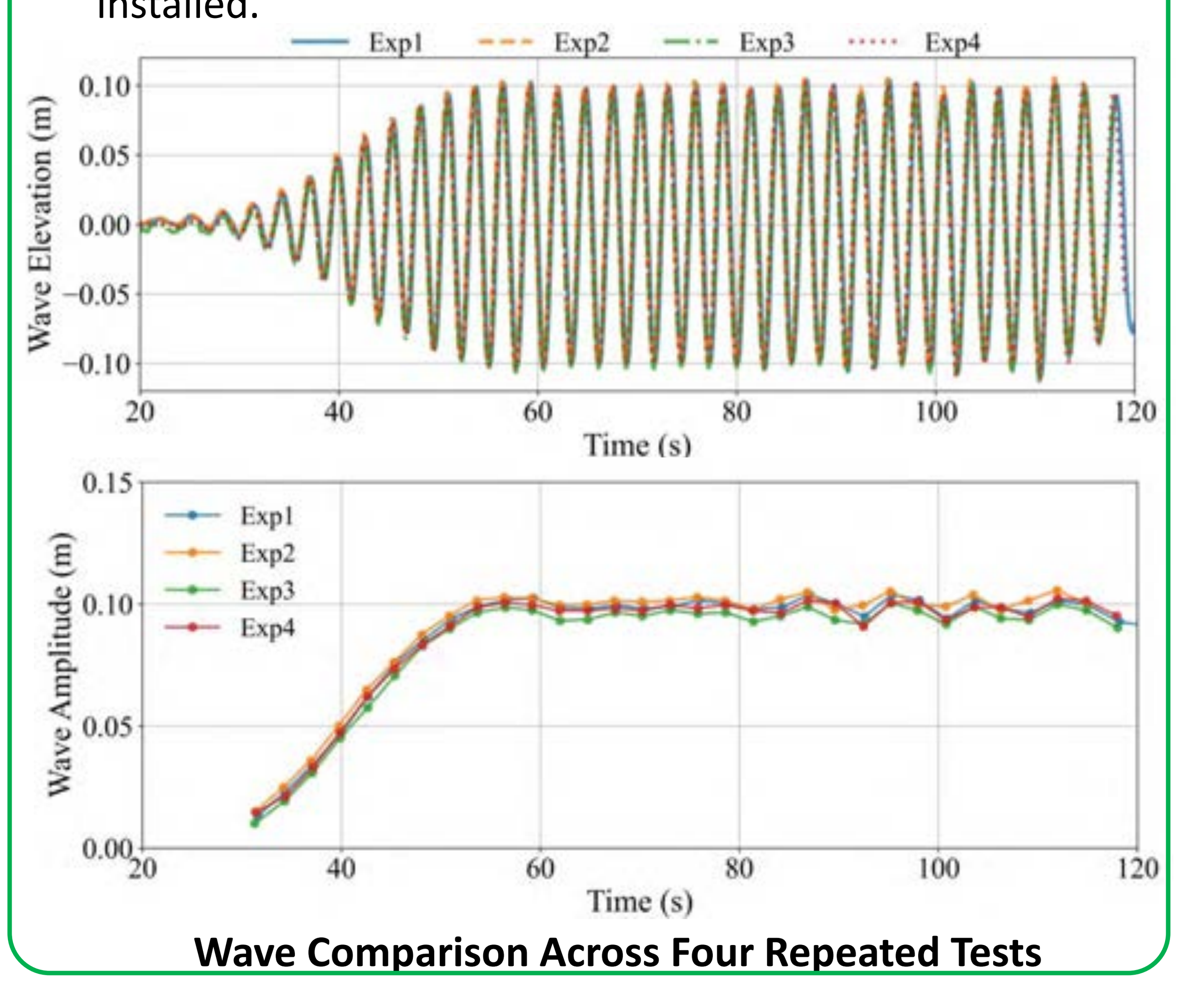

Wave Comparison Across Four Repeated Tests

- **Selection of stable wave cycles**
  Incident wave data analyzed for each case.
  Cycle-to-cycle variations in wave elevation and turbine torque of **less than 2%** result in **5-12 wave cycles** being identified for further analysis.
  The useful wave cycles identified from each test are combined with those obtained from repeated tests under the same conditions.

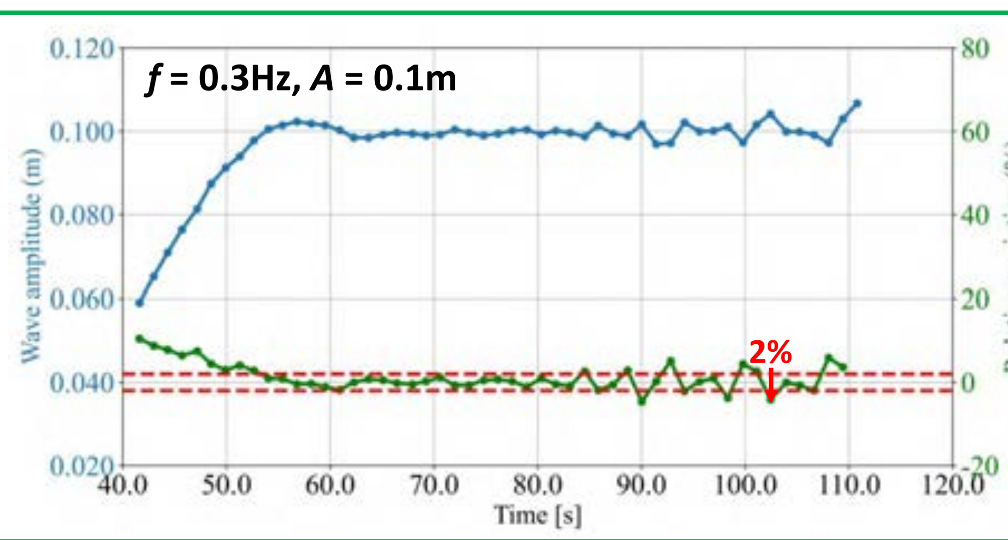

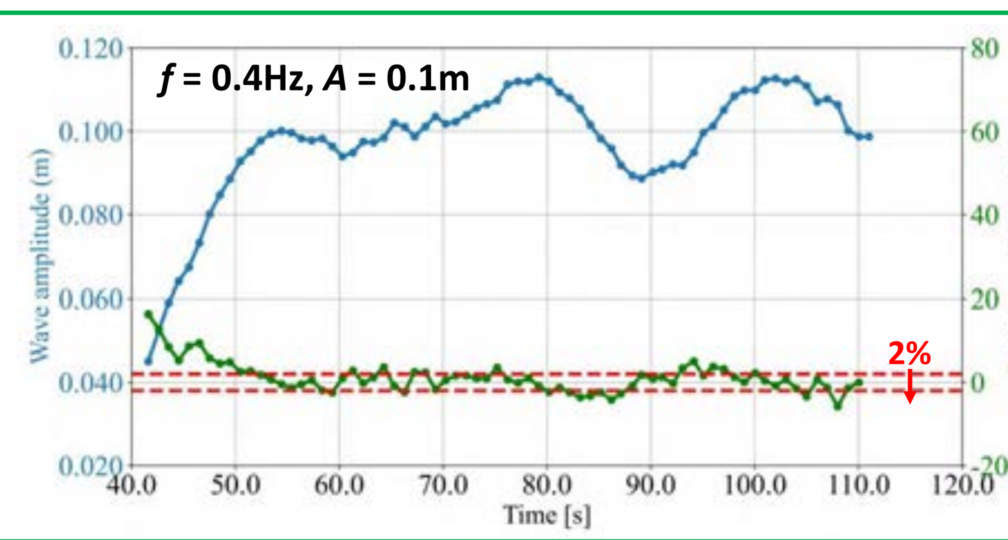

Acknowledgements

We would like to acknowledge the financial support of SuperGen ORE Hub EP/Y016297/1, RHJW's EPSRC Advanced Fellowship EP/R007322/1, and EPSRC Co-Tide EP/X03903X/1. We would also like to thank Xiaosheng Chen, Federico Zilic de Arcos, Timothy Rafferty, Thomas Clarke, Huw Edwards, Martina Lomele, Dylan Green, and Sarah Hudson for their valuable assistance throughout the experiments.

Tidal Resource Assessment for the Co-Tide Project

Fei He, Christopher Vogel, Thomas Adcock

INTRODUCTION

- Much of the global tidal current energy resource lies in the accelerated flows along narrow tidal channels that have the potential to produce 10–1000s of MW of electricity.
- However, realising 100MW of a channel's potential is much more complex than just installing 100 1-MW turbines and, more importantly, not all the tidal energy can be extracted due to different real constraints!
- Tidal Resource Assessment evaluates the potential of a tidal site for energy extraction using turbines arrays, providing insights into the feasibility and value of planning and deploying tidal energy projects.
- **The aim is to develop an analytical framework for quick tidal resource assessment.**

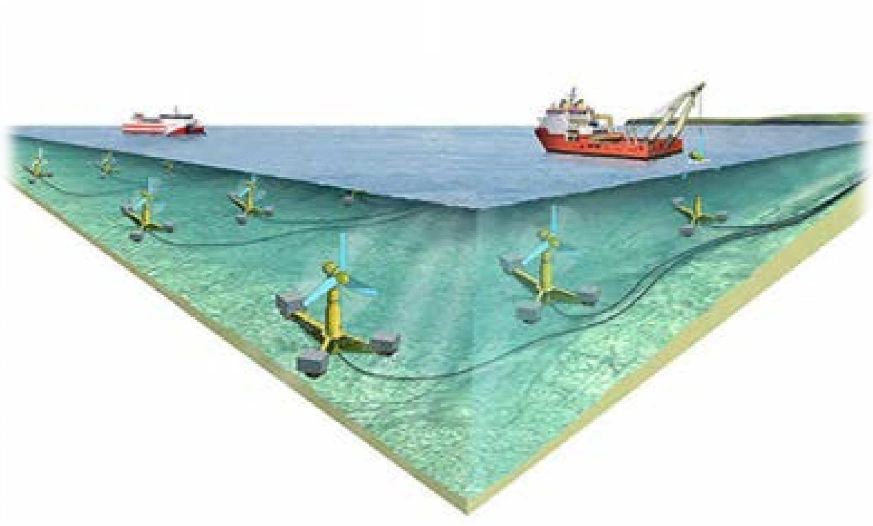

METHODOLOGY

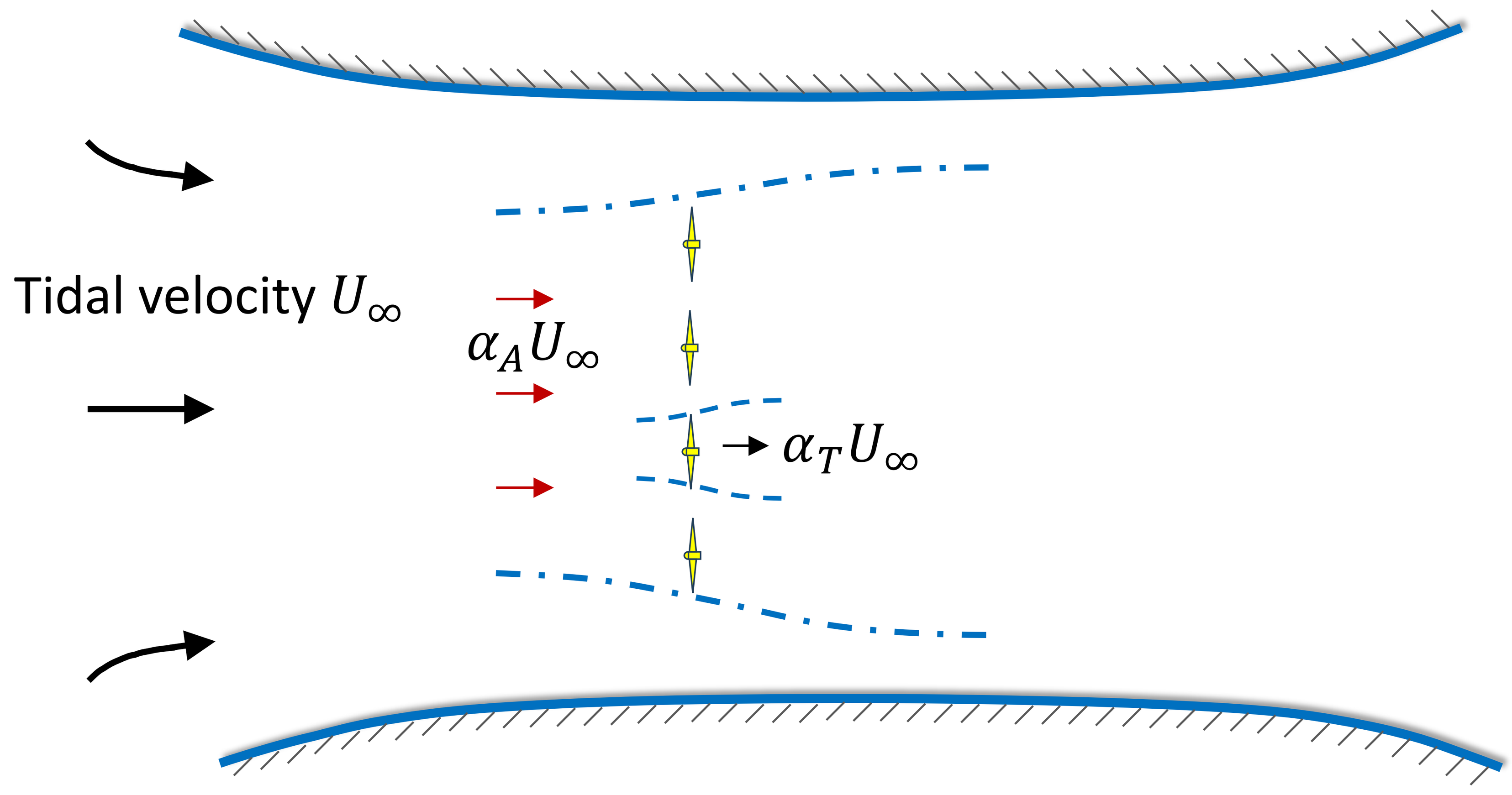

(a) Top-down view of a row of turbines in a tidal channel

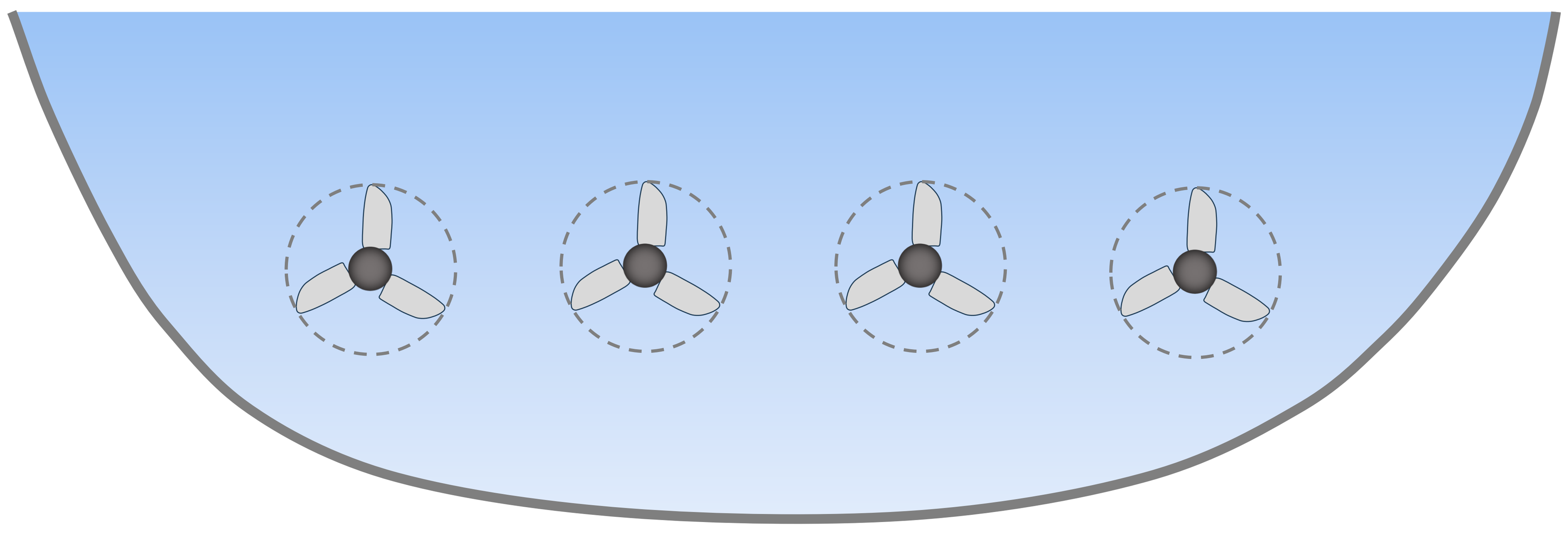

(b) Cross-sectional view of tidal turbines

Scale separation[1]

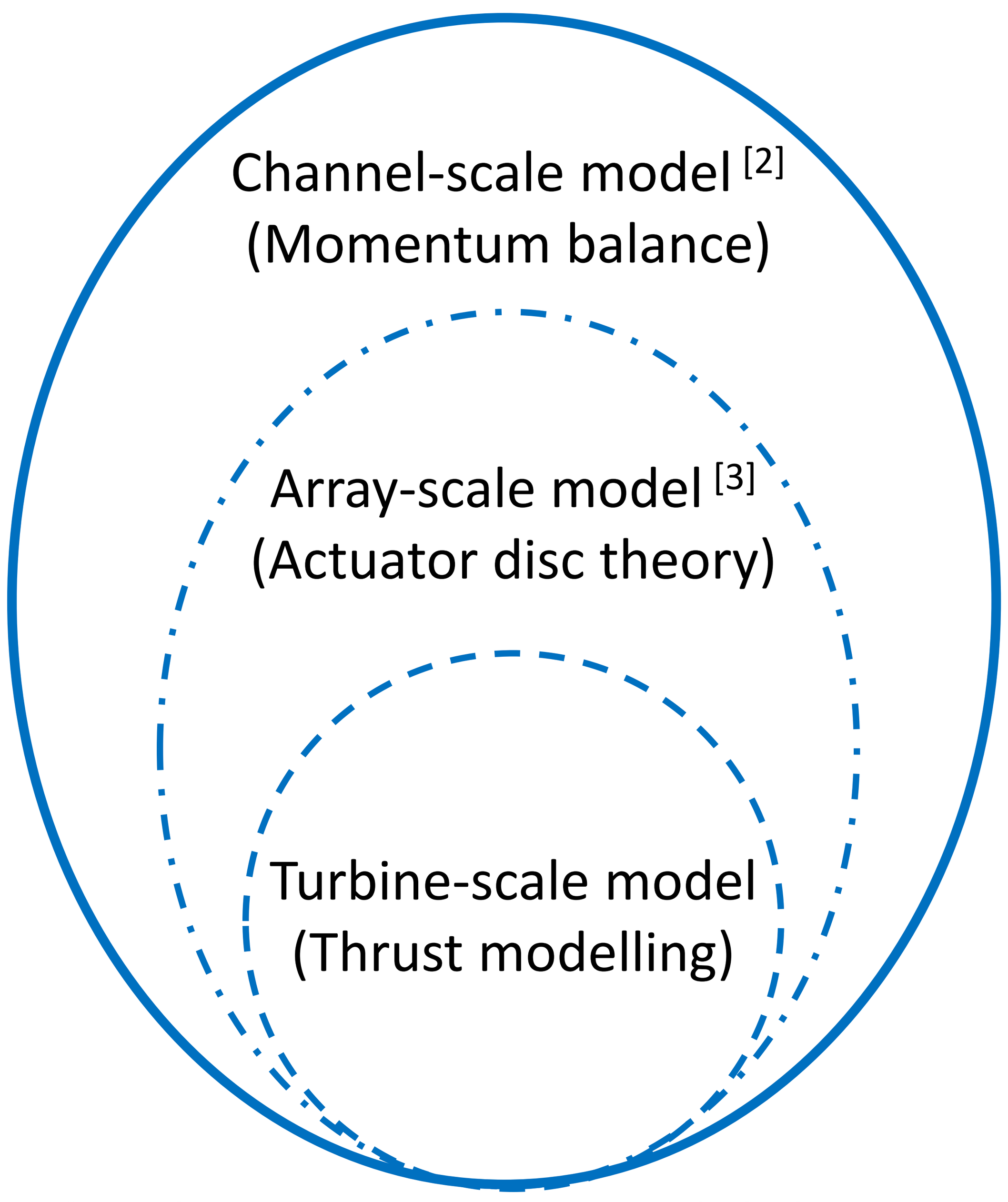

(c) Using idea of scale separation to model the system separately at different scales and then couple together through net thrust

RESULT

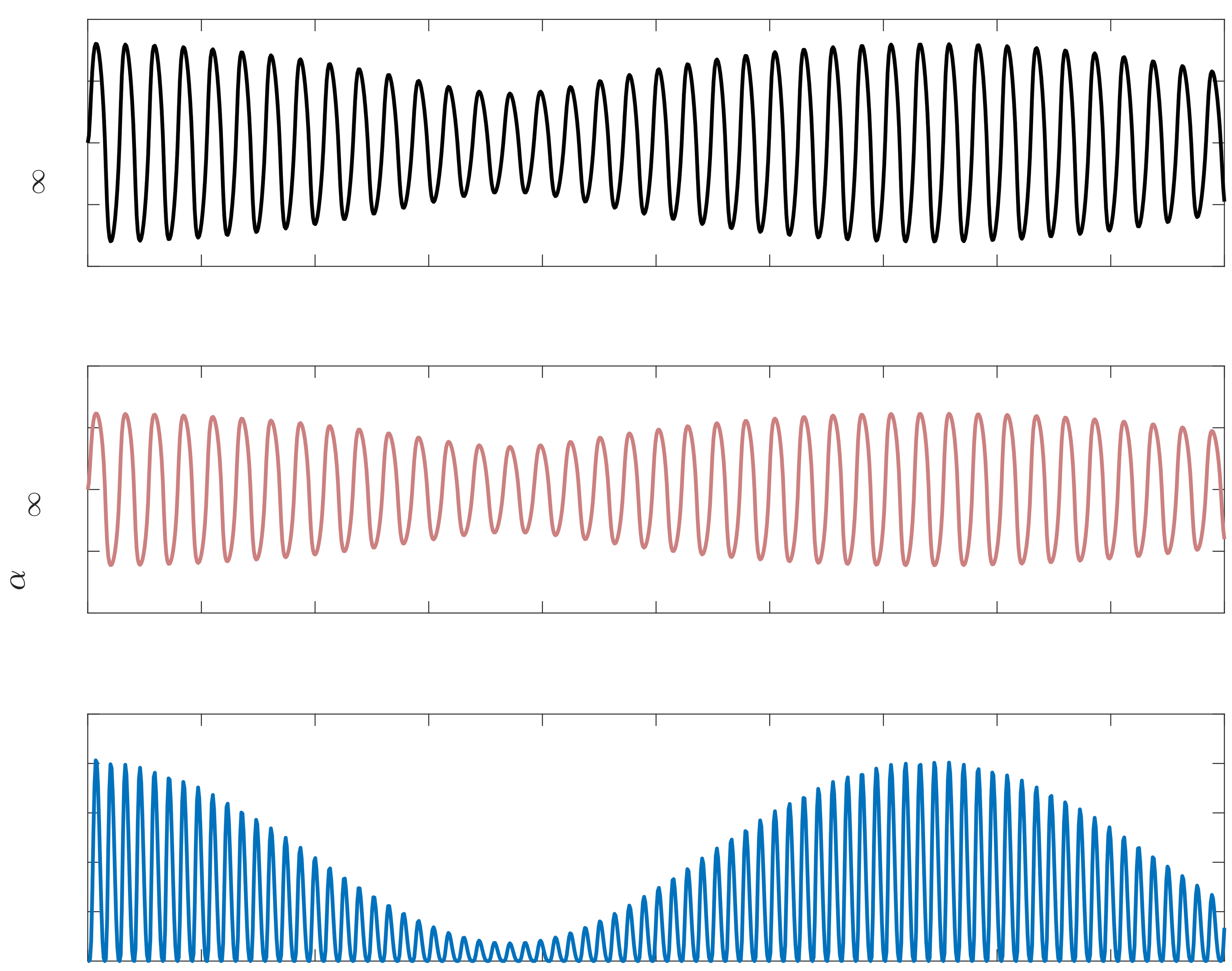

FUTURE WORK

- How does the 1-D analytical framework compare with 2-D numerical simulations?
- Can this framework be extended to an array of multiple rows of turbines and different channel geometries?
- Does arrangement of tidal turbines matter for power generation?

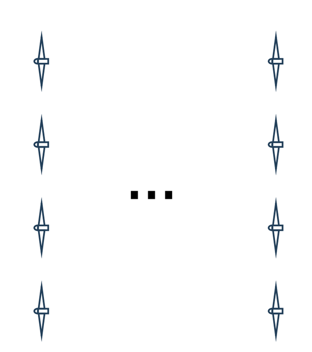

(a) Inline array

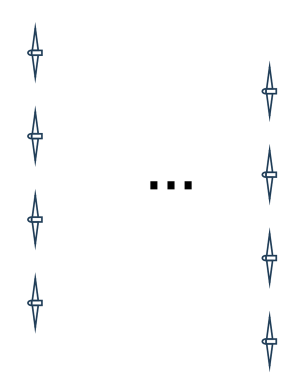

(b) Staggered array

Google Scholar

REFERENCE

[1] Nishino, T., & Willden, R. H. (2012). The efficiency of an array of tidal turbines partially blocking a wide channel.
[2] Garrett, C., & Cummins, P. (2005). The power potential of tidal currents in channels.
[3] Garrett, C., & Cummins, P. (2007). The efficiency of a turbine in a tidal channel.
[4] Image Credit: Andrey Armyagov/Shutterstock.com
[5] Image Credit: https://www.power-technology.com/projects/pentland-firth-tidal-power-plant-scotland

ACKNOWLEDGEMENT

EPSRC Engineering and Physical Sciences Research Council
Department of Engineering Science
Co-Tide Project

Distributed Optical Fibre Sensing for Monitoring of Large Bending Deformations of Subsea Power Cables

Dr. Madhubhashitha Herath[1] and Prof. James Gilbert[2]
[1] School of Engineering, Faculty of Science and Engineering, University of Hull, Hull, United Kingdom
[2] Energy and Environment Institute, University of Hull, Hull, United Kingdom

Introduction

Subsea power cables are critical assets for offshore renewable energy systems. Failures of subsea power cables lead to significant costs due to long outage times and high repair expenses [1]. The cable failures due to external mechanical loads during transportation, installation and operation are critical and condition monitoring of the cables can benefit to prevent unexpected damages [2]. This research intends to monitor the large bending deformations of the power cables using embedded optical fibre sensors.

Methods

In the initial stage of the research, a 6 m long and 40 mm diameter Polybutylene conduit (hollow) was used for experimental analysis of the bending behaviours of long cylindrical members subjected to large bending deformations. 125 μm diameter single mode optical fibres were attached to the outer surface of the Polybutylene conduit in two configurations, in parallel to the axis of the conduit and in helical windings around the conduit.

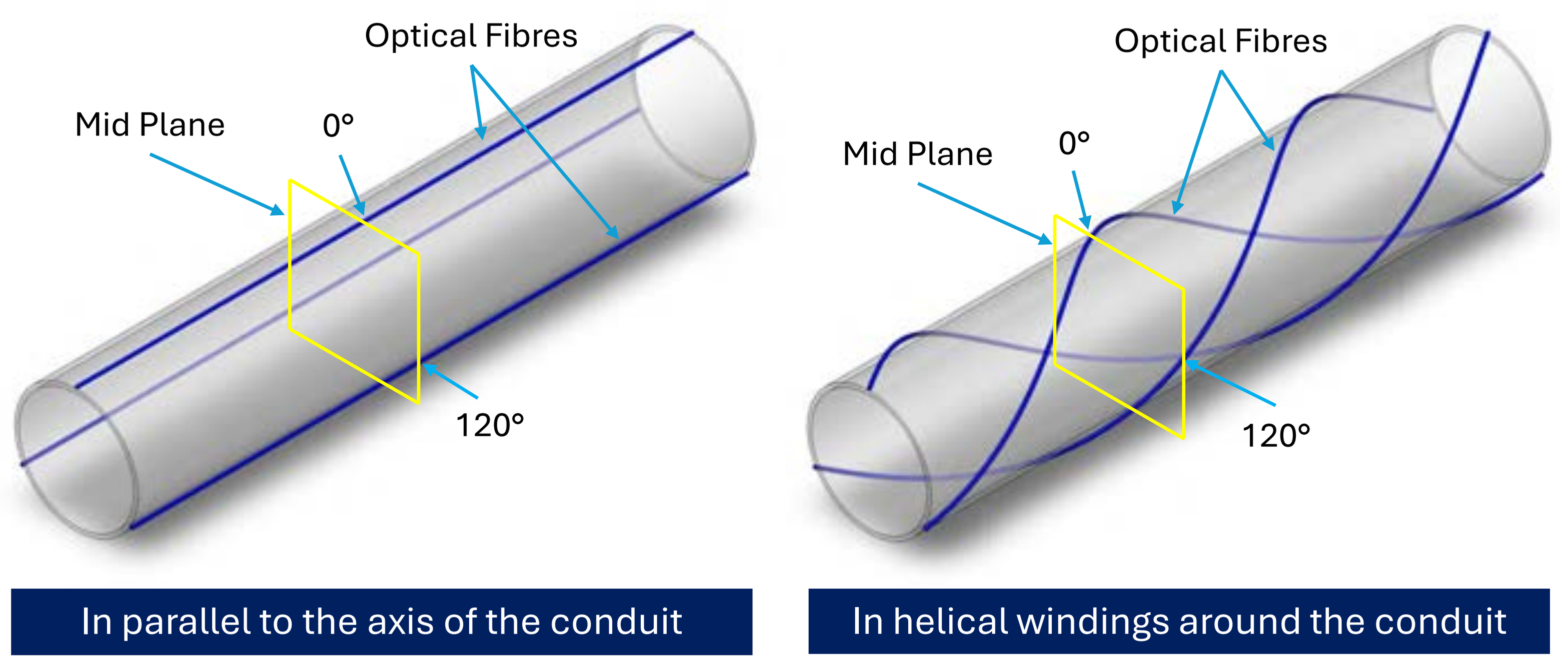

Figure 1: Configurations of the optical fibre attached to the outer surface of the Polybutylene conduit

A custom-made test rig was used to bend the conduit under 3-point bending and circular bending arrangements. The span for all the tests was 5 m. Both tests were conducted for five levels of deformations. The strain changes were measured using a VIAVI FTH-9000 Brillouin optical time domain reflectometer (BOTDR).

Table 1: Deformation magnitude levels of the bending tests

Midspan Displacements (MSD) of the 3 Point Bending Test	1.34 m	0.76 m	0.55 m	0.43 m	0.35 m
Bending Radiuses (BR) of the Circular Bending Test	3 m	4.5 m	6 m	7.5 m	9 m

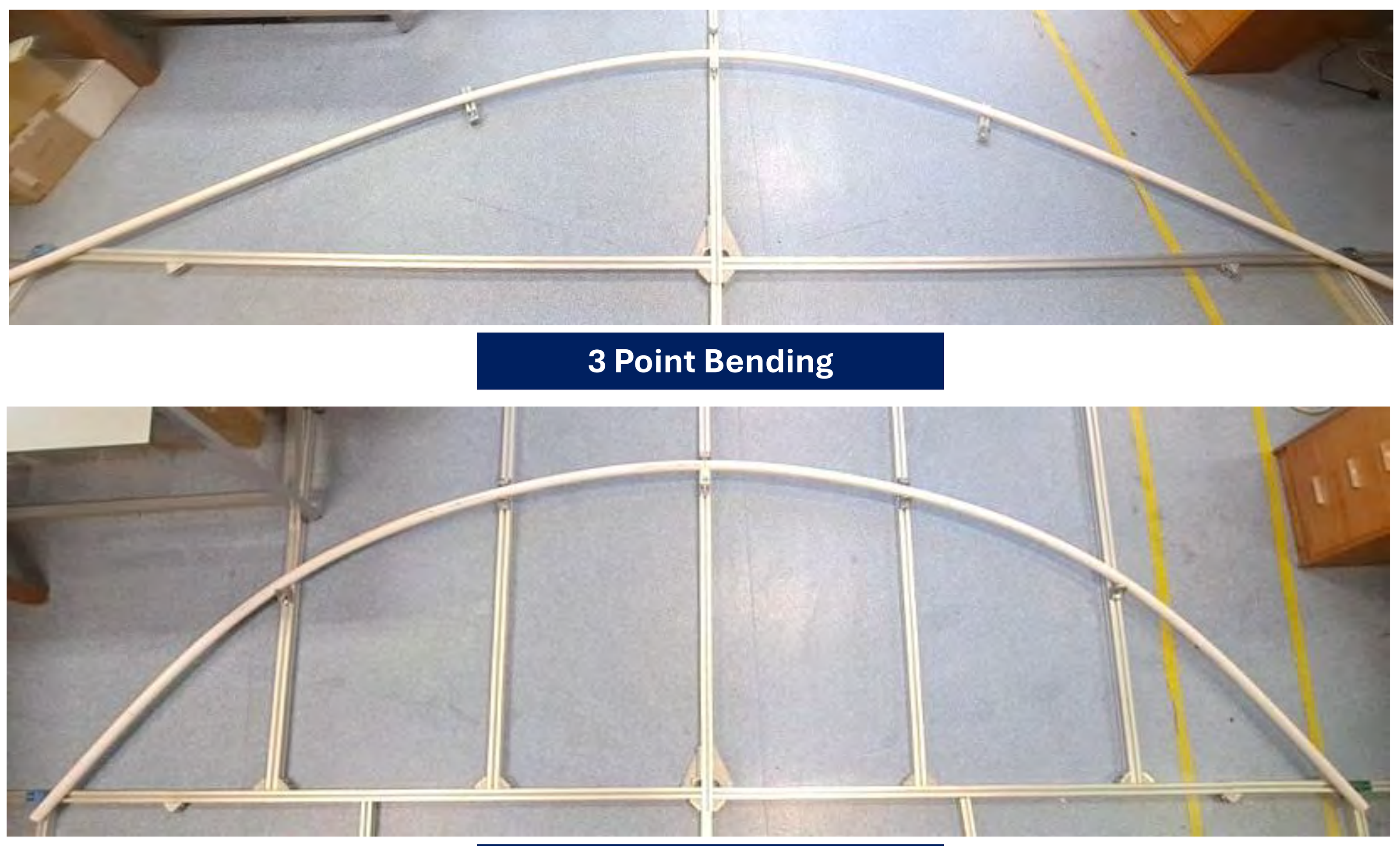

Figure 2: Bending configurations on the test rig

A series of 3 point bending tests were conducted to study the bending direction by changing the mid plane crossing location of the optical fibre sensor. The top dead centre of the mid plane was considered as 0° and CW rotational angles of 30°, 60°, 90°, 120°, 150° and 180° were considered for the experiment.

Results

The strain values along the fibre were proportional to the magnitude of the deformation. The strain patterns distinguish between the shapes of a 3-point bend and a circular bend. The strain measured by the optical fibre sensors at different mid plane crossing locations showed proportional magnitudes of tension and compression relative to the direction of the measured bending.

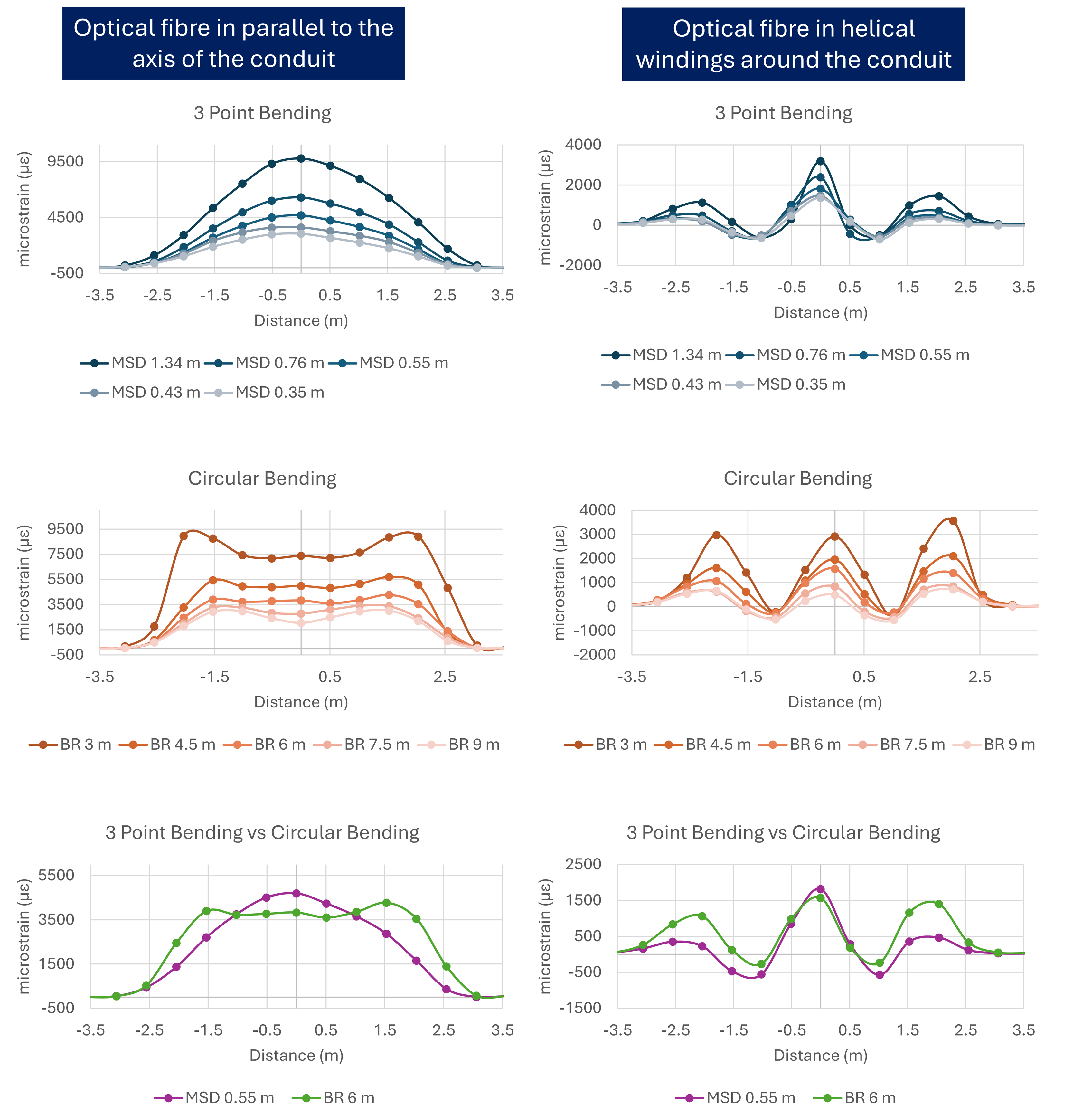

Figure 3: Strain data along the Polybutylene conduit under different magnitudes of the deformation.

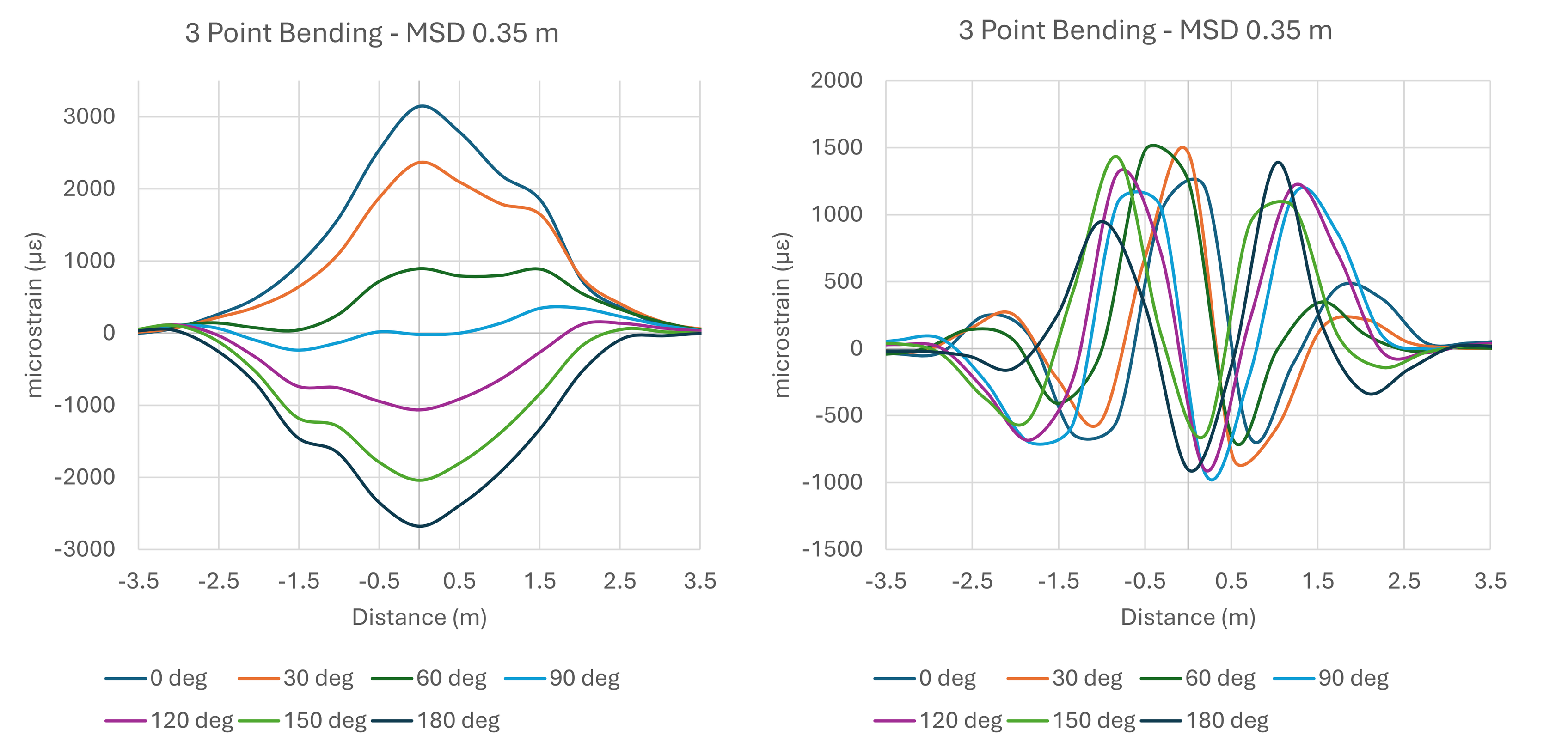

Figure 4: Strain data along the Polybutylene conduit measured by the optical fibre sensors with different mid plane crossing locations denoted by the rotational angle.

Conclusion and Future Directions

Employing three or more optical fibre sensors around a cylindrical member in parallel or helical configurations can analysis the magnitude and direction of the member subjected to a large bending deformation. Optical fibre embedded cylindrical sensing cables are propose to be integrated within three-core power cables to monitor and predict the bending throughout the different stages of their lifecycle.

References

1. Song, Y., et al., Online multi-parameter sensing and condition assessment technology for power cables: A review. Electric Power Systems Research, 2022. 210: p. 108140.
2. Cerik, B.C. and L. Huang, Recent advances in mechanical analysis and design of dynamic power cables for floating offshore wind turbines. Ocean Engineering, 2024. 311: p. 118810.

UNIVERSITY of HULL
UKRI Engineering and Physical Sciences Research Council
Supergen Offshore Renewable Energy

Data-Driven 1D Design Model for Monopile Foundations in Layered Soils

Ioannis Kamas, Harvey Burd & Byron Byrne
Department of Engineering Science, University of Oxford
Ioannis.kamas@eng.ox.ac.uk

Supergen Offshore Renewable Energy | Ørsted | University of Oxford

1. Introduction

The design of **monopile foundations** for offshore wind turbines (OWTs) is governed by **lateral loading** from wind, waves, and currents, generating large overturning moments.
Conventional design approaches model the monopile as a **1D beam with non-linear Winkler springs** but often **neglect interactions between adjacent soil layers in layered soils.**
Soil stratification significantly affects lateral response, and ignoring it can lead to inaccurate, conservative, or even unsafe designs.


Monopile Foundation [4]

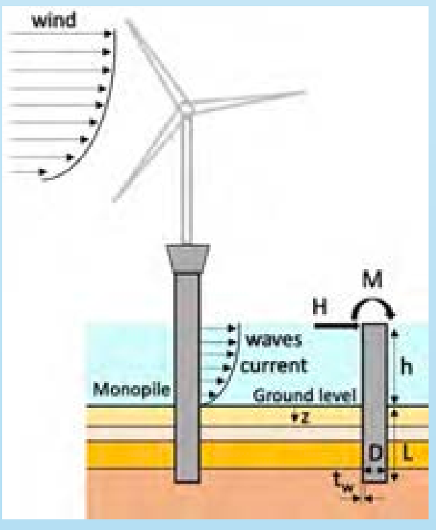

Loads applied on the OWT substructure

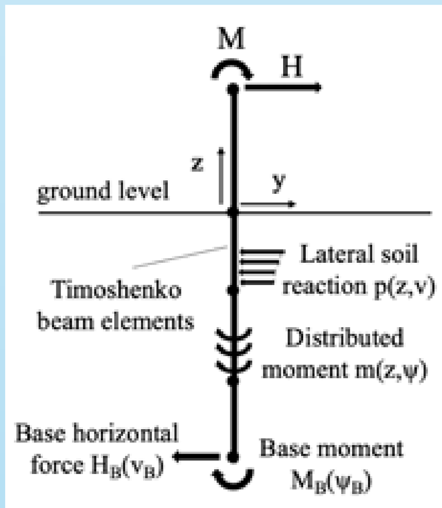

Pisa 1D FE Framework [2]

2. Objectives

Develop a **1D model** to predict the **monotonic lateral response** of monopiles in **layered soils**.
Calibrate the 1D model using **soil reaction curve data** from layered soil analyses
Capture **layer-to-layer interactions** and enable **rapid site-wide predictions**.
Account for **variations in soil parameters** (e.g., strength, stiffness) and **layer thickness** across the wind farm.

Key stages followed to develop a data-driven 1D design model for layered soils

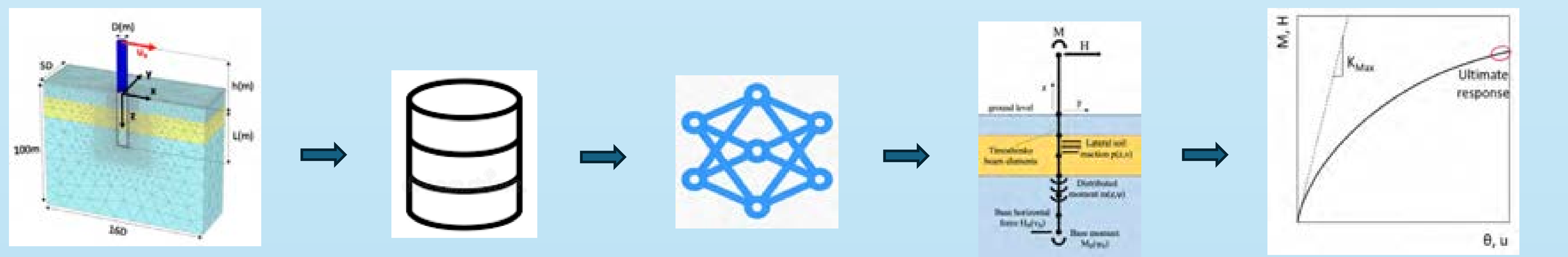

Calibration 3D FEA → **Soil reaction curves database** → **Machine learning model** → **PISA 1D framework** → **Prediction: Backbone curve**

3. Site Investigation

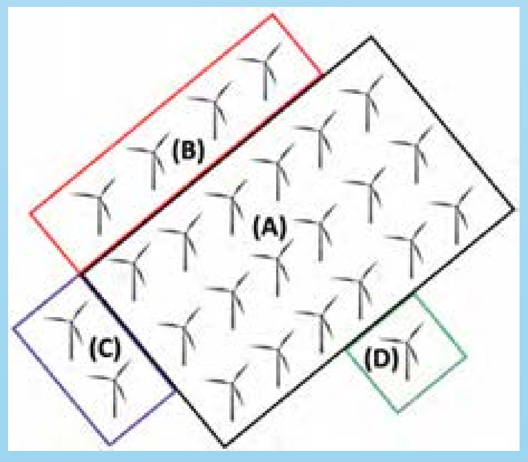

Identify OWT locations with similar soil configuration

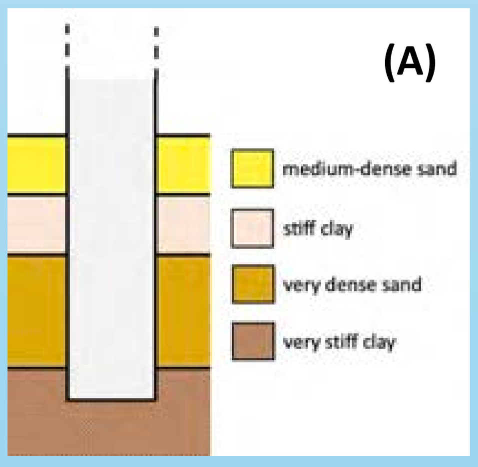

Analysed layered soil configuration

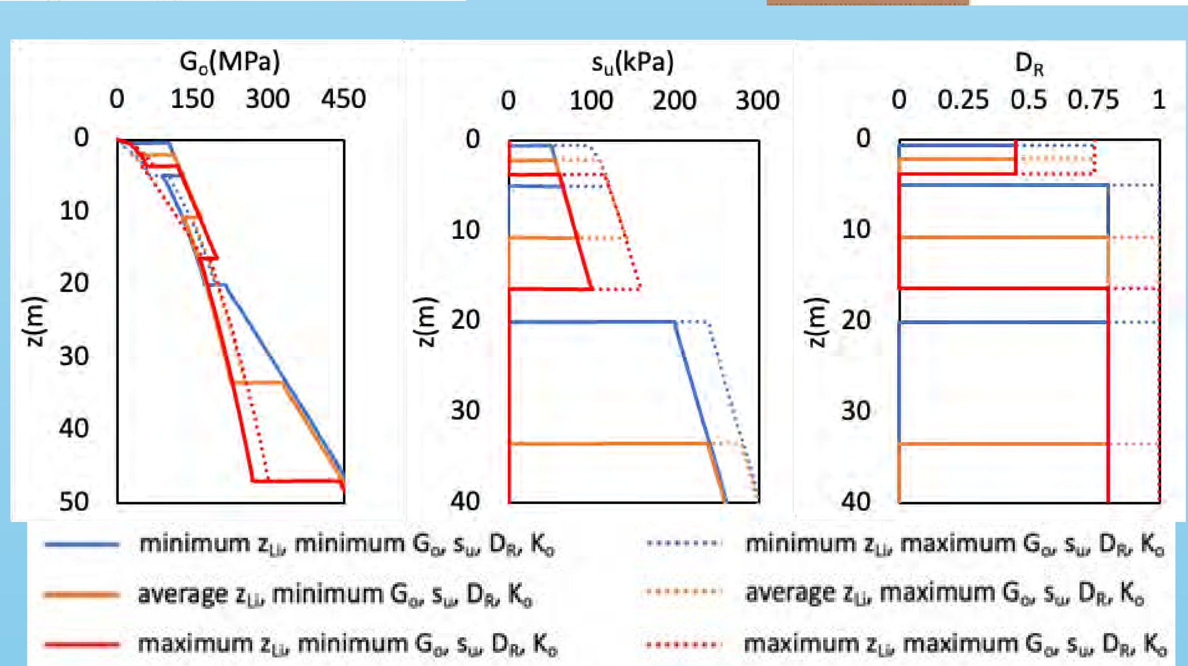

Identify site-wise soil parameters variation

4. 3D FEA Calibration Analyses

Current Study Setup:
Software: PLAXIS 3D [1]
Clay Model: NGI-ADP
Sand Model: HS-Small

Identification & Calibration Process:
Parametrise the problem to reduce the number of required 3D FEA.
Define a calibration space to capture spatial variability across OWF:
Pile geometry
Soil parameters variation
Layer thickness range

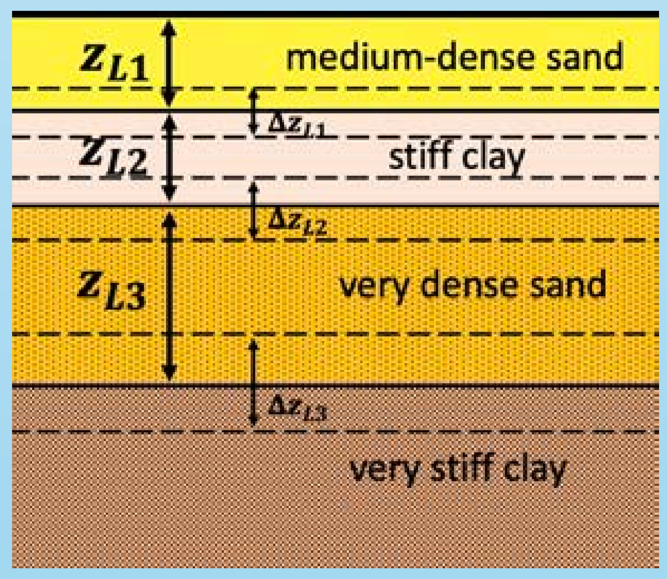

Site Wise Variation in Layered Thickness for Configuration A

5. Soil Reaction Curve Database

For each calibration 3D FEA, the following soil reaction components are extracted:
1) Distributed lateral reaction **2)** Distributed moment **3)** Base horizontal force **4)** Base moment

Soil reaction curves are normalised to a dimensionless form

Spline-Based Representation
Normalised curves follow: $\bar{y} = g(\bar{u})$
where: $\bar{u}$ = normalised displacement/rotation, $\bar{y}$ = normalised load/moment
Each curve is defined by 8 knot points, forming the basis of the data-driven model

knot-point parameters										
	$\bar{u}$	0	0.00004	0.0001	0.001	0.004	0.01	0.03	0.06	0.1
	$\bar{y}$	0	$\bar{y}_1$	$\bar{y}_2$	$\bar{y}_3$	$\bar{y}_4$	$\bar{y}_5$	$\bar{y}_6$	$\bar{y}_7$	$\bar{y}_8$

A PCHIP interpolation scheme [3] ensures smooth transitions between knots.

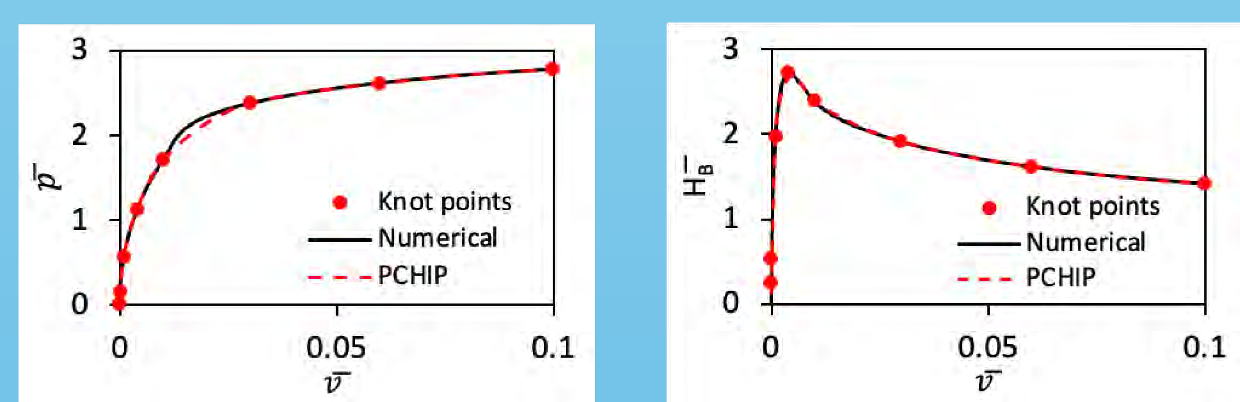

PCHIP spline soil reaction curve for use in the data-driven 1D design model

6. Training Features

(L/D): pile slenderness

(z/L): depth variation

(G_o/σ'_v), (s_u/σ'_v), (D_R): soil parameters

(z_{L1}/L): layer thickness

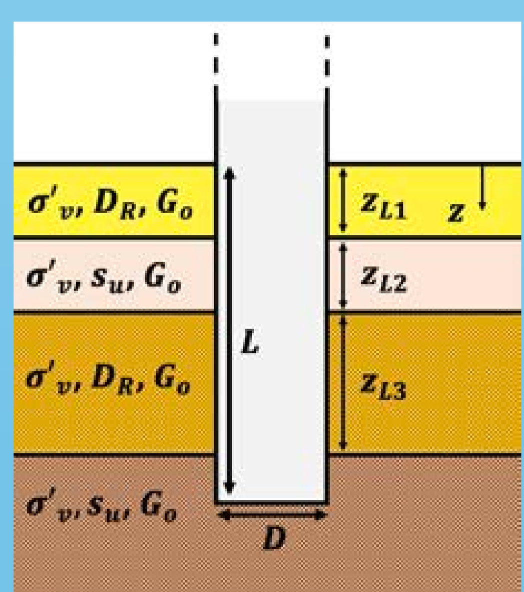

Layered Soil Configuration A

7. Machine Learning Model

A separate Gaussian process regression (GPR) model [5] is trained for each knot point in the spline.

GPR uses a zero mean function and a Matérn (v = 5/2) + White Noise kernel.

The dataset for each knot point is randomly split, with 80% used for training and 20% reserved for testing

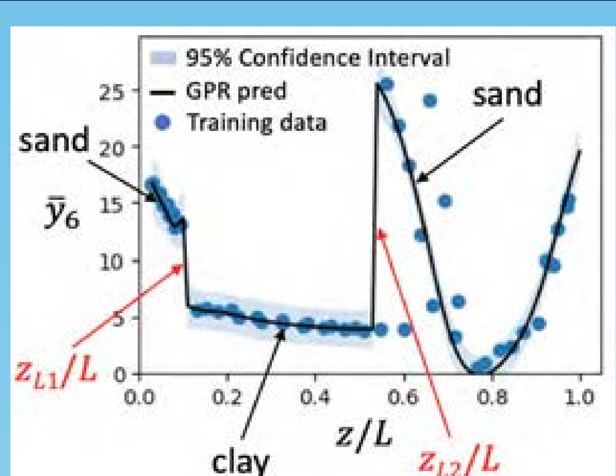

Example GPR outputs

8. Design Scenario – 1D Model Predictions

1D model tested on unseen conditions:
Pile geometries
Soil parameters
Layer thicknesses

1D model prediction
Ground-level response:
Load–displacement
Moment–rotation
Bending moments profile

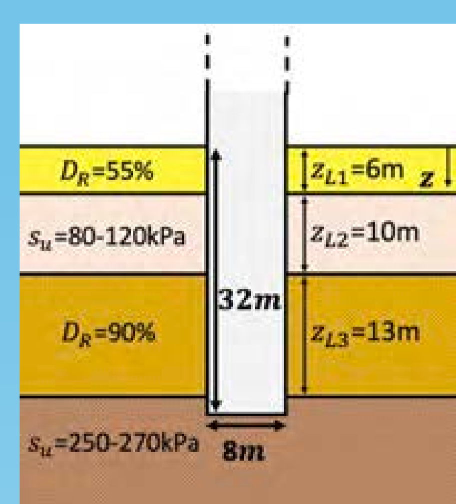

Design scenario

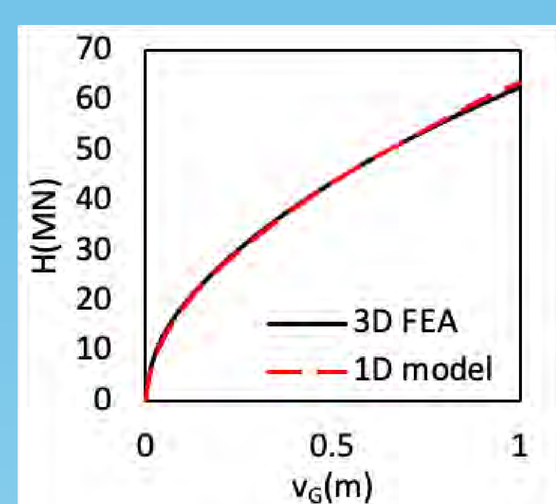

Load-displacement response

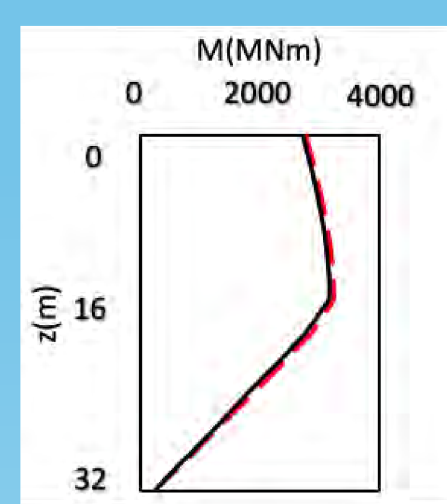

Bending moments profile

✓ Validated against 3D FEA – close agreement observed

REFERENCES:
[1] Brinkgreve, R.B.J., Kumarswamy, S. and Swolfs, W.M. (2018). Plaxis 2018. *Plaxis bv Delft*, the Netherlands.
[2] Byrne, B. W., McAdam, R. A., Burd, H.J., Beuckelaers, W. J. A., Gavin, K. G., Houlsby, G.T., Igoe, D. J. P., Jardine, R. J., Martin, C.M., Wood, A. M., Potts, D. M., Gretlund, J. S., Taborda, D. M. G., and Zdravković L. (2020a). Monotonic laterally loaded pile testing in a stiff glacial clay till at Cowden. *Géotechnique* 70, No. 11, 970–985.
[3] Fritsch, F.N. and Carlson, R.E. (1980). Monotone Piecewise Cubic Interpolation, SIAM. *Journal on Numerical Analysis*, 17, pp. 238-246.
[4] Kallehave, D., Byrne, B.W., LeBlanc Thilsted, C. and Mikkelsen, K.K. (2015). Optimization of monopiles for offshore wind turbines. Philosophical Transactions of the Royal Society A: Mathematical, Physical and Engineering Sciences, 373(2035).

Intelligent Fault-Tolerant Control of Offshore Wind Turbines via Deep Reinforcement Learning

Dr. Hongyang Dong[1] and Dr. Shuyue Lin[2]

Abstract

Methodology

➢

➢

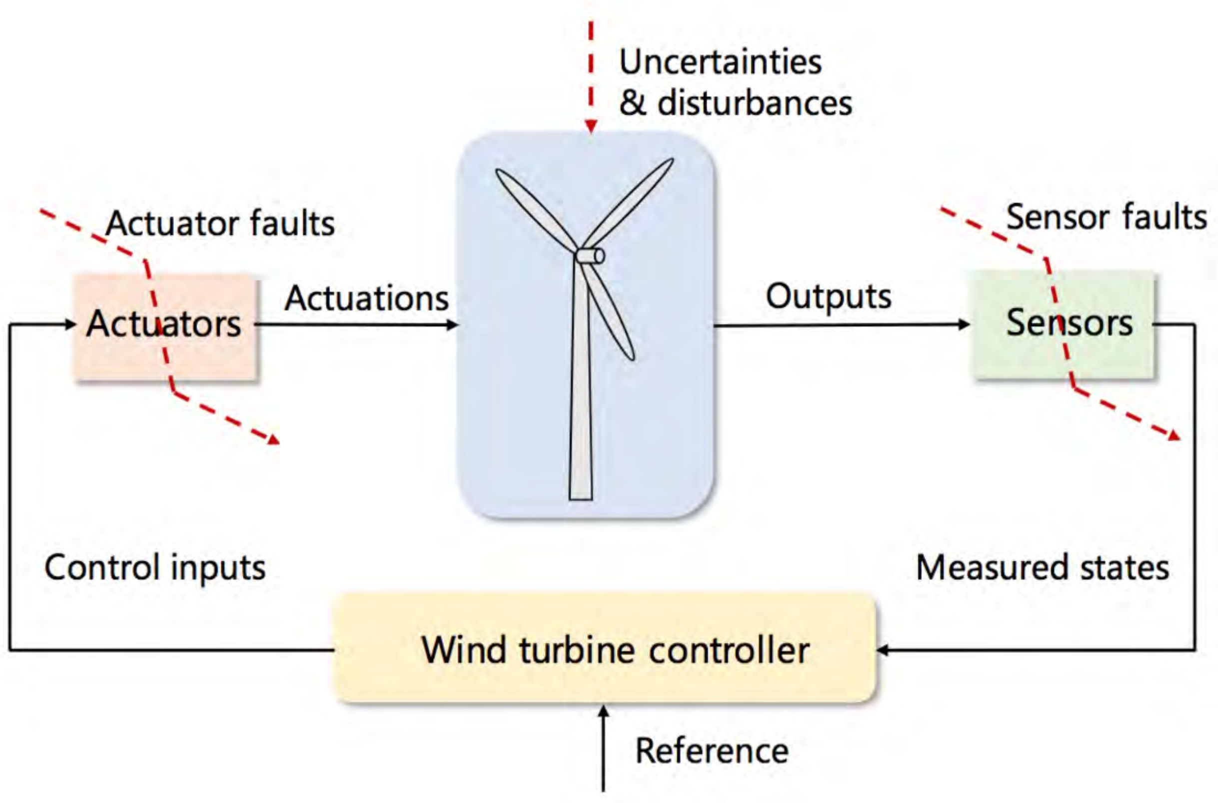

Figure 1. Offshore wind turbine control system with actuator and sensor faults [1].

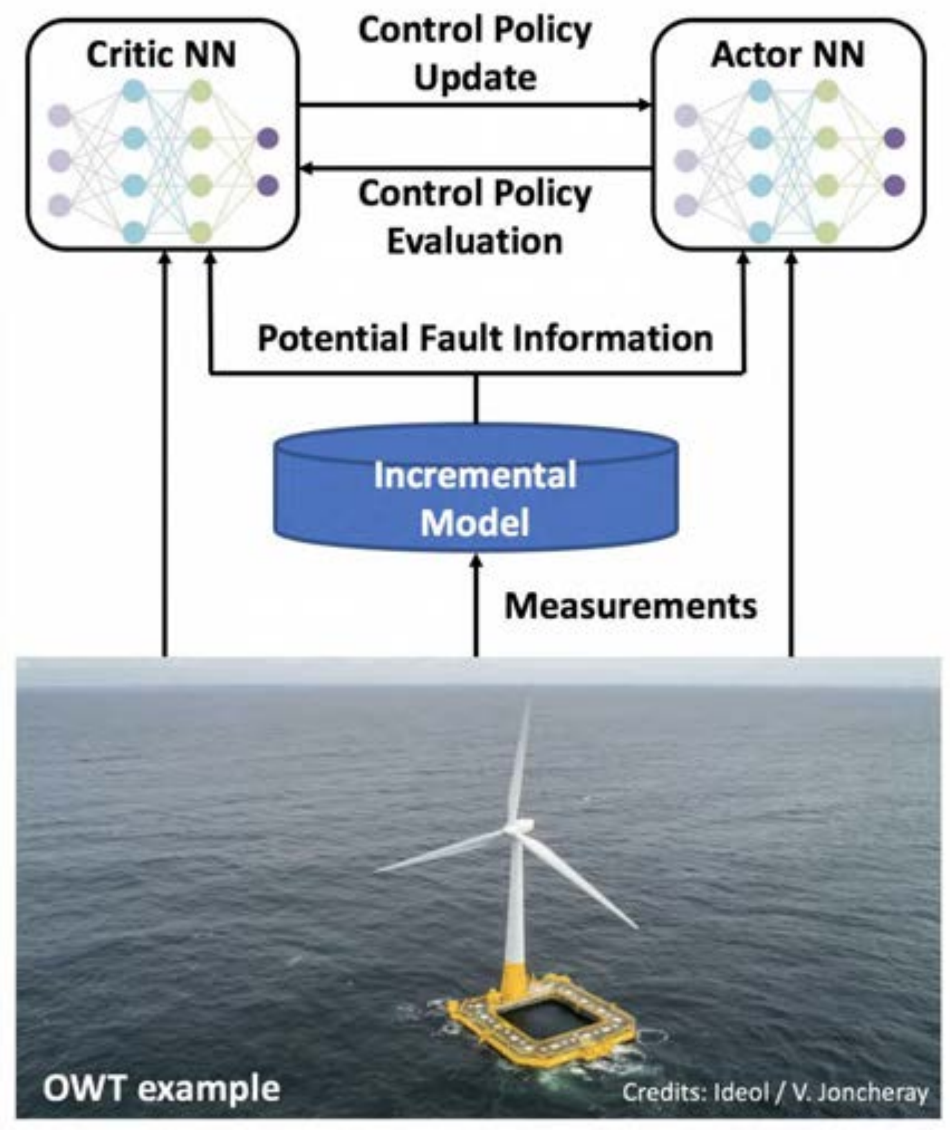

Figure 2. A brief illustration of the proposed control strategy [1].

Simulation and Discussion

➢ An incremental model to capture potential online system changes with real-time measurements.

➢ A critic-actor RL structure to achieve high-performance fault-tolerant control.

➢ Better performance than commonly-used methods (incl. PI and MPC) under faulty conditions.

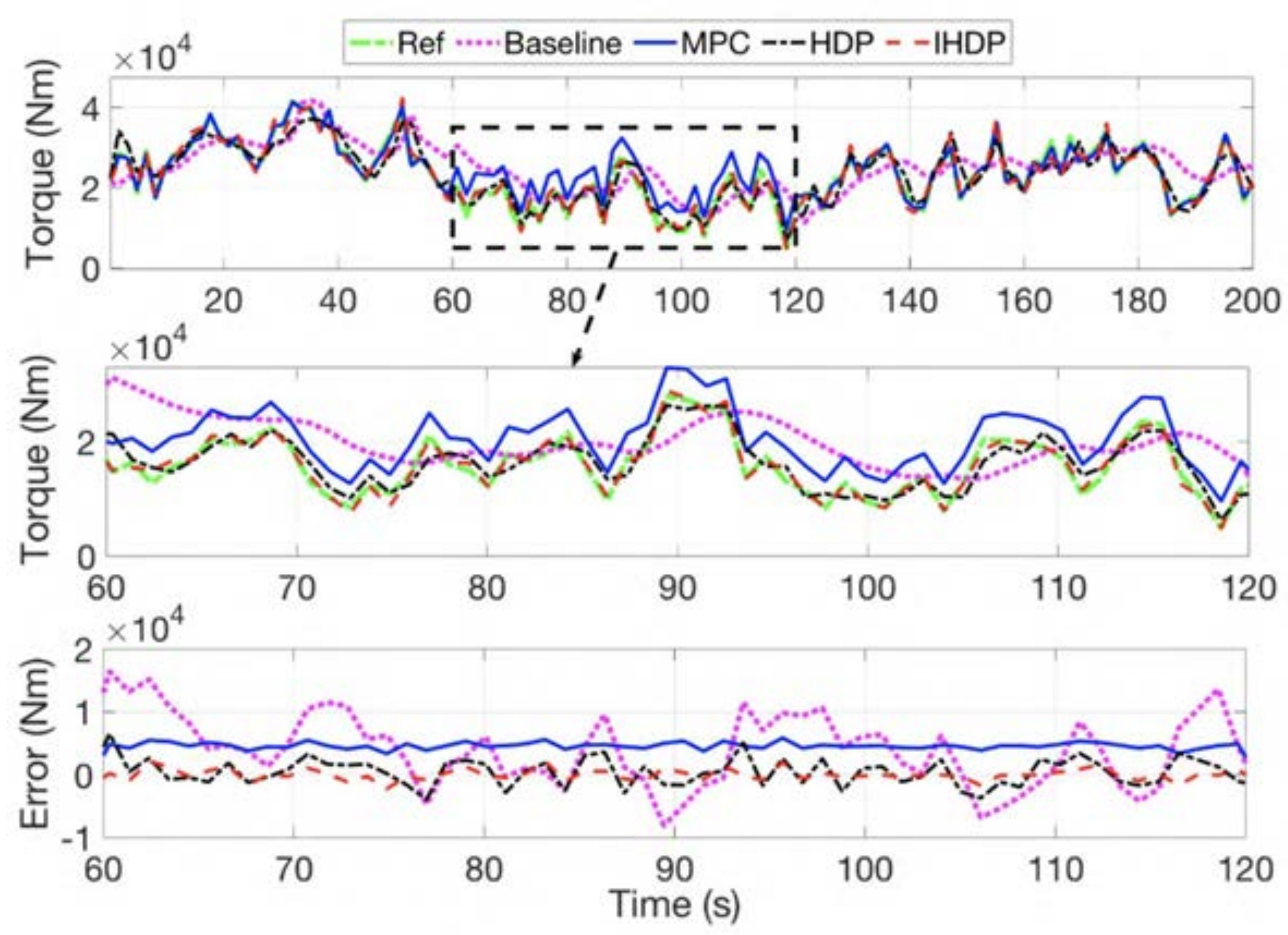

Figure 3. Generator torques under different controllers subject to the offset fault (+5000 N m) – IHDP is the proposed method, which leads to smallest errors [1].

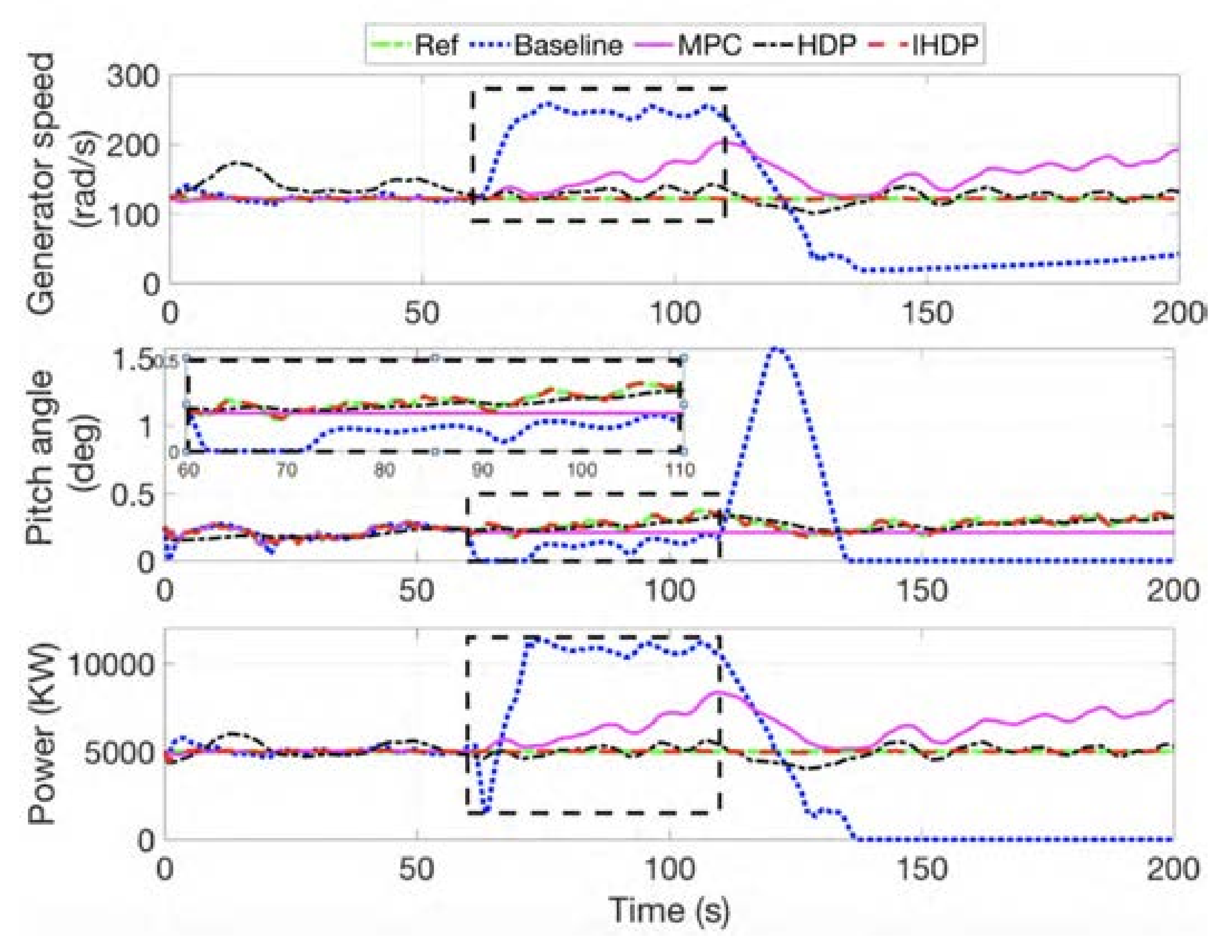

Figure 4. Control performance of different controllers under partial failure sensors and parameter uncertainties – IHDP is the proposed method, which leads to best performance [1].

Reference -

IEEE Transactions on Automation Science and Engineering

Supergen ORE Hub Early Career Researcher Forum 2025

Adapting Building-Structure Bolt Design Practices for Offshore Wind Applications

University of Dundee

Xuemei Lin

Introduction

high-strength steel stainless steel shape memory alloy 200+ physical tests and 1,100+ finite element simulations

Key research outcomes (HSS & stainless steel bolted connections)

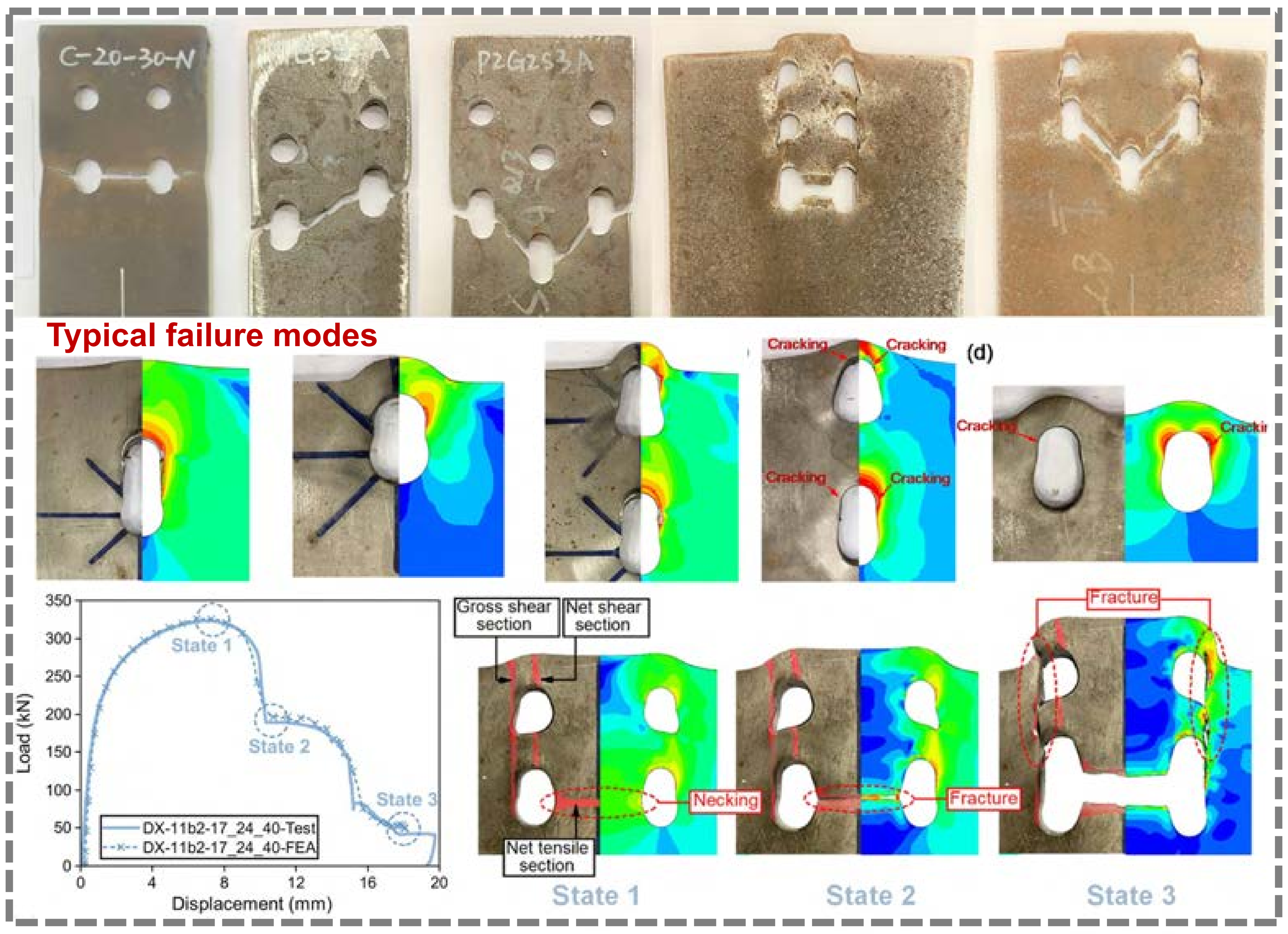

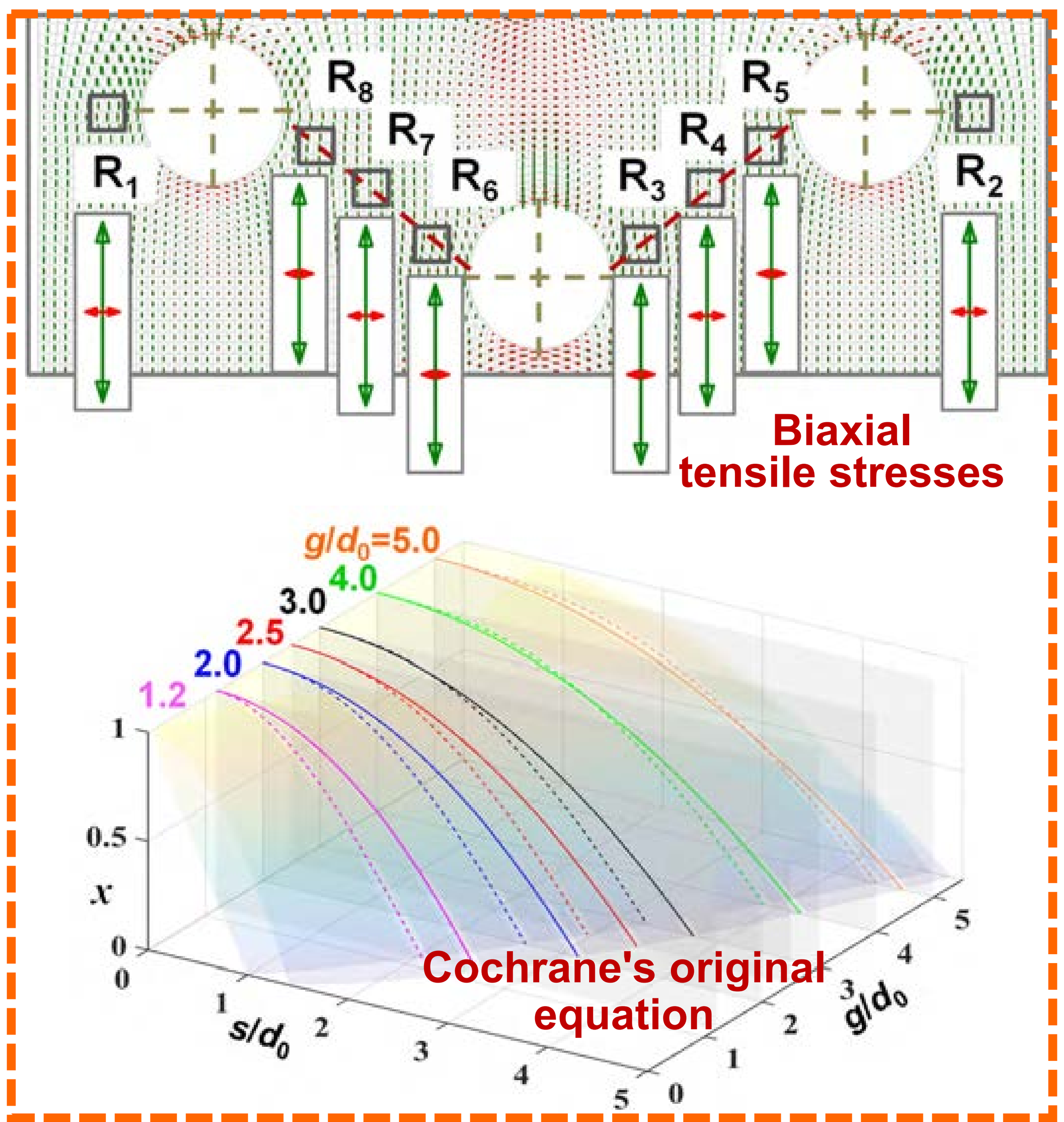

Key research outcomes (SMA-hybrid system)

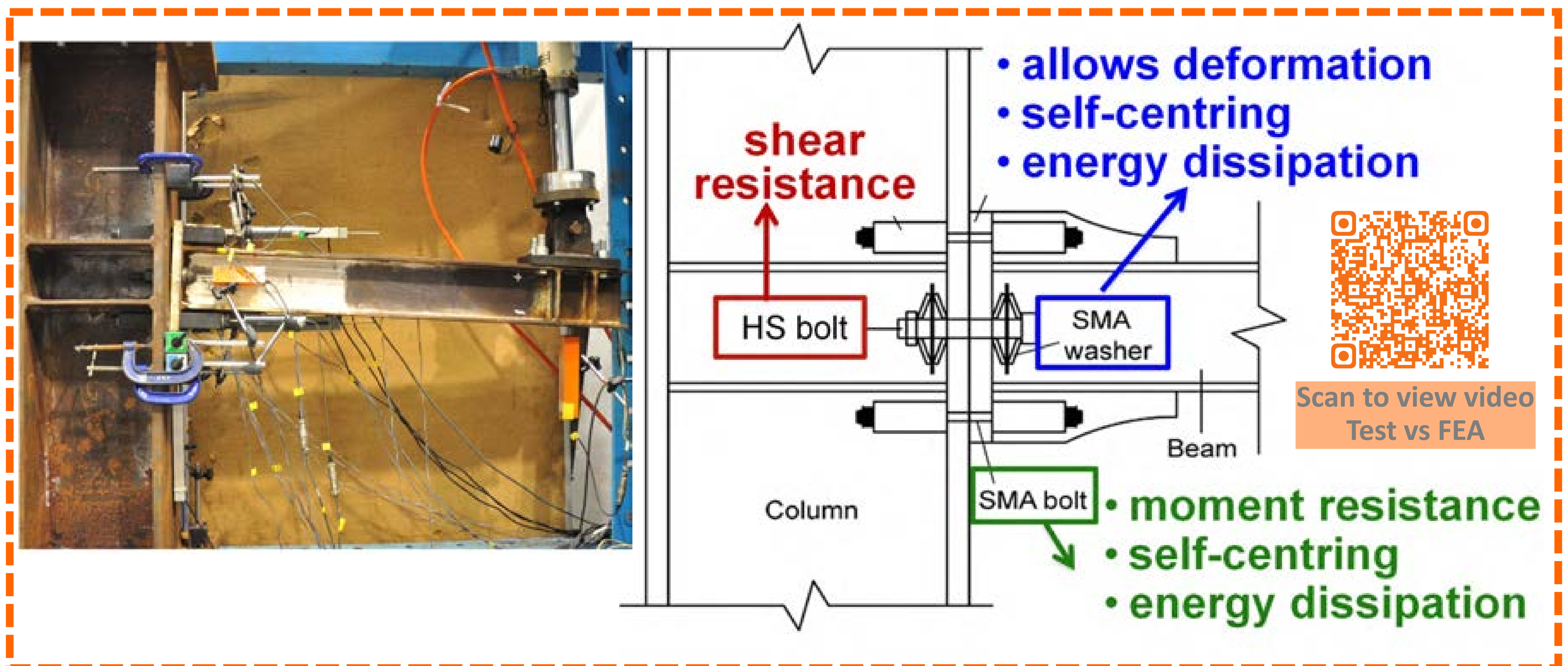

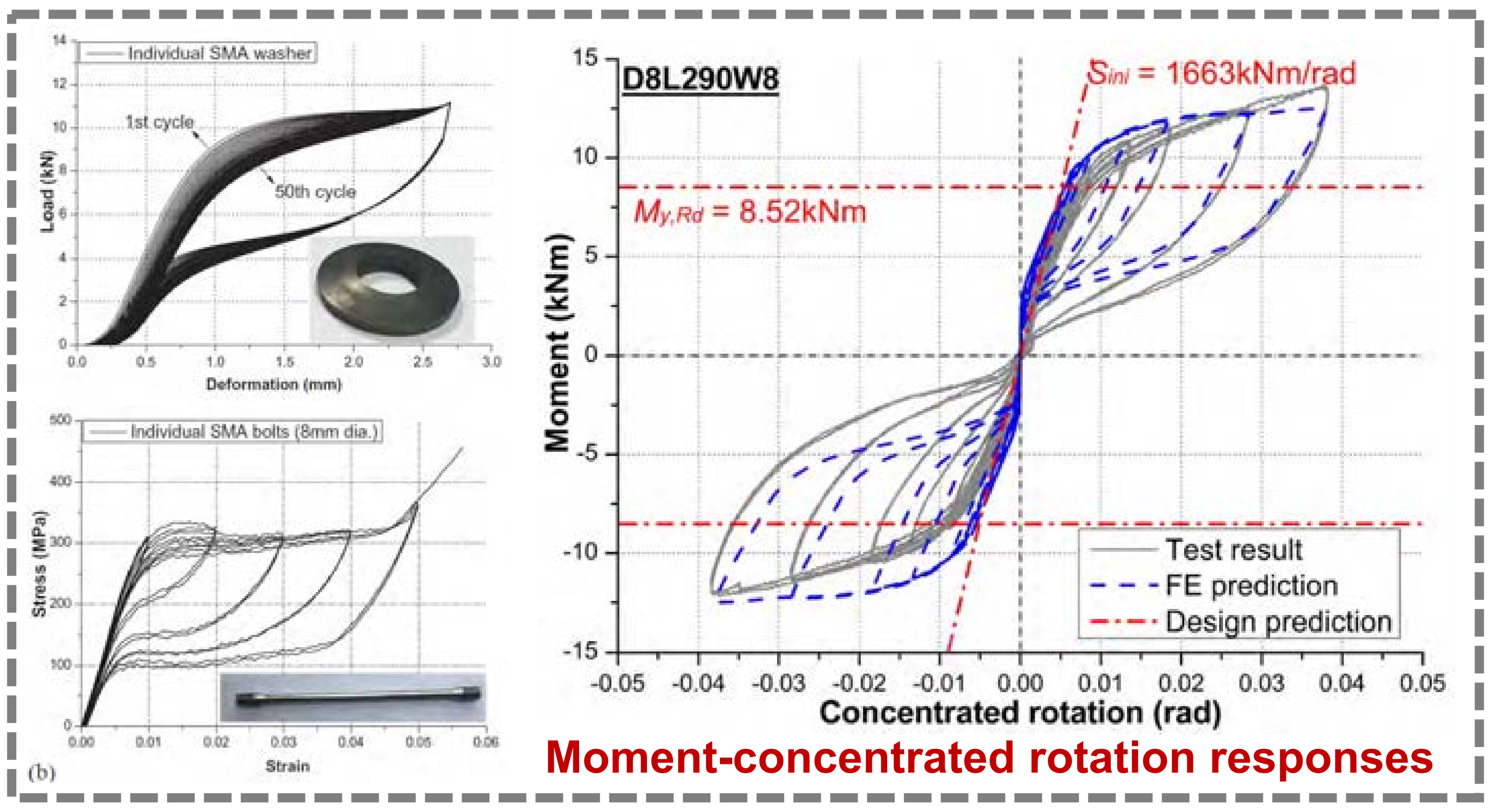

Potential marine applications

Engineering Structures, 247
Thin-Walled Structures, 205

Email: xlin001@dundee.ac.uk

EUROCODES
The Hong Kong Polytechnic University 香港理工大學
SCI Steel Knowledge
Supergen Offshore Renewable Energy
Tongji University
國家鋼結構工程技術研究中心香港分中心 Chinese National Engineering Research Centre For Steel Construction (Hong Kong Branch)

Advancing Floating Offshore Wind Turbine (FOWT) Stability and Performance through Coupled Aero-Hydro-Mooring Analysis

Rizwan Haider [a,b], Wei Shi [b], Zaibin Lin [c]

[a] School of Hydraulic Engineering, Faculty of Infrastructure Engineering, Dalian University of Technology, Dalian, 116024, China
[b] State Key Laboratory of Coastal and Offshore Engineering, Dalian University of Technology, Dalian, China
[c] School of Engineering, University of Aberdeen, King's College, Aberdeen, AB24 3UE, the UK

Introduction

Context: FOWTs harness deep-sea wind energy but face challenges from coupled aerodynamic, hydrodynamic, and mooring dynamics.
Problem: Existing models often oversimplify interactions, limiting accuracy in predicting stability and efficiency.
Research Gap: Fully coupled simulations integrating real-world platform motions and mooring dynamics are computationally demanding and underexplored.

Objectives

1. Develop a **validated CFD model** for fully coupled aero-hydro-mooring analysis of FOWTs.
2. Investigate the impact of **Centre of Gravity (COG)** height on platform stability and energy capture.

Methodology

Tools: OpenFOAM-based CFD solver with:
- *turbinesFoam* (Actuator Line Model for aerodynamics).
- *waves2Foam* (wave generation/absorption).
- *MoorDyn* (dynamic mooring system, Coulling et al., 2013).
- *sixDoFRigidBodyMotion* (6-DOF platform dynamics).

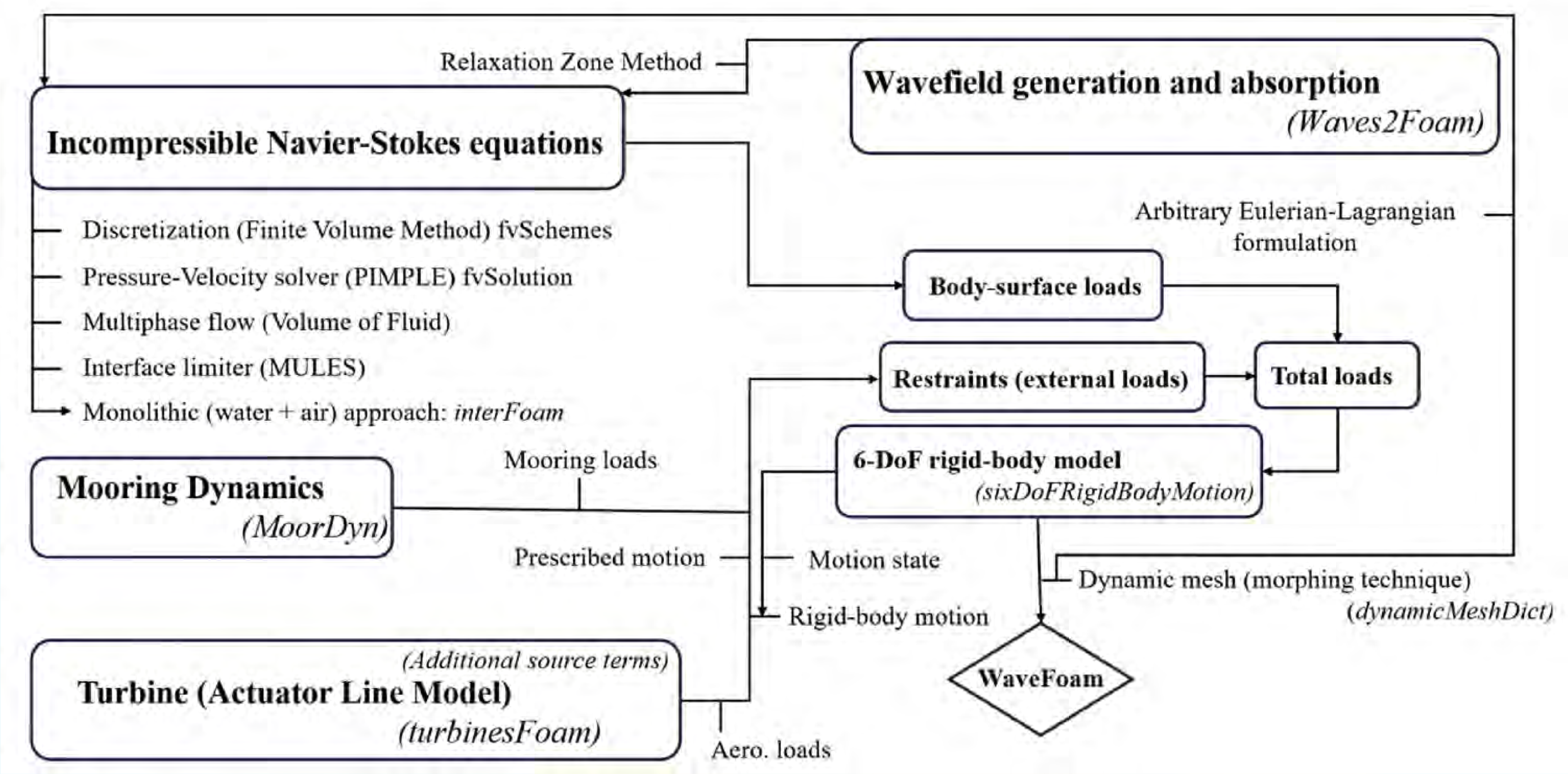

Figure 1: Flowchart of the FOWT fully coupled model

Model Validation: NREL 5 MW OC4 semi-submersible FOWT validated against experimental and numerical benchmarks.

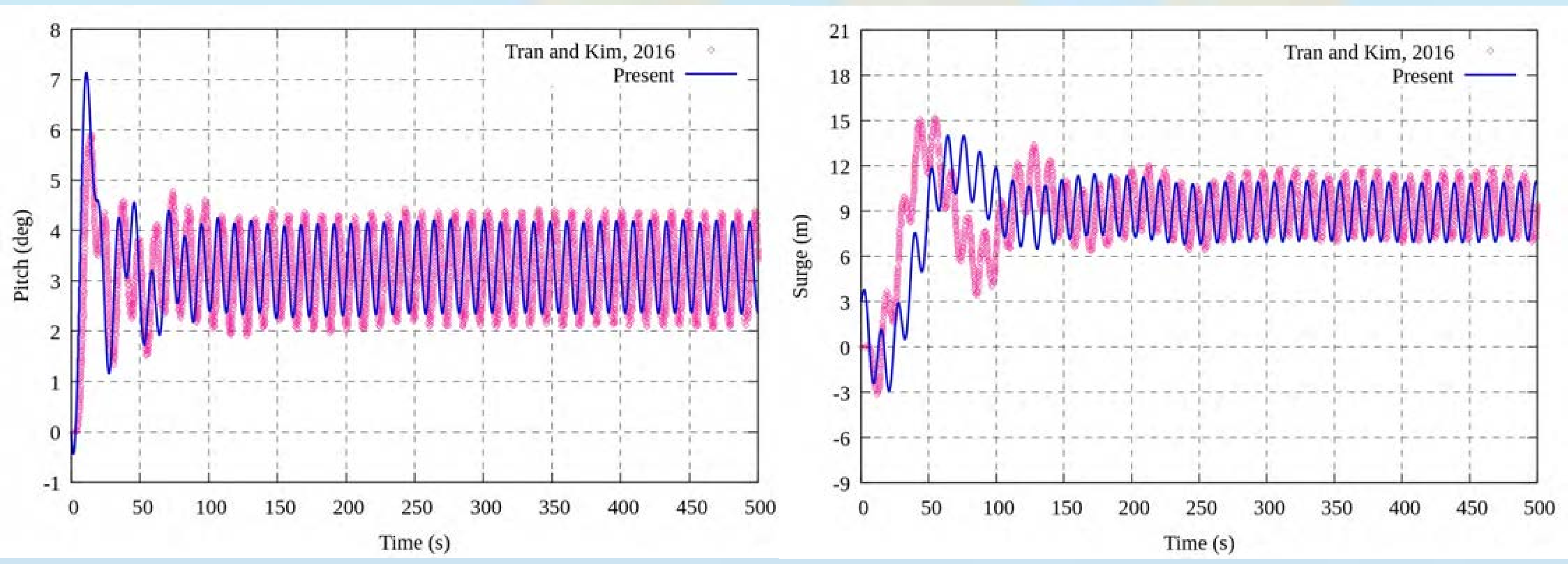

(a) Pitch response (b) Surge response

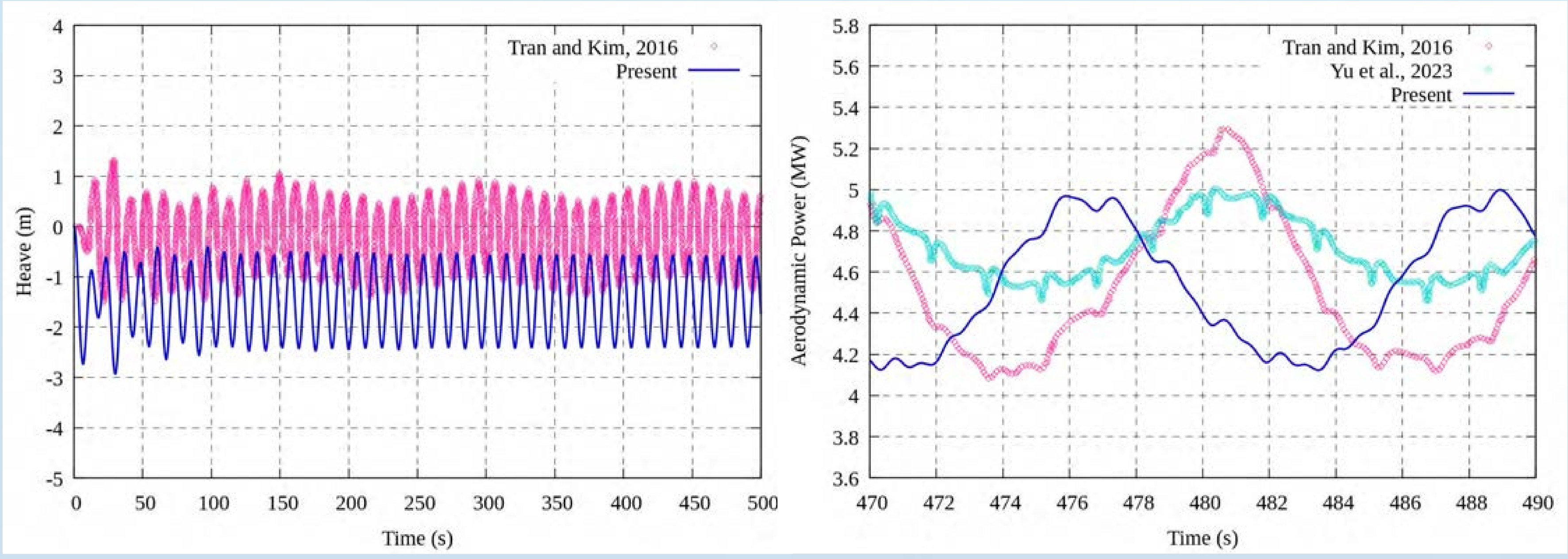

(c) Heave response (d) Power

Figure 2: Comparisons for the platform motion response and power under the case LC1 in Table 1

Key Results

COG Impact: Lower COG reduces **pitch motion by 20%** and mooring tension by **8.6%**, improving FOWT stability but also fluctuating the power output.

Table 1: Environmental conditions and load cases for the FOWT

Environmental conditions				
Inflow Wind Speed (m/s)	Wave amplitude (m)	Wave Height (m)	Wave Period (s)	Rotor Speed (rpm)
11.4	3.79	7.58	12.1	12.1
Load Cases#				
COG (m)	LC1	LC2	LC3	LC4
	-10.2	-12.2	-14.2	-16.2

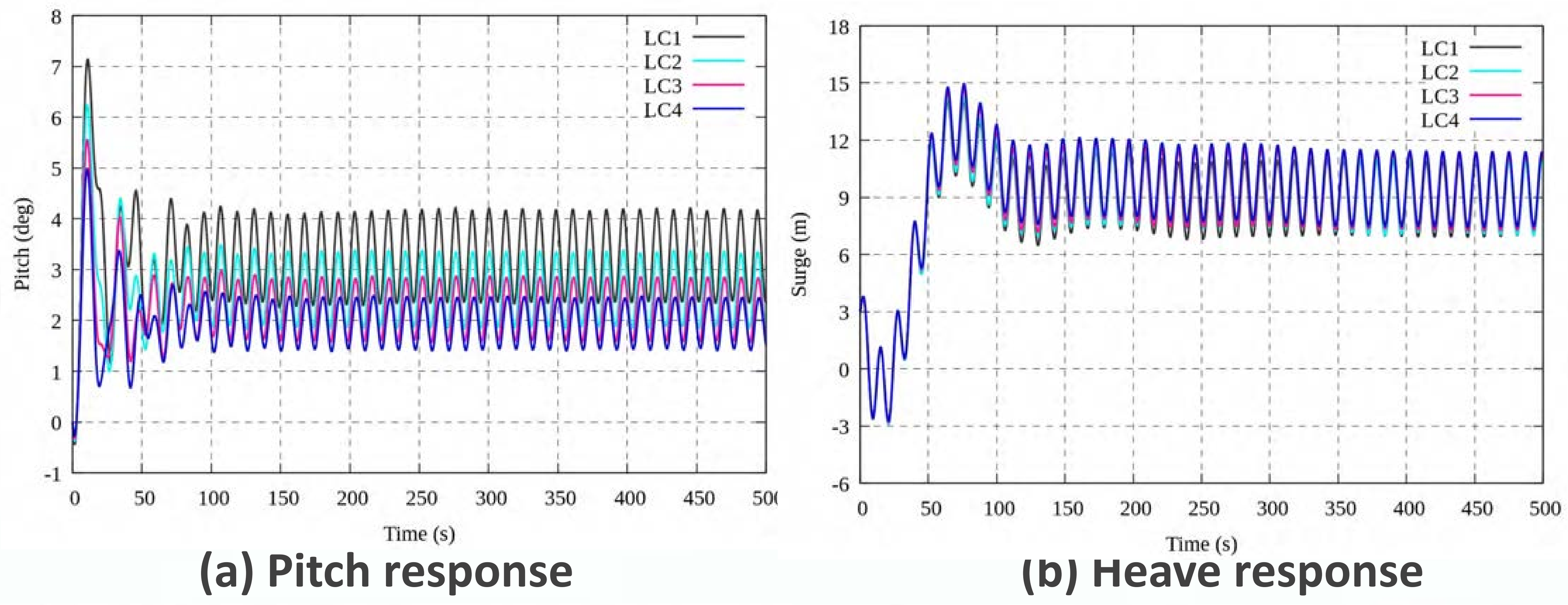

(a) Pitch response (b) Heave response

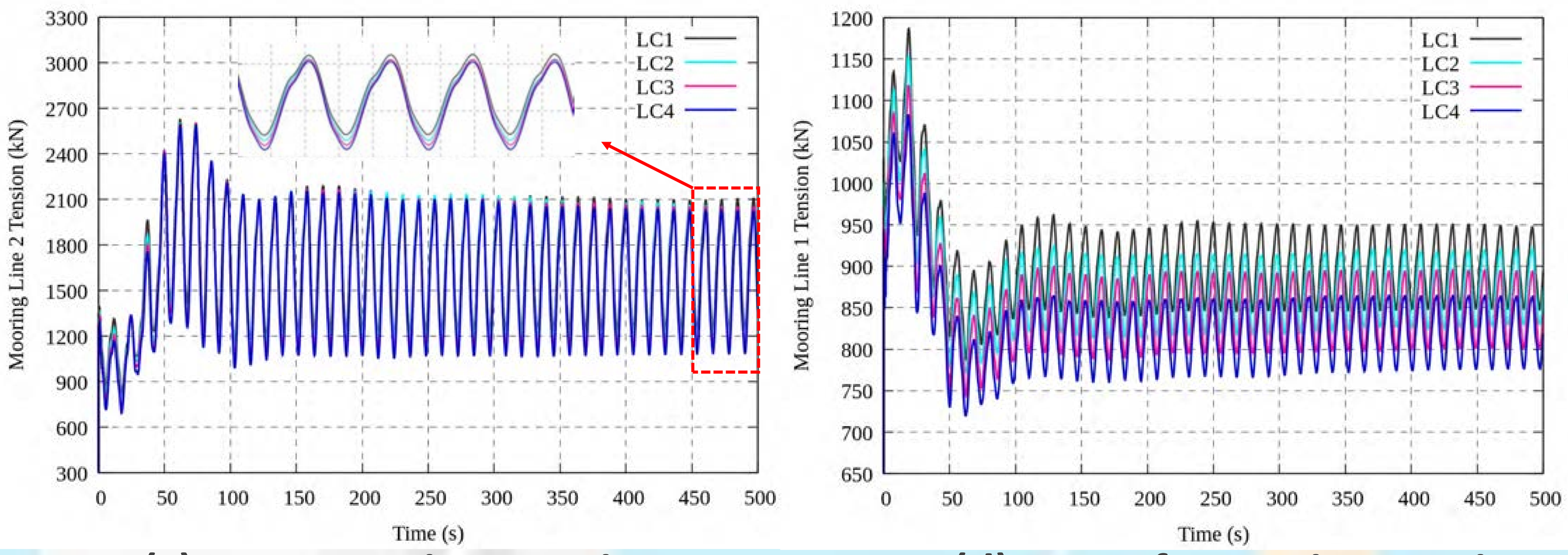

(c) Fore mooring tension (d) Port-aft mooring tension

Figure 4: Pitch, heave, and mooring tension under cases LC1-4.

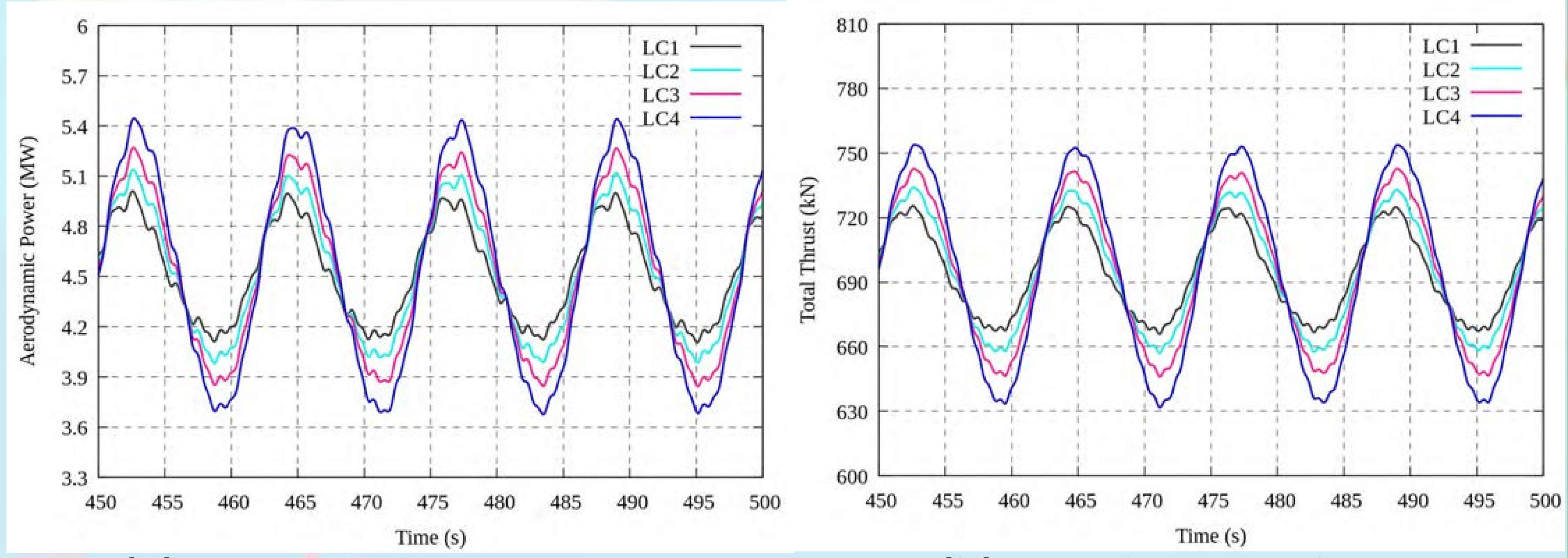

(a) Aerodynamic power (b) Aerodynamic thrust

Figure 5: Aerodynamic power and thrust under cases LC1-4.

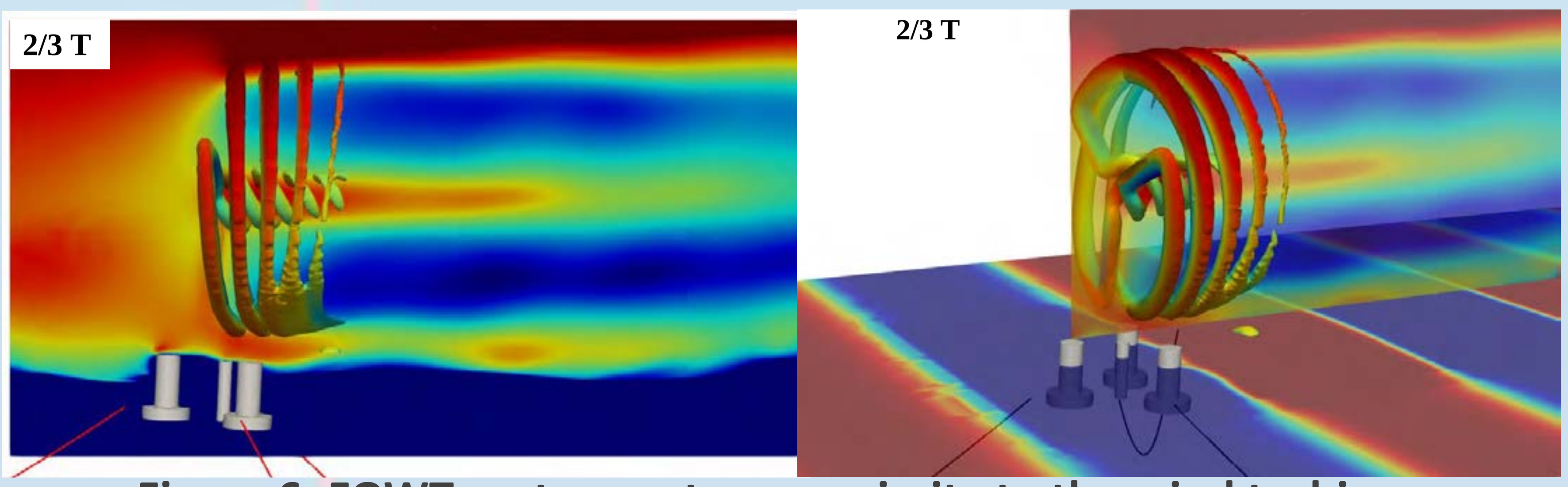

Figure 6: FOWT vortex contour proximity to the wind turbine and midplane flow field under the case LC1

Conclusion

The coupled model accurately predicts FOWT dynamics.
Reducing COG enhances the pitch and mooring tension of the FOWT system, but leads to fluctuations in power output.
Mean power output was increased by 0.9% due to improved platform stability.

Sponsor: Engineering and Physical Sciences Research Council; Supergen Offshore Renewable Energy; The Royal Society; HEC-WSI a High End Computing Consortium for Wave Structure Interaction

Personal website

Key reference

Haider et al. (2024). *Renewable Energy 237, 121793*.
Tran and Kim (2016). *Renewable Energy, 90, 204-228*.
Coulling et al. (2013). *J. Renew. Sustain. Energy 5, 023116*.

Origami-Enhanced Dielectric Fluid Generator for Wave Energy Conversion

Chenying Liu[1], Maozhou Meng[2,*], Jingyi Yang[1,3], Liang He[1], and Zhong You[1,*]

[1] Department of Engineering Science, University of Oxford
[2] School of Engineering, Computing and Mathematics, University of Plymouth
[3] Singapore Institute of Manufacturing Technology, A*STAR
[*] Contact: maozhou.meng@plymouth.ox.ac.uk and zhong.you@eng.ox.ac.uk

UNIVERSITY OF OXFORD

UNIVERSITY OF PLYMOUTH

1 Introduction

Ocean waves offer a vast, largely untapped, and sustainable energy resource. In the UK, wave energy has the potential to generate up to 30 TWh/year, about 10% of nation's electricity demand.

Dielectric elastomer generators (DEG) and dielectric fluid generators (DFG) use **mechanically variable capacitors** to convert wave motions into electricity. A parallel-plate capacitance is

$$C = \frac{\varepsilon_0 \varepsilon_r A}{d}$$

where ε_0 is vacuum permittivity and ε_r is relative permittivity.

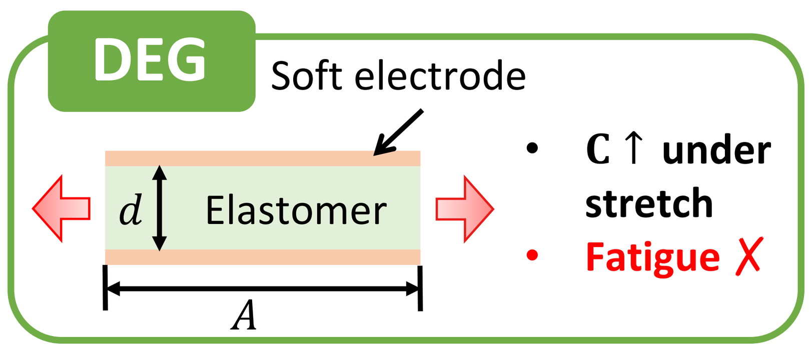

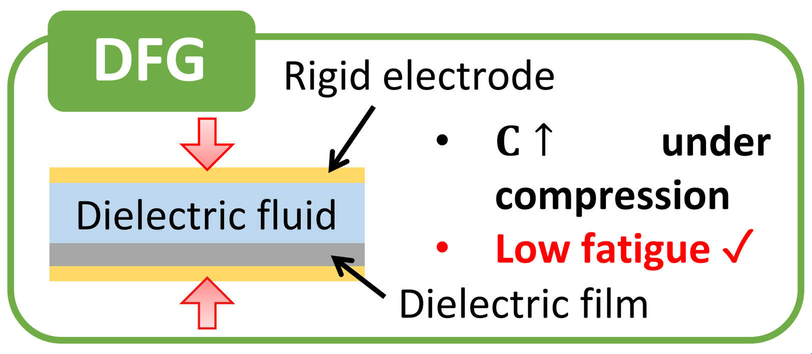

2 Why Origami?

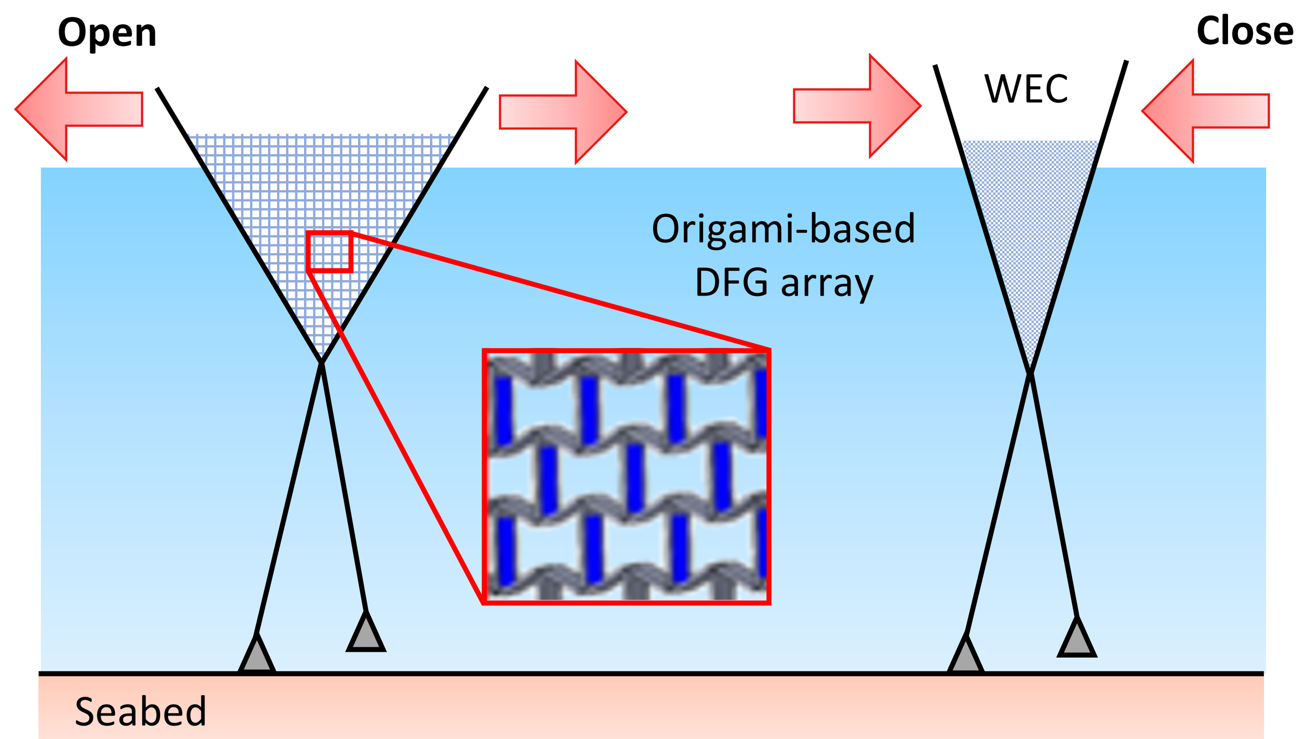

- ✓ **Easily stackable** for scalable arrays in wave energy converters.
- ✓ **Stress isolated to flexible joints** further enhances fatigue life.
- ✓ **Precise control** of electrode displacement improves efficiency.

3 DFG Working Cycle

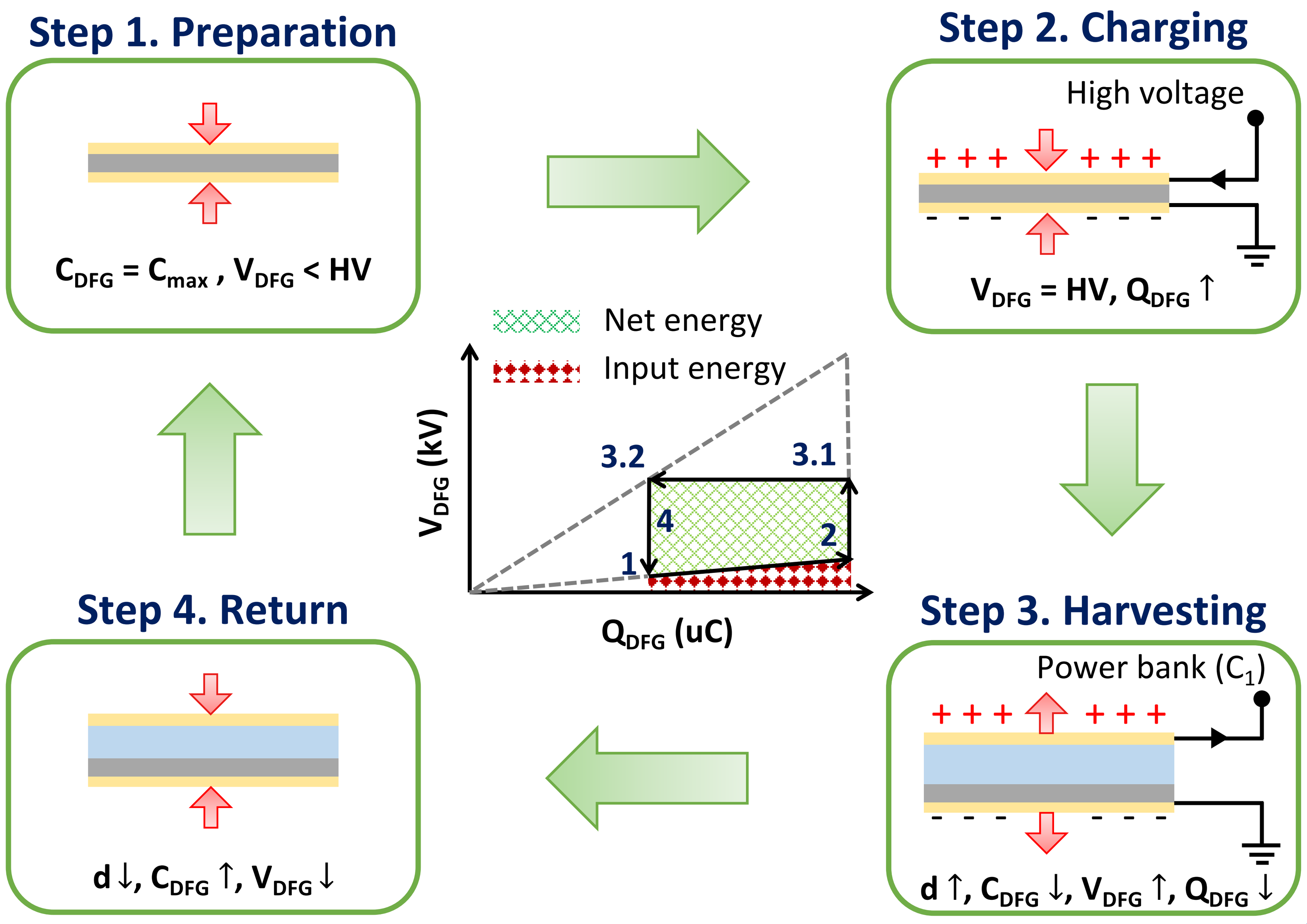

4 Circuit Design and Control

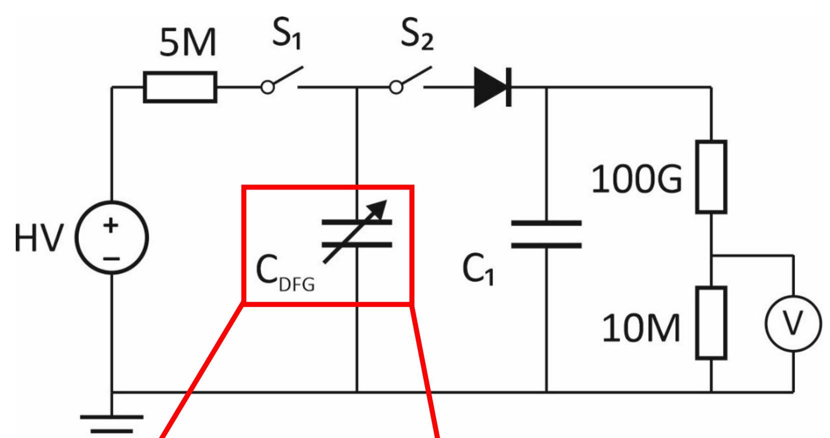

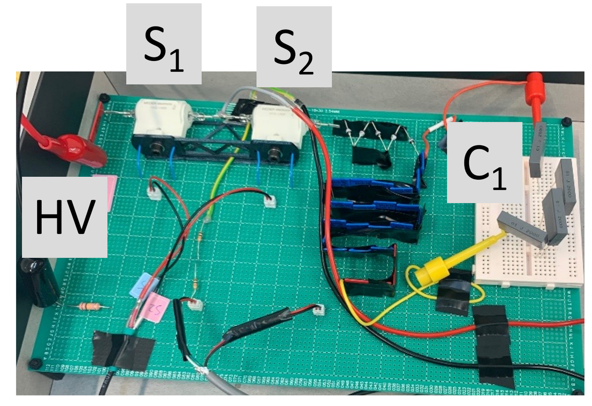

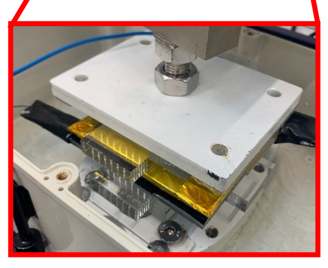

- Electrode size: 60 × 60 mm²
- Electrode material: copper and conductive silicone
- Dielectric film: polyimide ($\varepsilon_r \approx 3.1, E_{ds} \approx 200$ MV/m)
- Dielectric fluid 1: air ($\varepsilon_r \approx 1, E_{ds} \approx 3$ MV/m)
- Dielectric fluid 2: oil ($\varepsilon_r \approx 3, E_{ds} \approx 45$ MV/m)

Step 1 ⇒ S1 and S2 open, high voltage (HV) on, DFG idle
Step 2 ⇒ S1 and S2 close, DFG is charged to HV
Step 3 ⇒ S1 opens and S2 closes, DFG upper electrode lifts up
Step 4 ⇒ S1 and S2 open, DFG upper electrode lowers down

5 Single DFG in One Wave Cycle

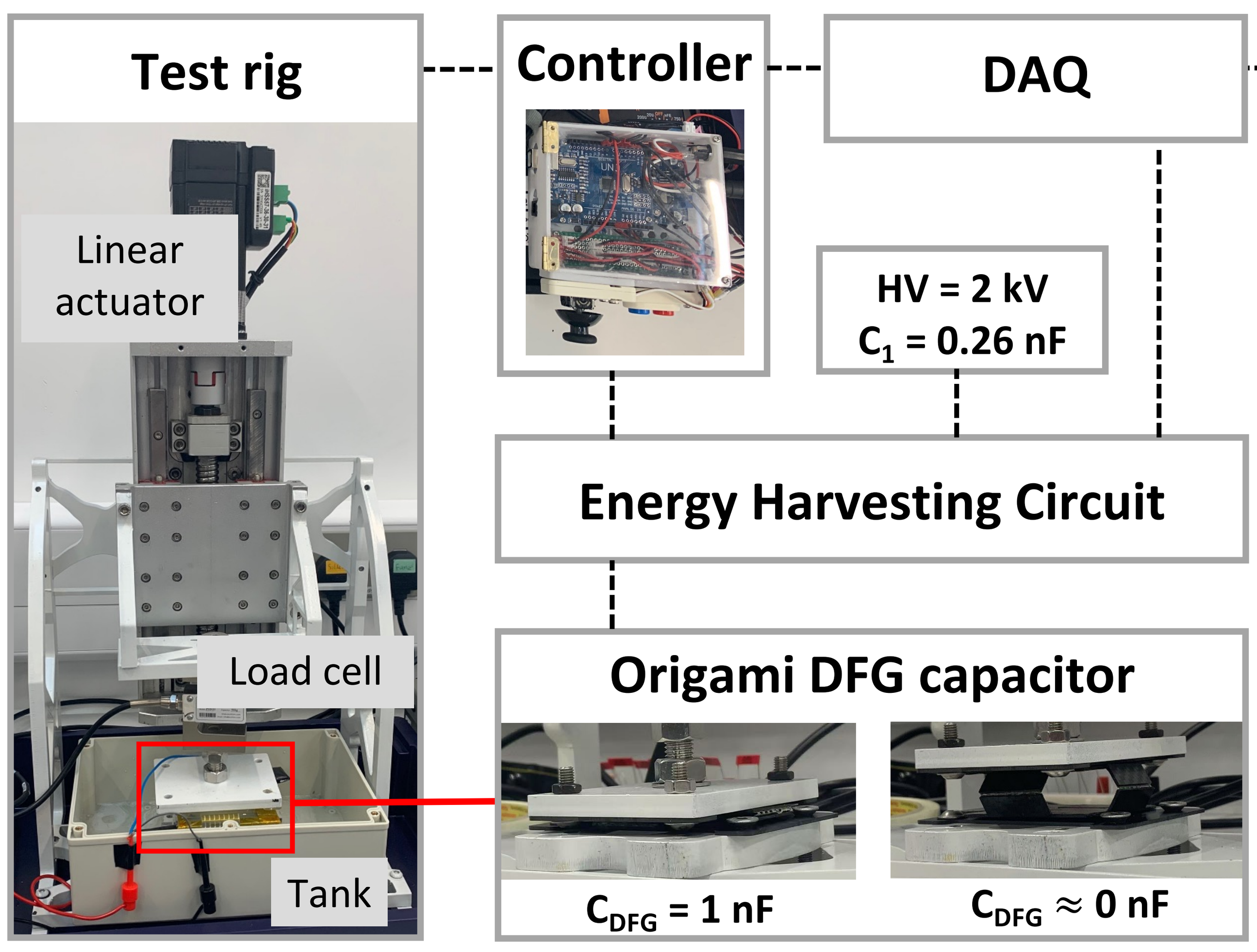

Actuation frequency (f) and speed (v) are tuneable to match wave dynamics. Electrode displacement (d) is precisely controlled.

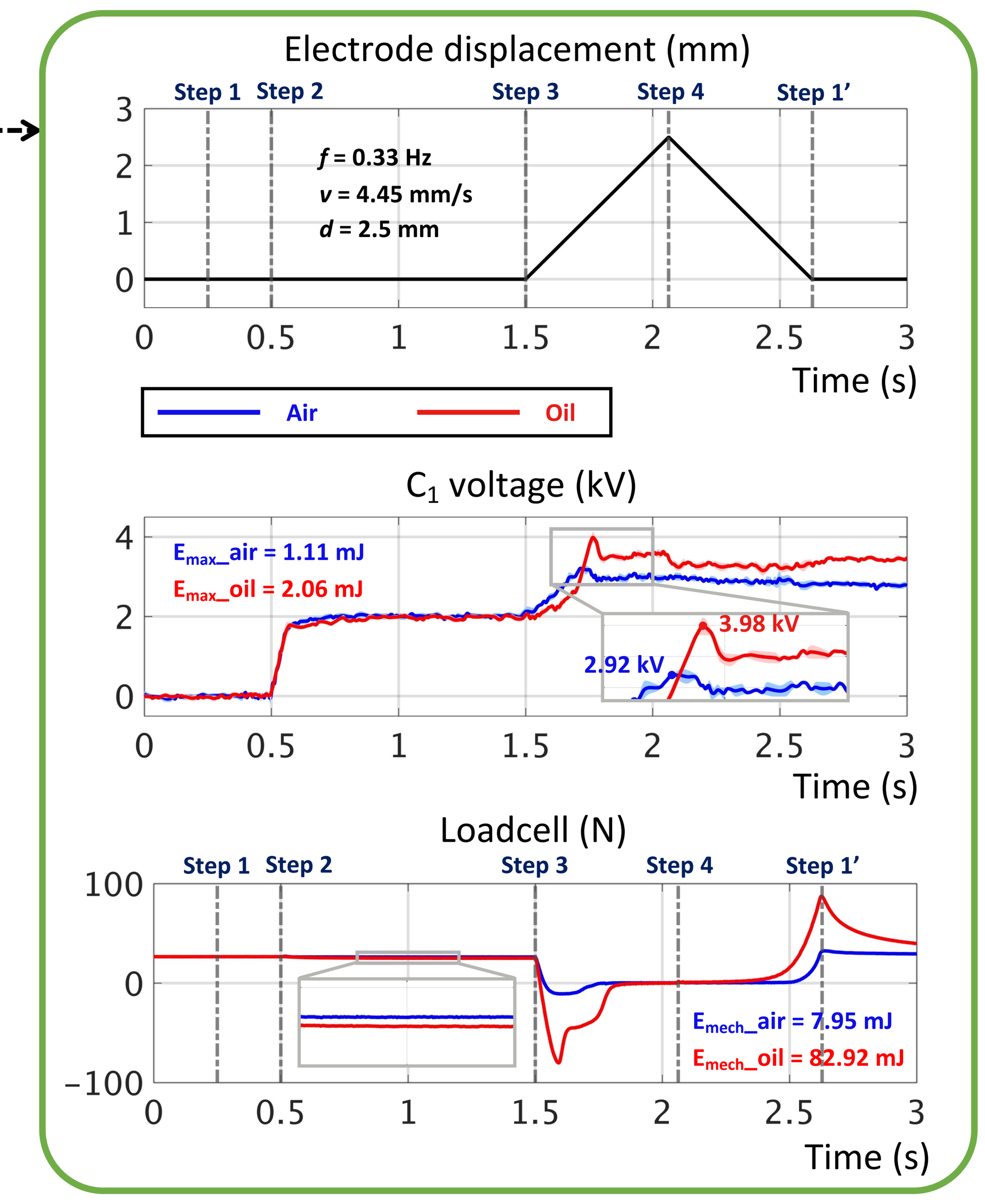

DFG in air

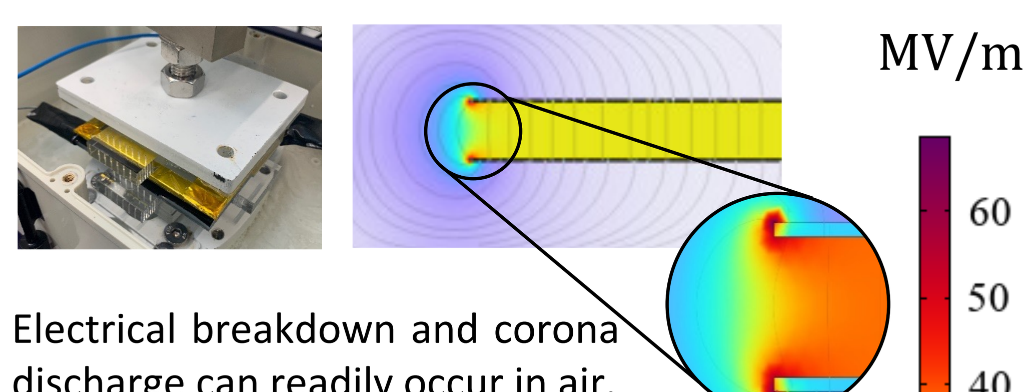

Electrical breakdown and corona discharge can readily occur in air.

DFG in oil

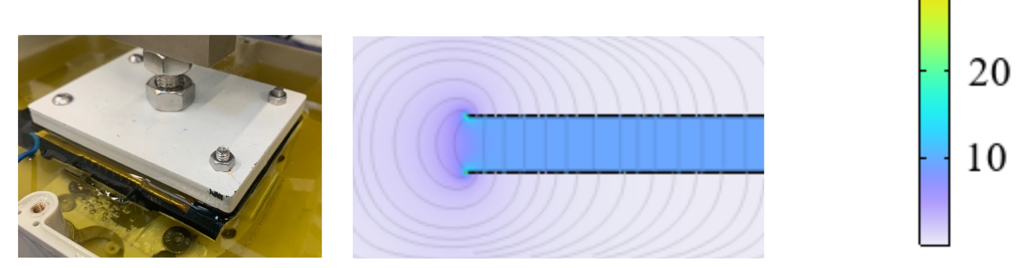

The higher permittivity and breakdown strength of oil help prevent ionisation and suppress corona discharge, boosting output energy by 85.6%. However, its high viscosity increases mechanical energy demand per cycle, reducing conversion efficiency from 14.0% to 2.5%. Speed control can help improve efficiency.

We gratefully acknowledge support from the Supergen ORE Hub and Wave Energy Scotland for the Flexible Fund Project (FF2023-1041), and from EPSRC for the FlexWave Project (EP/V040227/1).

UKRI Engineering and Physical Sciences Research Council

Supergen Offshore Renewable Energy

wave energy SCOTLAND

UNIVERSITY OF CAMBRIDGE
DEPARTMENT OF ENGINEERING

Supergen Offshore Renewable Energy

UKRI Engineering and Physical Sciences Research Council

Controlling Tip Vortices with a Grooved-tip Design

THE UNIVERSITY of EDINBURGH School of Engineering

ROYAL COMMISSION EXHIBITION OF 1851

THE ROYAL SOCIETY

Background and Concept

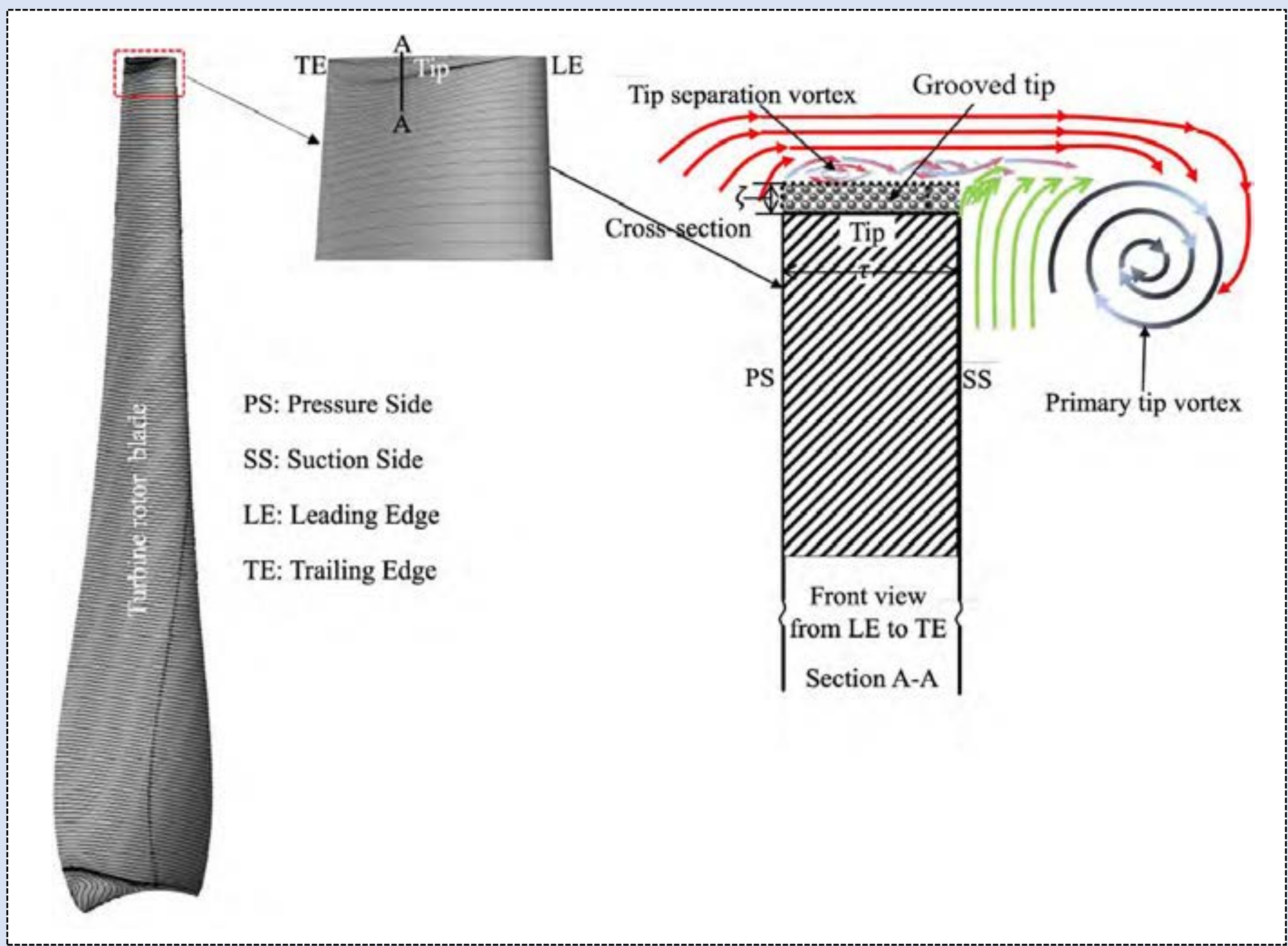

Key Research Outcomes and Ongoing Work

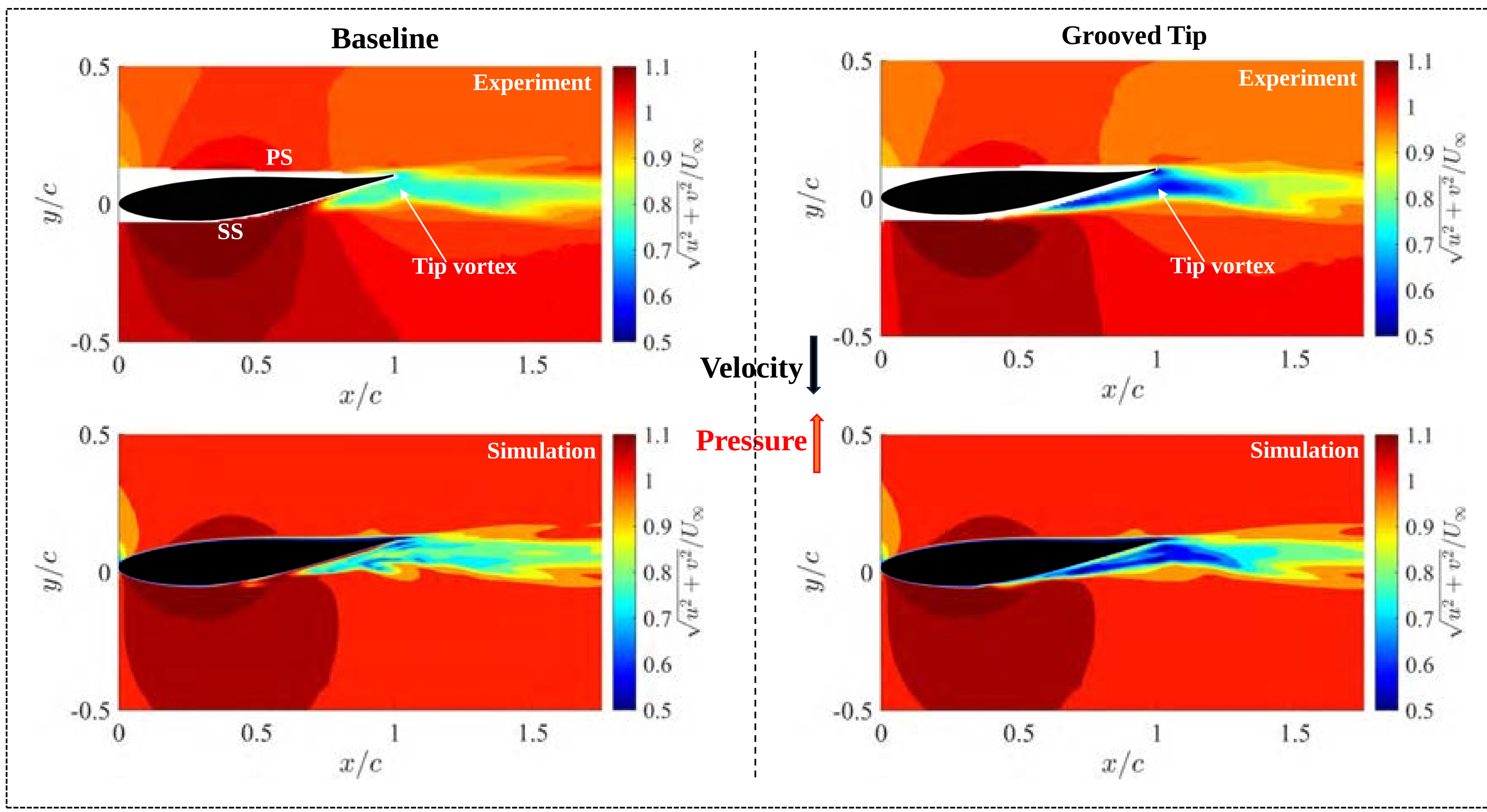

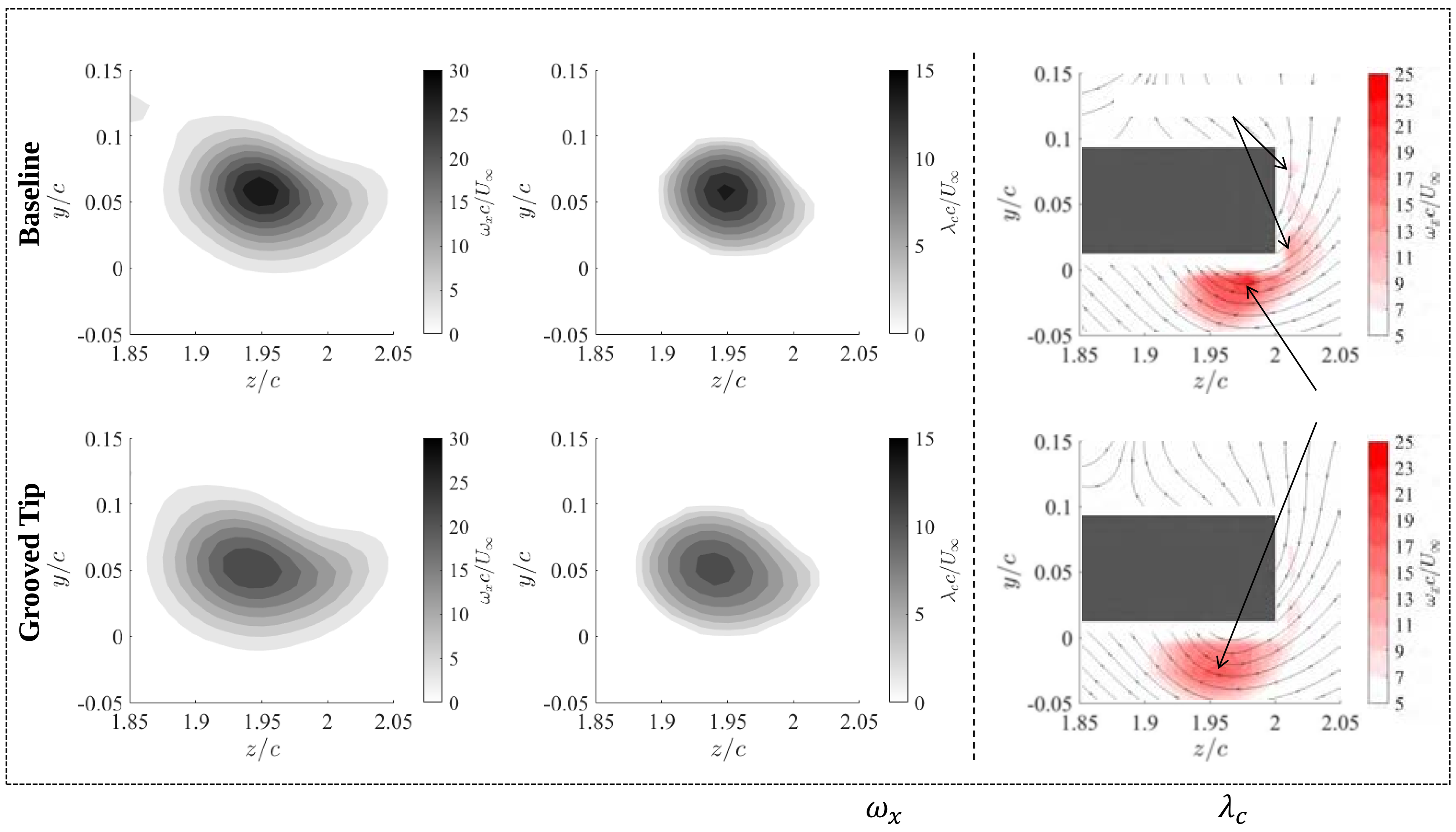

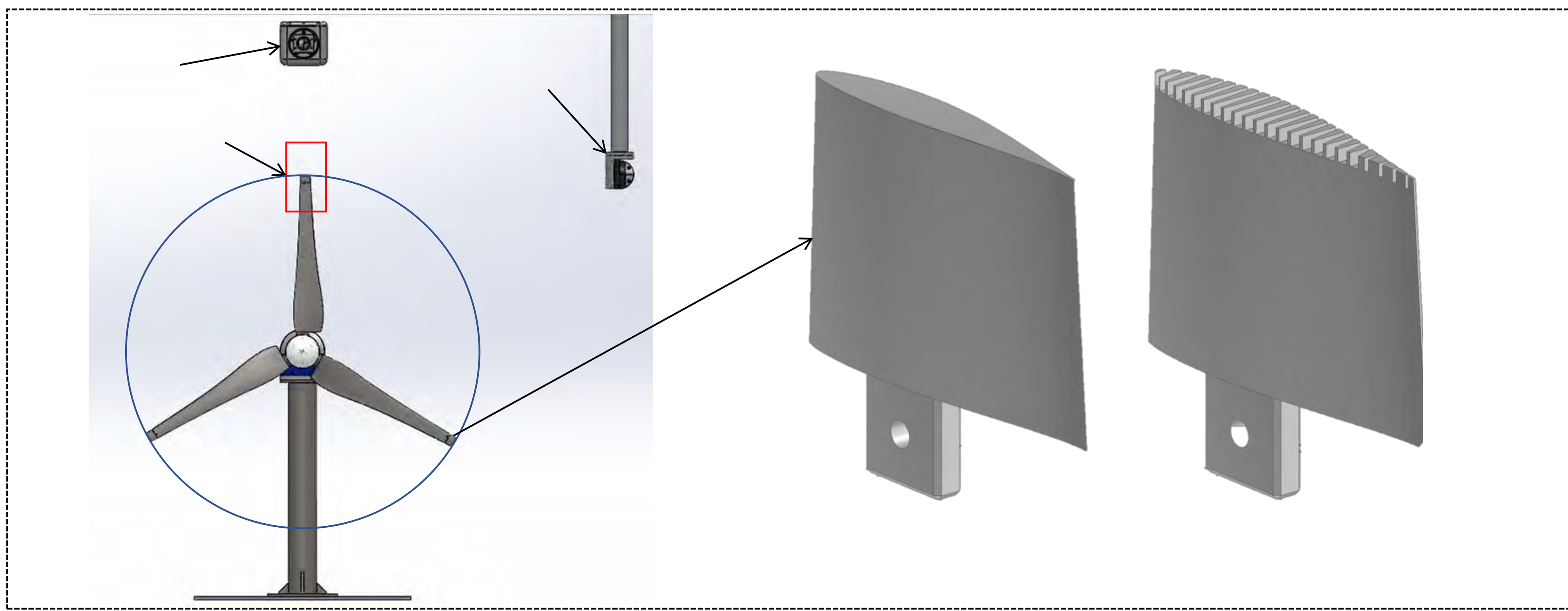

Experimental Methodology

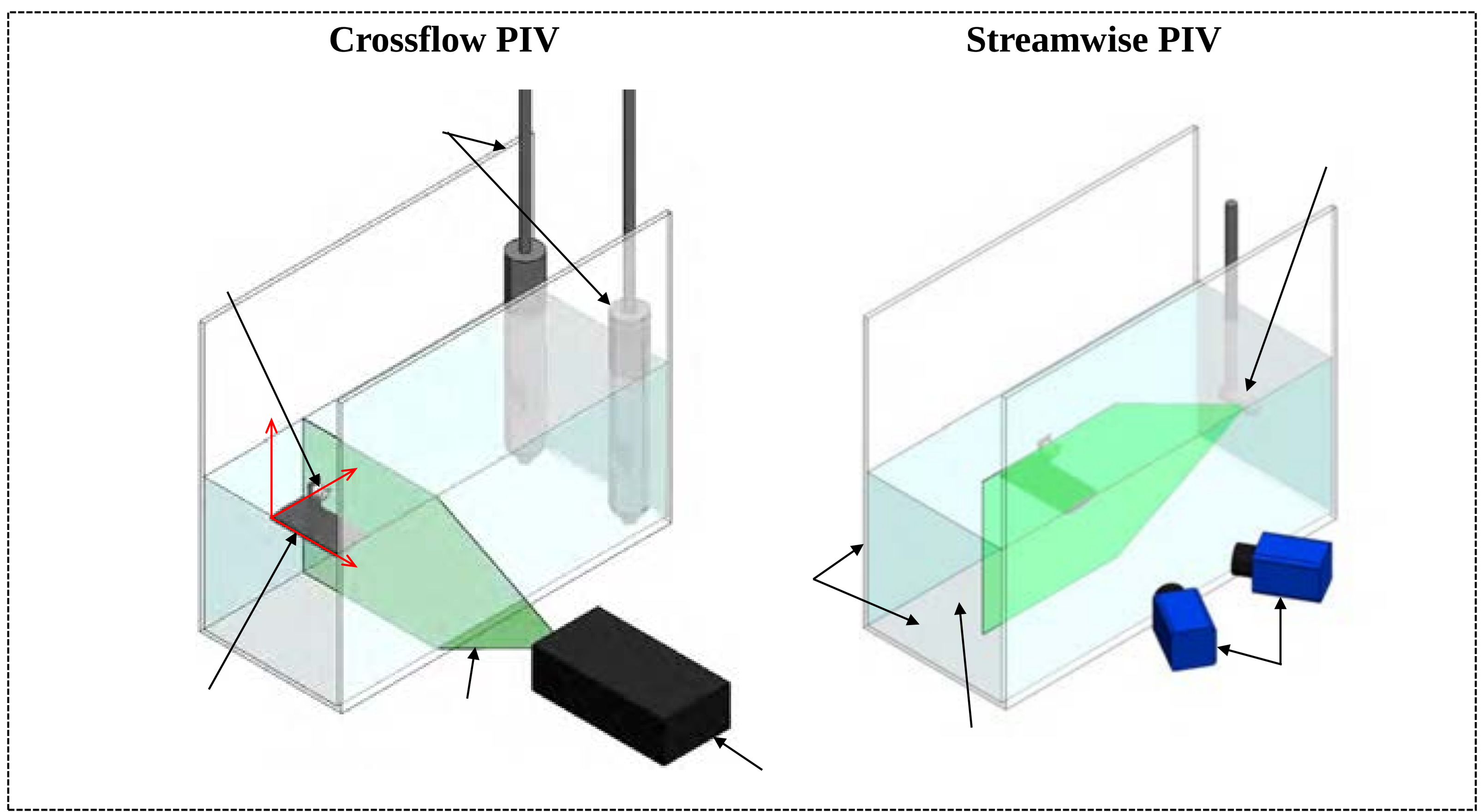

Test parameters:

❑

❑ $U_\infty = 0.3$

❑ $\alpha = 6°$

❑

Conclusions

✓

✓

✓

✓

✓

THE UNIVERSITY *of* EDINBURGH

Wide-Bandgap Power Electronics Topologies for Wave Energy Dielectric Elastomer/Fluid Generators

Sebastian Neira Castillo – s.neira@ed.ac.uk

Motivation: Advance the technology readiness level of Dielectric Elastomer Generator systems by developing wide-bandgap power converters

Dielectric Elastomer Generators (DEGs) and Dielectric Fluid Generators (DFGs) offer high energy densities and low mechanical complexity, particularly attractive for marine environments.

Power take-off systems require bidirectional power capabilities and to withstand efficiently high peak power levels (several kW), to perform the charge/discharge process, but low average output power

Gallium Nitride (GaN) power electronics offer significant advantages over traditional silicon-based devices, including higher efficiency, lower losses, and increased power density.

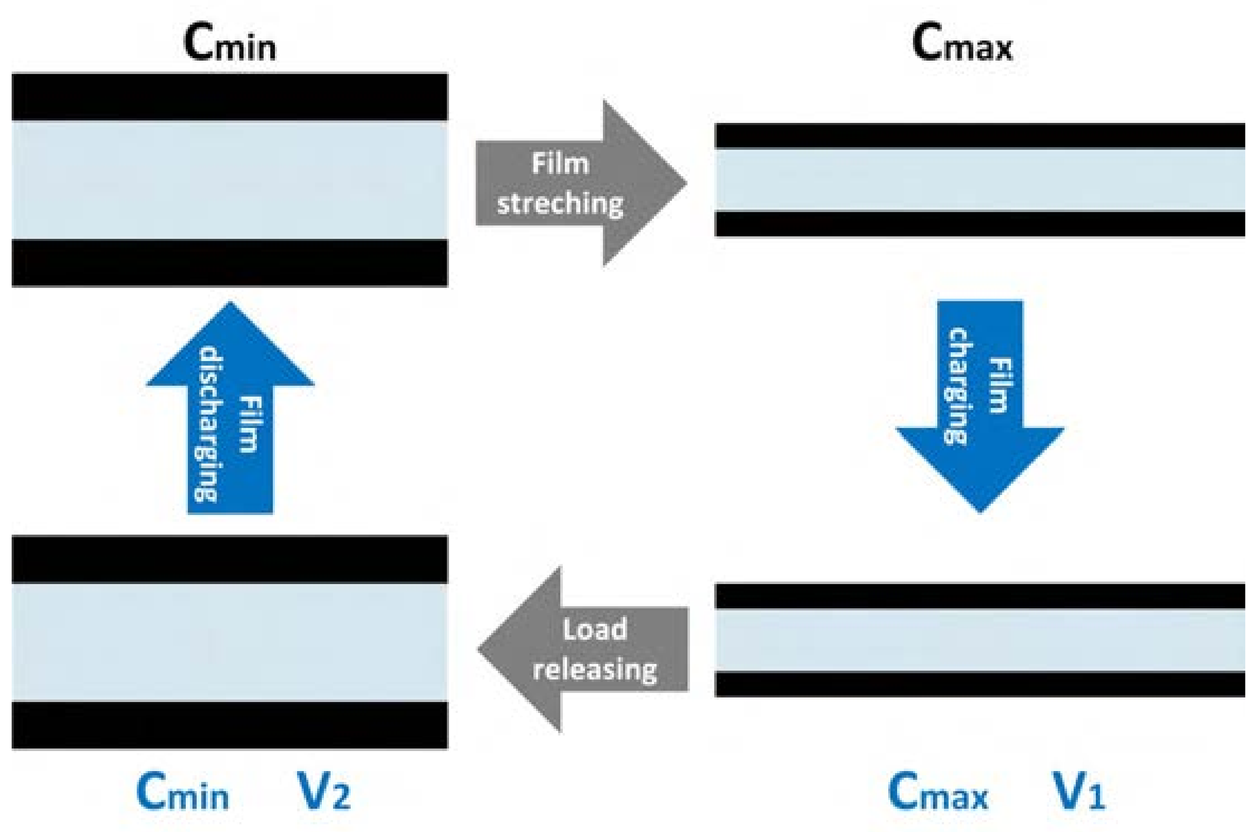

The project will result in the implementation of a 5-kW laboratory prototype of a wide-bandgap semiconductor-based DC-DC converter, designed for the studied DEG specifications.

The main goal of the proposed research is to develop high-voltage high-frequency DC-DC power converter topologies using wide-bandgap semiconductors, such as GaN, capable of performing the power take off process in an efficient and reliable manner for future wave energy systems.

The specific objectives to achieve the outlined goal are defined as follows:

Objective 1: Conceptualisation and design of a 10 kV capable DC-DC converter using GaN devices, currently rated for 650 V, using modular strategies.

Objective 2: Analysis and construction of resonant links and their respective control and modulation strategies to maximise the efficiency of the charge/discharge process of the DEG given the high peak power levels.

Objective 3: Implementation of a Power Hardware-in-the-loop system emulating the dynamics of the DEG for validating the operation of the developed power converters.

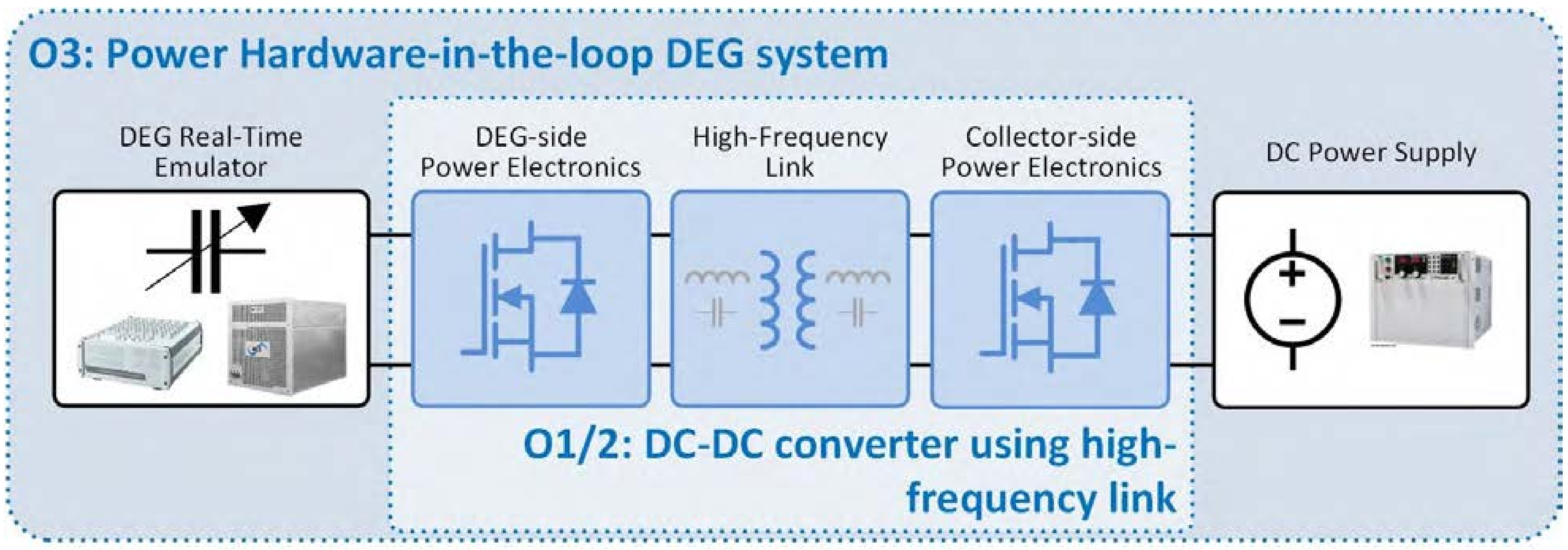

Conclusions & Future Work

Resonant Isolated DC-DC converters based on GaN technology offer enhanced efficiency to perform priming and energy harvesting processes of DEGs and DFGs.

Power hardware in the loop strategy will allow validating a 5 kW prototype, with the DEG/DFG dynamic implemented in a real-time simulator.

The developed power converter will be validated at the University of Edinburgh Power Conversion laboratory with capability for testing devices up to 2000 V and 2000 A.

The author would like to acknowledge the support of Supergen ORE Hub ECR Research Funding

University of Bristol

APPLIED BIFURCATION METHODS FOR EFFICIENT AIRBORNE WIND ENERGY GENERATION

KITEMILL

Universidad Carlos III de Madrid

1. AIRBORNE WIND ENERGY

100 kW
16 m wingspan
5 tons

Operating altitude:
300-700 m

100 kW
26 m diameter
50 tons

Hub height:
30 m

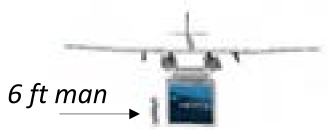

Easy transport

Use in remote areas, low-wind regions, disaster relief, military deployment (in testing with Dutch army)

24h operation

Strong and consistent wind at high altitudes

Reduced life cycle carbon footprint

60% lower cumulative energy demand *(Hagen, 2023)*

Similar energy cost to wind turbines *(Malz, 2020)*

2. THIS FELLOWSHIP

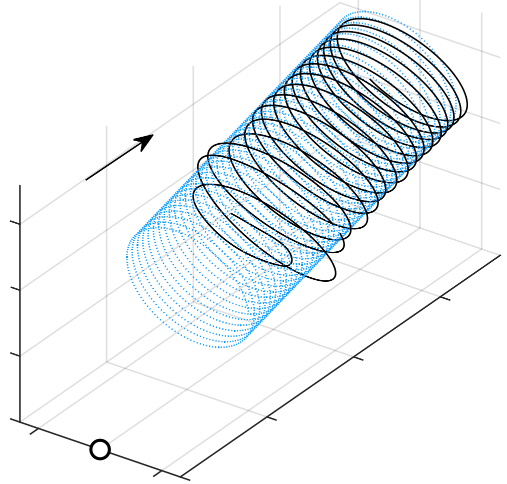

CHALLENGE: realising theoretical predictions

Optimal flight paths established.

How can the aircraft follow that path automatically?

RESULTS

Derived a general control framework to guide the aircraft along a desired path.

Novelty: use of a non-static reference frame. Works with simple PI controller.

Eliminated the angle-of-attack during power production.

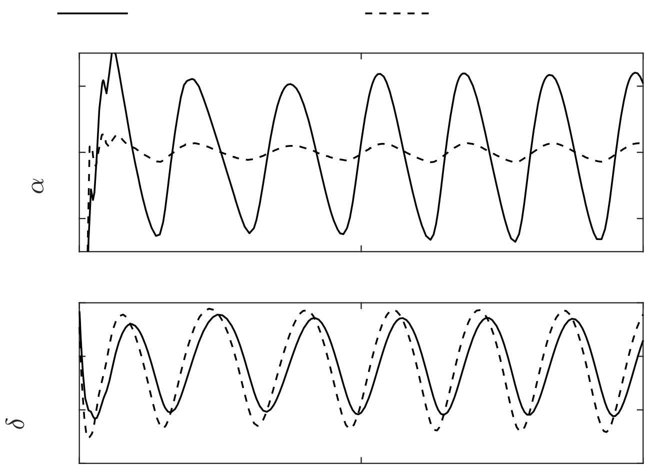

NEXT STEPS

Verify the theoretical predictions using simulations and potentially test flights.

DUC H. NGUYEN

ACADEMIC APPOINTMENTS

December 2023-present
Lecturer in Flight Dynamics and Control
University of Bristol

2022-2024
Lead Tutor in Control Engineering
University of Cambridge Online

2021-2023
Postdoctoral researcher
University of Bristol

EDUCATION

2019-2021
PhD Aerospace Engineering
University of Bristol

2015-2019
MEng Aerospace Engineering
University of Bristol

CURRENT PROJECTS (100% FTE)

Airborne wind energy
EPSRC postdoctoral fellowship
Collaboration with Norwegian startup
Kitemill (see figure)
£375k, PI
2024-27

Folding wingtips
Innovate UK grant
£870k, co-I
2024-26

OTHERS

Private pilot license (2018)

Kitemill's KM1 airborne wind prototype

Multi-axis motion analysis of TALOS Wave Energy Converter under realistic sea states

Charikleia L.G. Oikonomou[1], Wanan Sheng[2], Gerasimos Korres[1], George Aggidis[2]

1. Hellenic Centre for Marine Research - HCMR, Greece

2. Renewable Energy Group, Energy Engineering, Lancaster University

Lancaster University

hcmr ΕΛΚΕΘΕ

Introduction/Motivation

TALOS, developed at Lancaster University, is a novel wave energy converter (WEC) designed to extract power from multiple motion modes—surge, heave, and pitch—via a multi-axis omni-directional Power-Take-Off (PTO) system.
This study evaluates its performance under four representative wave climates using both frequency-domain and stochastic modeling, guiding device optimisation for deployment.

Methodology

Wave climate locations analysed (1–4)

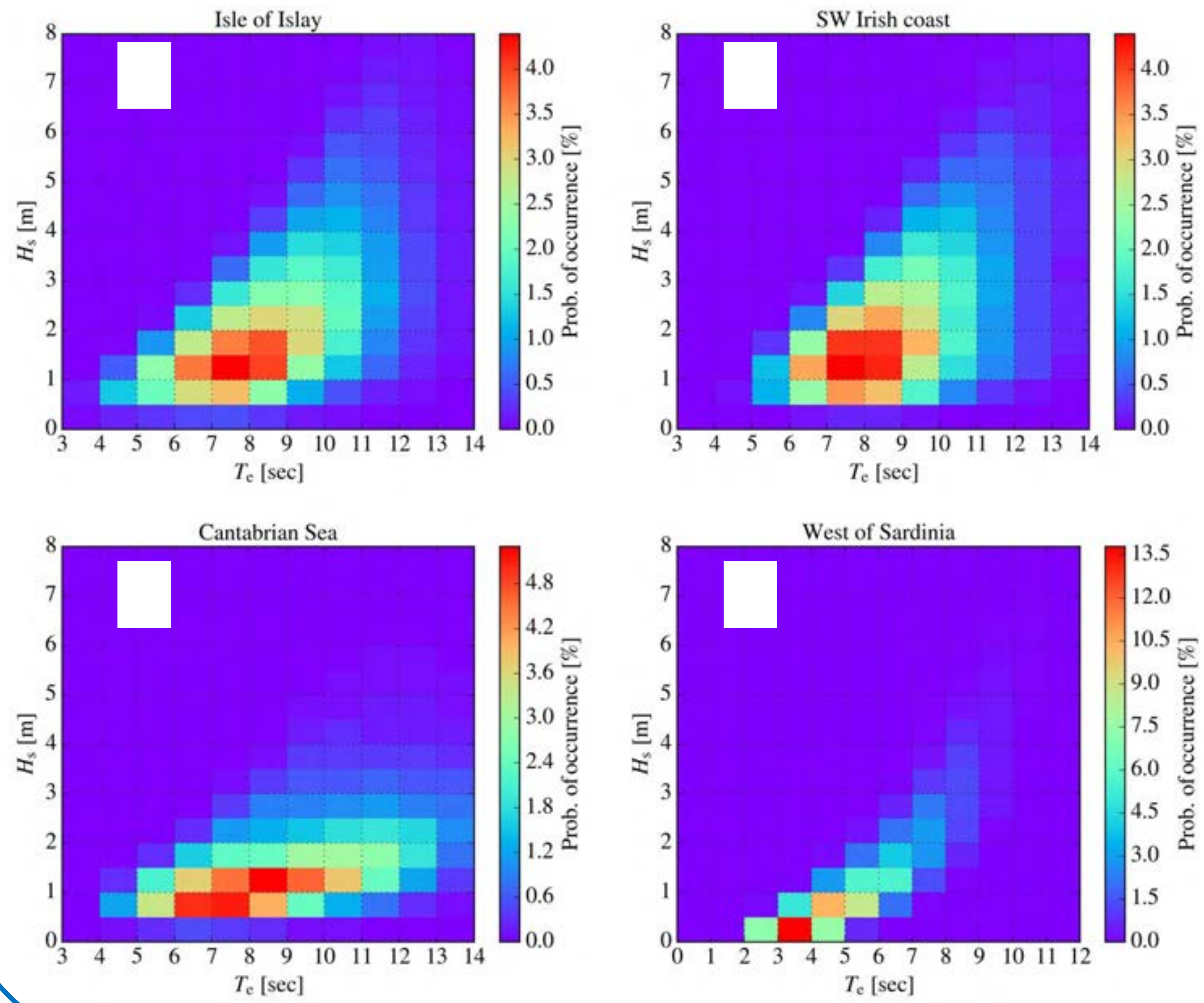

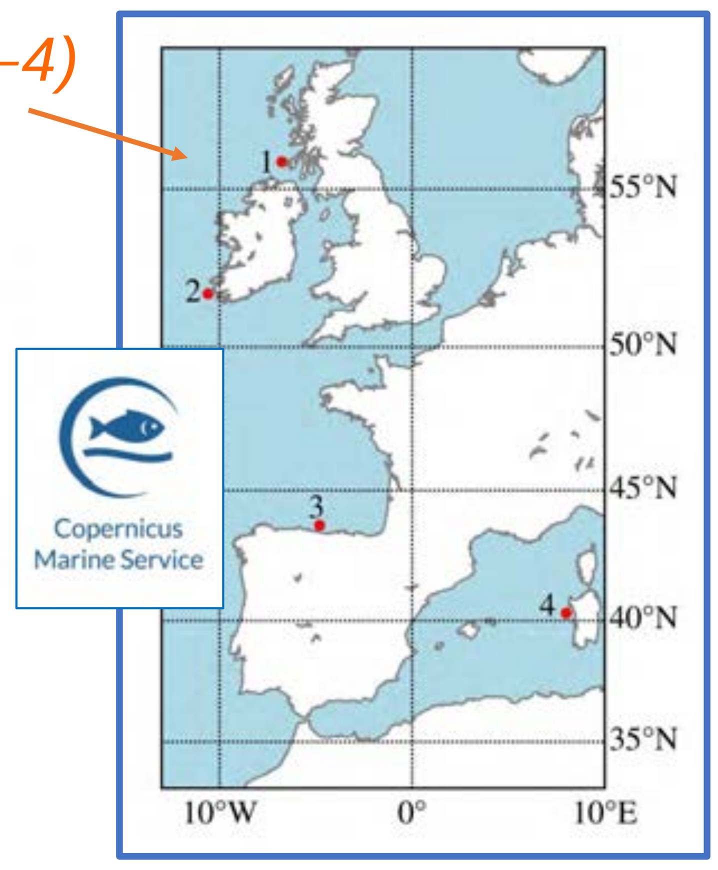

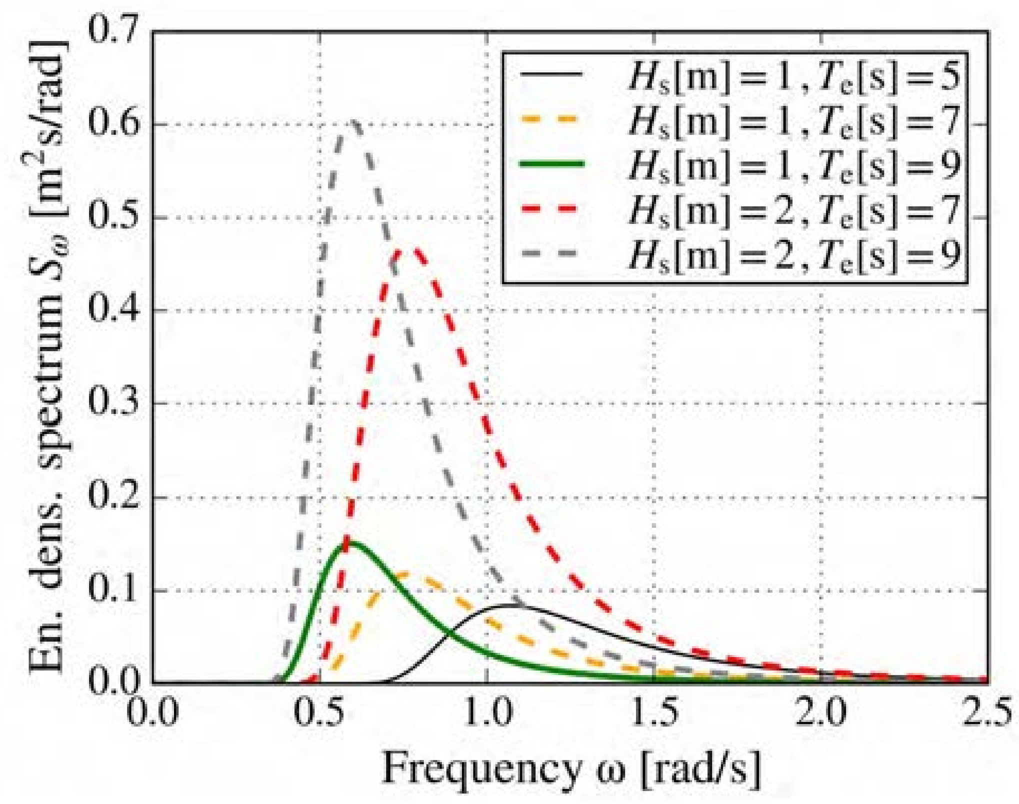

Hydrodynamic analysis was conducted using both frequency-domain and stochastic approaches. A semi-empirical Bretschneider wave spectrum was modelled to represent realistic sea states (wave data were retrieved from the Copernicus Marine Service). Key parameters included significant wave height and energy period. Response Amplitude Operators (RAOs) and standard deviations were computed using panel methods (WAMIT) and statistical estimations to assess TALOS motion.

Results and discussion

Stochastic model results: Standard deviation of motion response per location

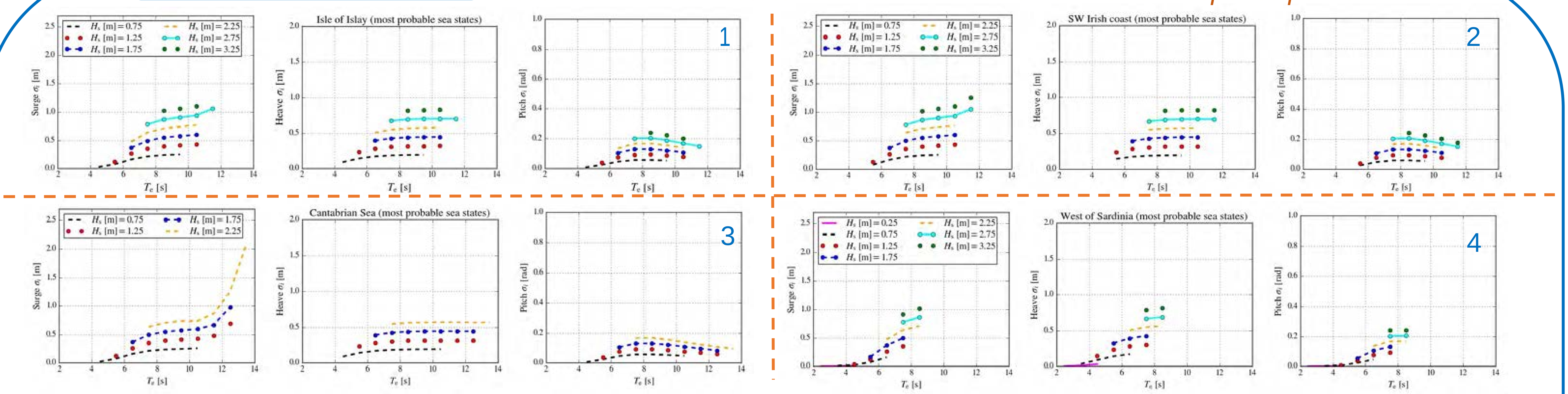

Size optimisation

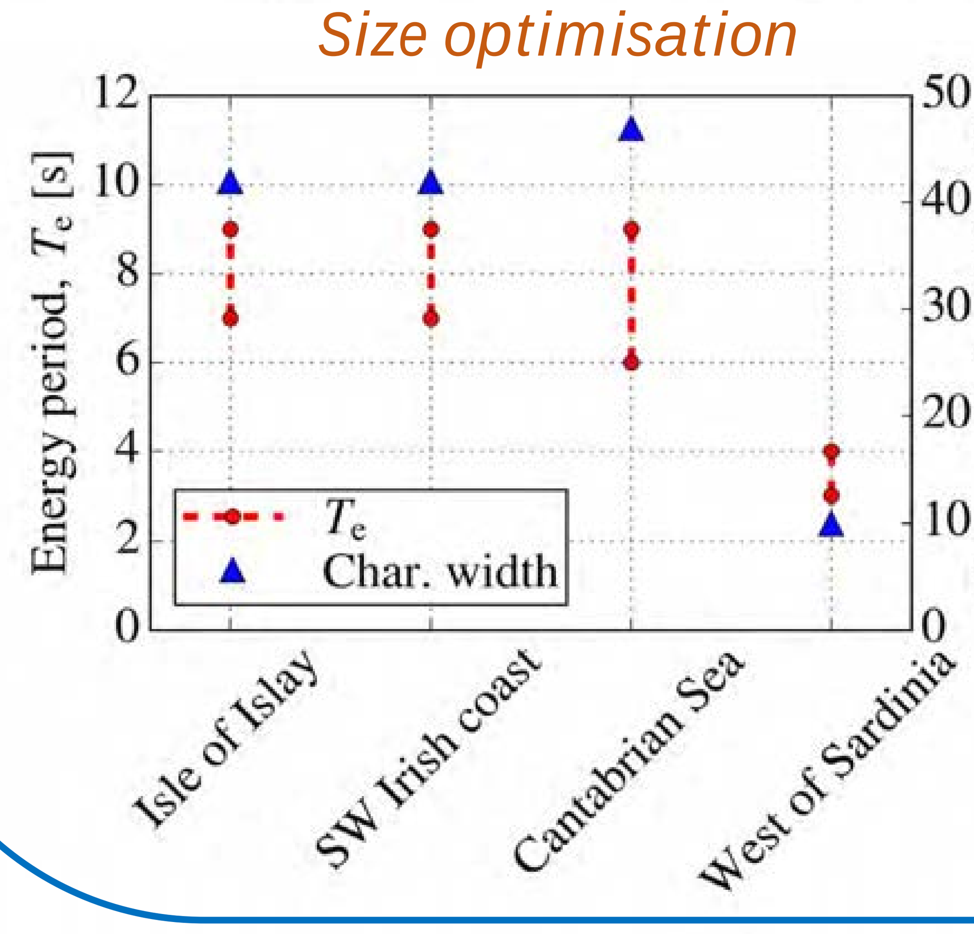

By analysing the most probable sea states from wave reanalysis data, we determined ideal adjustments to TALOS's width for resonance-based tuning using the Froude scaling law.
These recommendations aim to align the device's heave resonance with the most common incoming wave periods at each location

Scan to learn more about the TALOS WEC Project Lancaster University

Access to wave climate Copernicus Marine Service data

Original paper:
Oikonomou, C. L. G., Sheng, W., Korres, G., & Aggidis, G. (2023). *Operating of TALOS wave energy converter in different wave climates.* Paper presented at the ISOPE International Ocean and Polar Engineering Conference. (Paper No. ISOPE-I-23-094)

Assessing Operational Profiles for Offshore Renewable Energy: A Data-Driven Approach for Hydrogen Production Feasibility

University of Strathclyde Glasgow

Claudio A. Rodríguez, Maurizio Collu, Feargal Brennan

Department of Naval Architecture, Ocean & Marine Engineering

Background

Ref: Buchan Offshore Wind @ LinkedIn.com

Decentralised Floating Wind-H_2 System

- 15-MW IEA RWT
- Integrated H_2 facilities
- ERA5 hindcast metocean data (2002 – 2021)
- AEKs typical operational requirements: rated capacity at 80% of rated WT power, minimum load of 20% rated capacity.

Wind Energy Resource

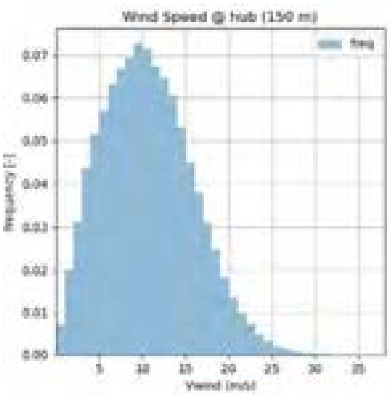

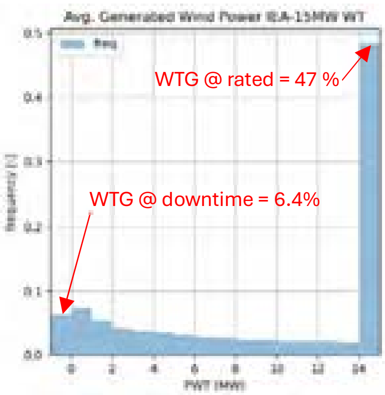

15-MW WTG capacity factor = 64.5%

Operational Profile of H_2 facility

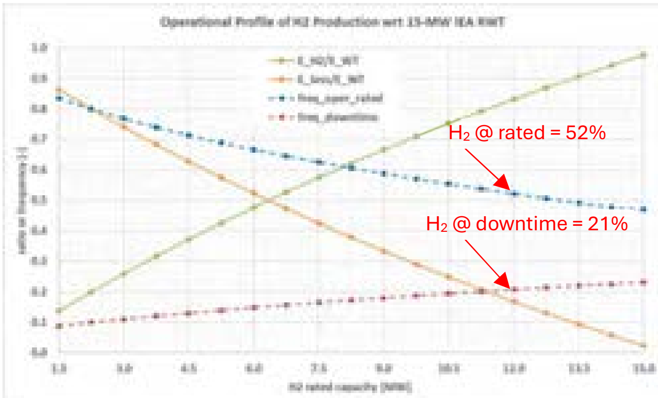

12-MW AEK oper. factor = 83.1% (wrt WT gen. power)

Persistence downtime: AEK & Hs

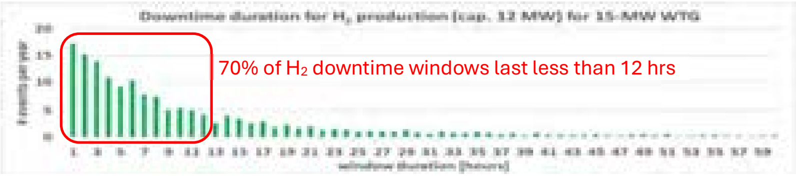

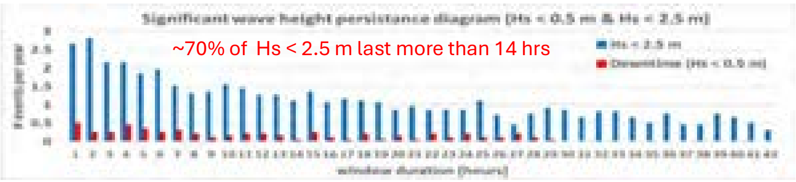

Complementary ORE potential

- Required complementary power (15-MW WTG & 12-MW AEK):

  0.20 * 12.0 = 2.4 MW

Thus:

- 10 WECs (~250 kW), or
- 02 tidal devices (~1.2 MW)
- Fuel cells?

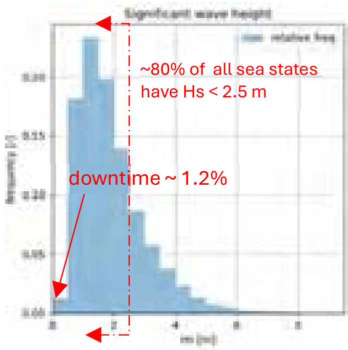

Conclusions & Future work

- ✓ Number of shutdown/start-up events are critical for H_2 production feasibility assessment;
- ✓ Downtime wind energy persistence diagrams evidence the need to complementary energy resources;
- ✓ Wave energy seems to be a promising complementary resource: power and persistence;
- ○ Investigate wind–wave joint occurrences and correlation;
- ○ Investigate WECs and other ORE devices suitable for WTG & AEK downtime windows.

Ocean REFuel

Supergen ORE Hub Early Career Researcher Forum

Explore the latest research and innovation in offshore wind, wave and tidal energy

Supergen Offshore Renewable Energy

Numerical Simulation of Laterally Loaded Monopiles for Offshore Wind Turbines using an Advanced Hyperplasticity Model

UNIVERSITY OF OXFORD

Introduction & Problem Statement

Monopiles

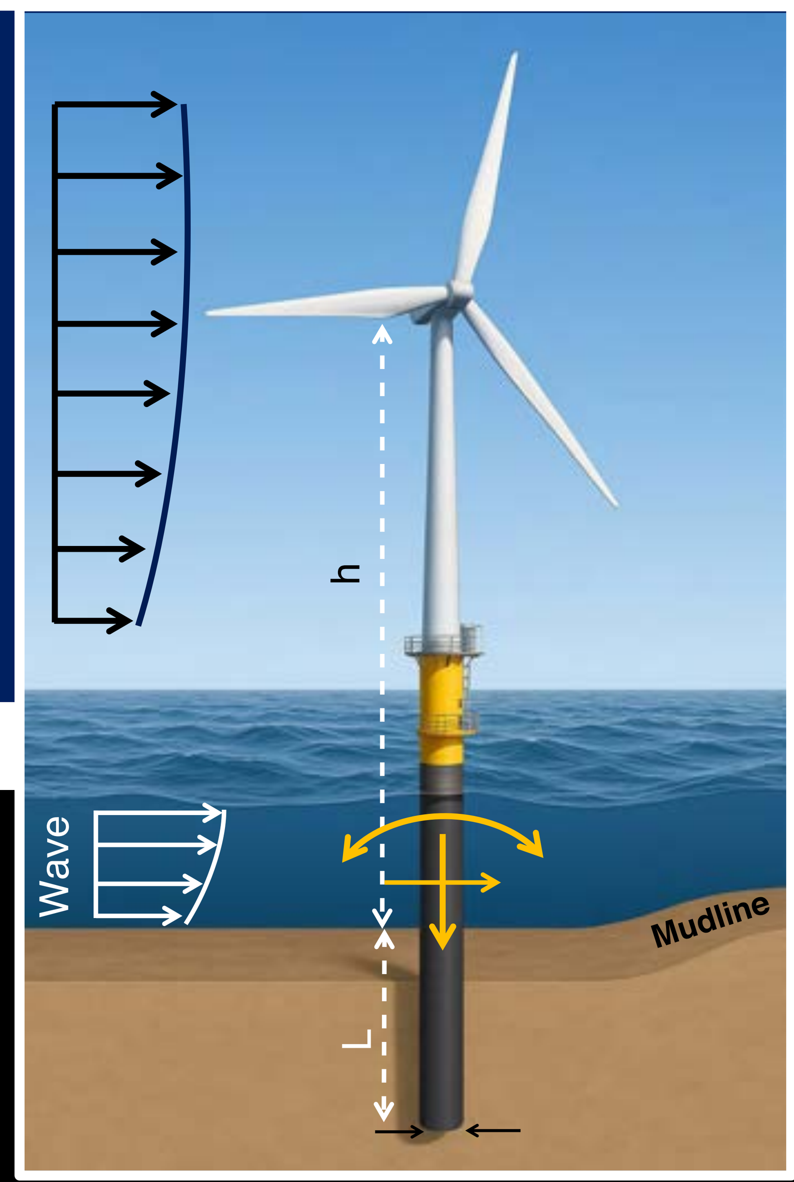

Objective

1 HySand Model Development

HySand

Gibbs energy function (g):

Yield functions (y):

Model parameters:

2 Model Calibration

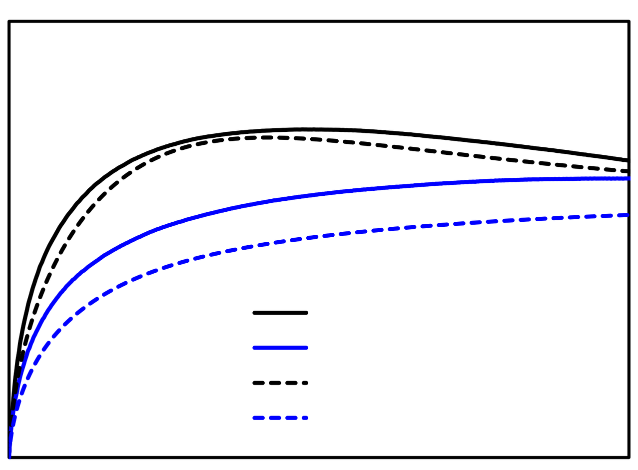

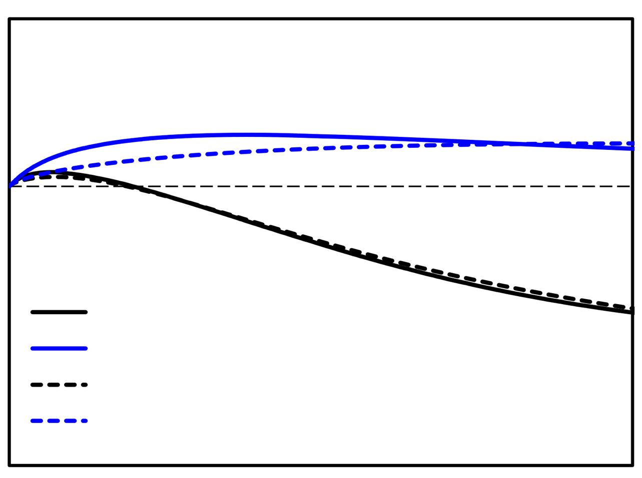

3 Implementation & Application

3D FE Model:

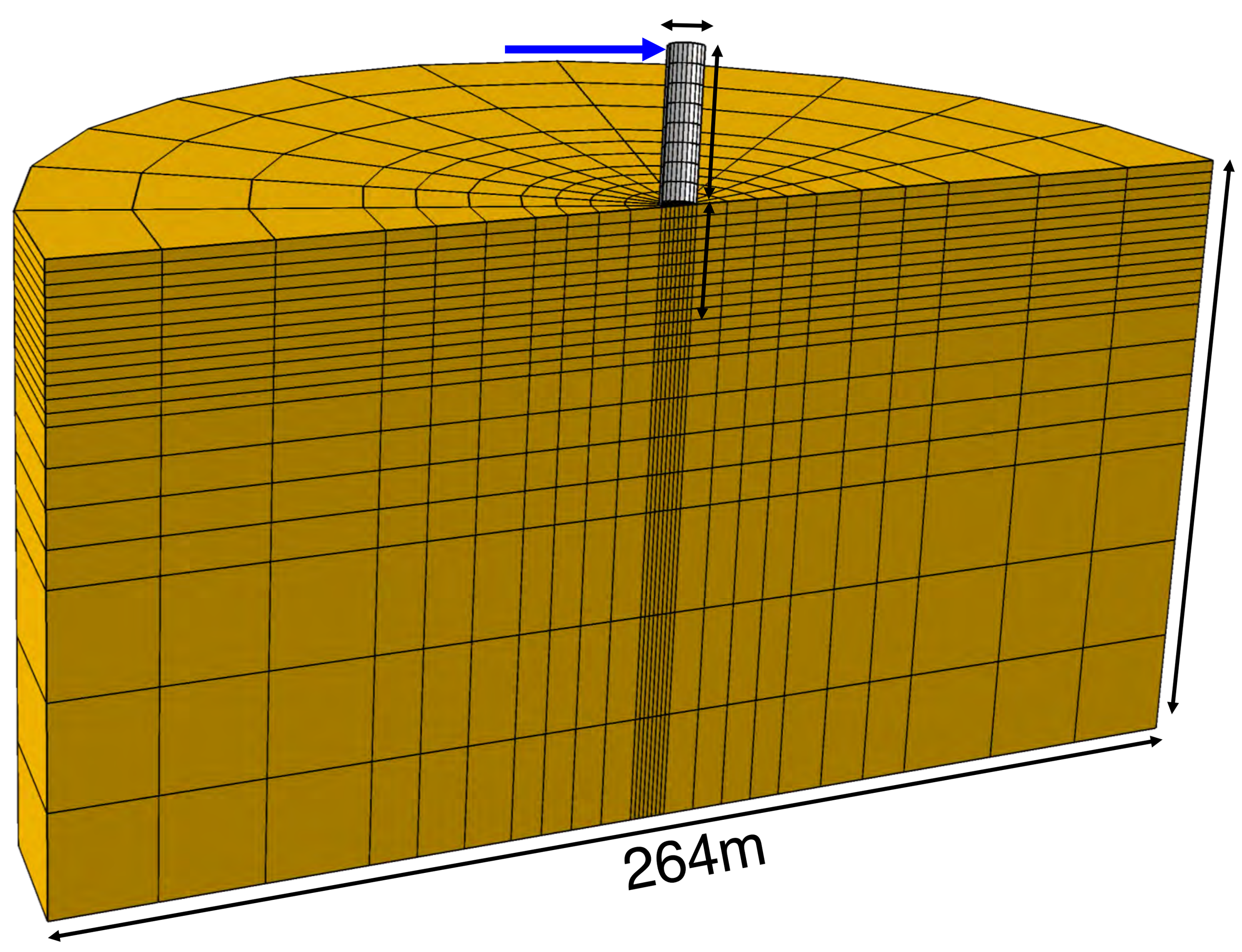

Numerical results:

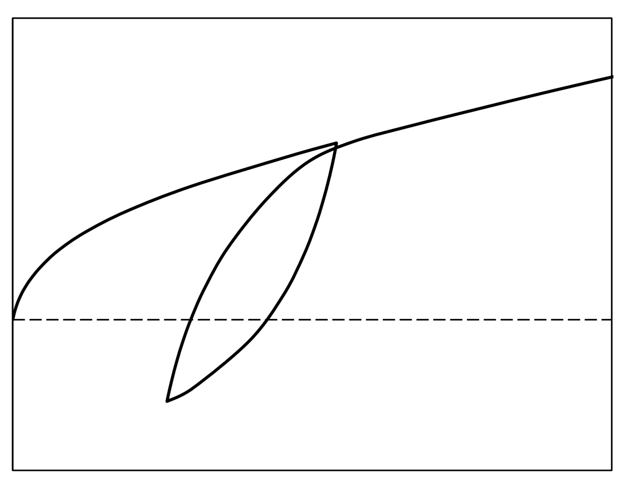

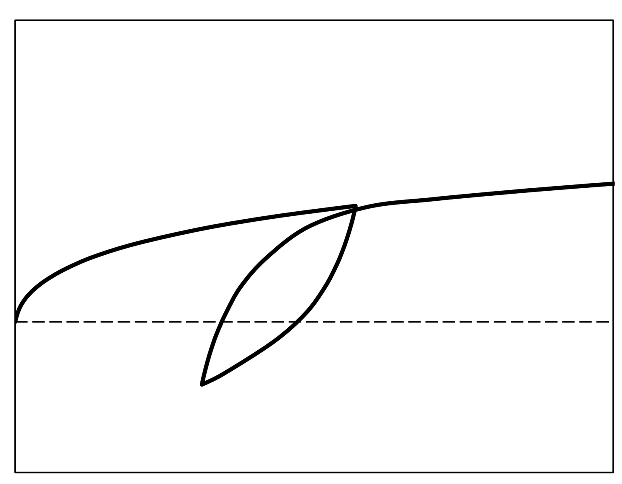

References:

-
-
-

Ørsted

Supergen Offshore Renewable Energy

REDUCING UNCERTAINTY FOR BAYESIAN ANALYSIS IN WIND ENERGY SYSTEMS

Isha Saxena, University of Durham, isha.saxena@durham.ac.uk

Supervised by:

Dr. Behzad Kazemtabrizi, Prof. Matthias Troffaes, Prof. Christopher J Crabtree

MOTIVATION 1

About 25-35% of the Levelised Cost of Electricity(LCOE) of modern wind farms is incurred in the operation and maintenance (OPEX) of the wind farms. A more data-driven approach can be useful in more precise costs estimation and decreasing LCOE.

Lack of data for wind turbine failures and repairs gives rise to uncertainty in case of wind turbines makes it harder to calculate the hyperparameters for the prior.

Bayesian parameter estimation, utilizing prior knowledge and observed data, provides a robust framework for modelling the failure rates of wind turbines, essential for optimizing performance and reducing costs.

QUESTION 2

How can sensory data be used to optimise installation and operation and maintenance procedures of a wind farm using statistical analysis?

How can uncertainties be addressed in case of a Bayesian estimation utilisation?

METHODOLOGY 3

Sensory Data → Processed Data →

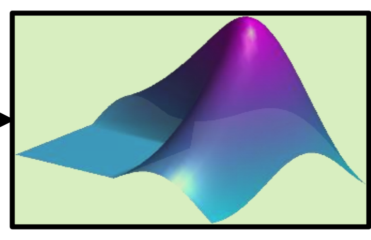

→ **Output**

Statistical Model

SCADA data, and turbine logs are used for this project. The SCADA data consists of the SCADA signals like generator RPM, total active power, etc. This data needs to be converted into times to failure and times to repair for modelling.

The power production from real time SCADA Data and wind turbine's wind vs power curve are used to determine times to failure and repair of the wind turbines at this stage.

A new statistical model characterising the times to failure or number of failures per year for each turbine is prepared to understand the impact of the environment on the wind turbines' failures. The parameter estimation for the model is carried out by using Bayesian inference and the results are compared with maximum likelihood estimation.

PRIOR ELICITATION 4

{Using Historical data} For a homogeneous process, let N(t) ~ Po(tλ) be the number of wind turbine failures in the time t, with failure rate λ ~ *Gamma*( ). The prior predictive distribution is:

$$N(t) \mid \quad \sim NB\left(\quad \frac{}{t+}\right)$$

The expectation and variance of N(t) given are:

$$E(N(t)) = \frac{}{} \text{ and } Var(N(t)) = \frac{t+}{} E(N(t)).$$

Prior elicitation can be done if the expectation and variance are known. The data below is obtained from [2].

Years t	Number Failures per turbine	Number of failures (N(t))
1	10.75	2375.75
2	10.18	2249.78
3	11.01	2433.21
4	9.41	2079.61
5	7.44	1644.24
6	13.32	2943.72
7	9.91	2190.11
8	7.94	1754.74

Based on the failure data for offshore wind turbines over 8 years for 1,768 turbine hours, as shown in Table 1, the hyperparameters and of the prior Gamma distribution were estimated for the failure rate (λ). Using the sample variance of 165,993.8 and the total number of failures 17,671.16 for N(t = 1768 turbine years) and the values for N(t =221), we obtain = 29.8 and = 2.98. The value of variance can also be inflated if the sample variance does not fully represent the uncertainty of the data. These values are used to visualize the prior predictive distribution (Negative Binomial) and the Gamma prior distribution. This analysis applies only to wind farms in similar situations as the data.

POSTERIOR INFERENCE 5

{Using Current Data} Let $T_1,\ldots,T_n$ be i.i.d. random variables representing wind turbine failure times, with density P(t_i |θ). Here, model 1 assumes a Weibull distribution:

$$T_i \mid \lambda, k \sim Weibull(\lambda, k)$$

Model 2 assumes an exponential distribution (Weibull with *k*=1):

$$T_i \mid \lambda \sim Weibull(\lambda, 1)$$

Where, *λ ~ InverseGamma*( ), and for *k ~ Uniform(,)*.

Hyperparameter Selection: We assume that k and λ are a priori independent. Once initial hyperparameters are chosen according to the values obtained from Ref [2], they are iteratively adjusted until a reasonable prior predictive distribution is achieved.

Dataset for analysis for this section is sourced from EDP Renewables [3], encompassing SCADA and log data from a wind farm of 16 turbines, each rated at 2MW, with a focus on a subset of 5 turbines. Here, within Bayesian framework, Markov Chain Monte Carlo algorithms are used for sampling data from posterior distribution effectively.

	k (Expo)	λ (Expo)	k (Weibull)	λ (Weibull)
MLE	1	21.03	0.87	19.71
Bayesian Estimation	1	21.7	0.84	20.31

Model Validation: The data can be divided into two parts: test data and training data. The training data is used to train the statistical model and to obtain parameters for the curve. The test data, which represents around 20% of the total dataset, is used to test the performance of the model based on parameters obtained from the training dataset.

TAKE AWAYS

This research focuses on determining a more generalised statistical model pertaining to times to failure (and repair) in offshore wind turbines, leading to better estimations of impacts of failure/repairs on key performance indicators.

REFERENCES

[1] R. Billinton and R N Allan. Reliability evaluation of engineering systems: concepts and techniques. 2nd ed. New York: Plenum Press, 1992. 453 pp. ISBN:978030644063

[2] Carroll, J., McDonald, A., and McMillan, D. (2016) Failure rate, repair time and unscheduled O&M cost analysis of offshore wind turbines. Wind Energ., 19: 1107–1119. doi: 10.1002/we.1887

[3] Data. en. https : / / opendata . edp . com / open - data / en / data . html. Accessed: 2023-6-2

Durham University

aura

Enhancing Marine Concrete Performance: Fatigue Mechanics of Polymer-Modified Concrete

Concrete challenges in the marine environment

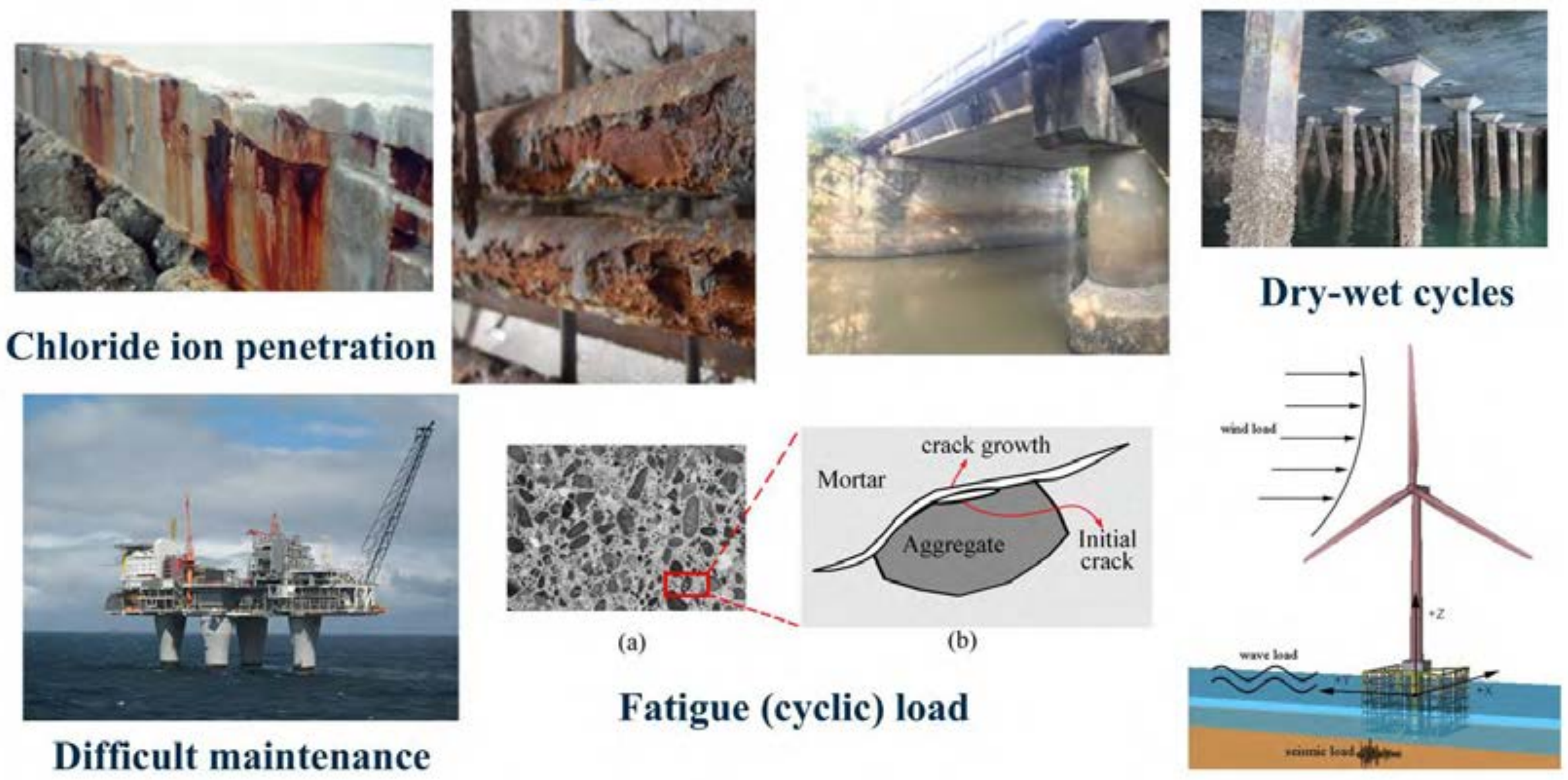

What is polymer modified concrete (PMC)

PMC is a cement-based composite where polymers (e.g., latex, epoxy) are added to improve mechanical properties, durability, or workability compared to conventional concrete.

Polymers added to the concrete

Enhancement of PMC in current state of research

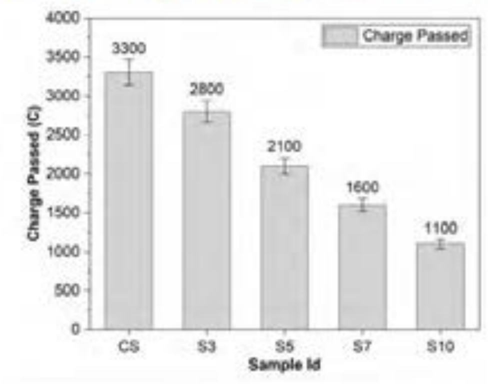

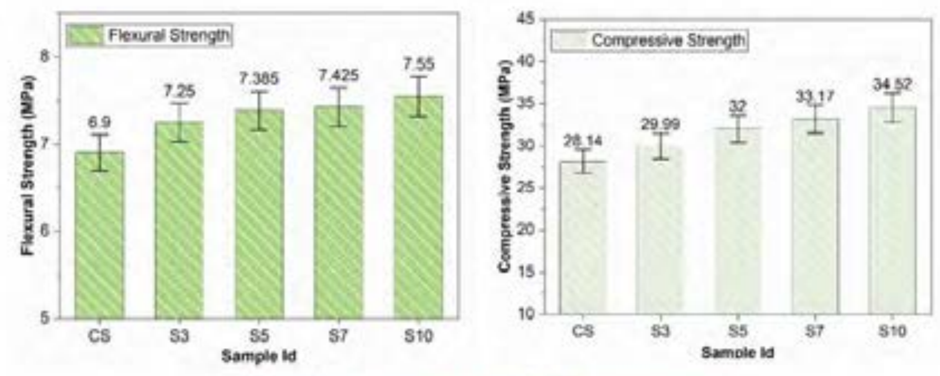

0%, 3%, 5%, 7%, and 10% SBR modification

Aims and objectives

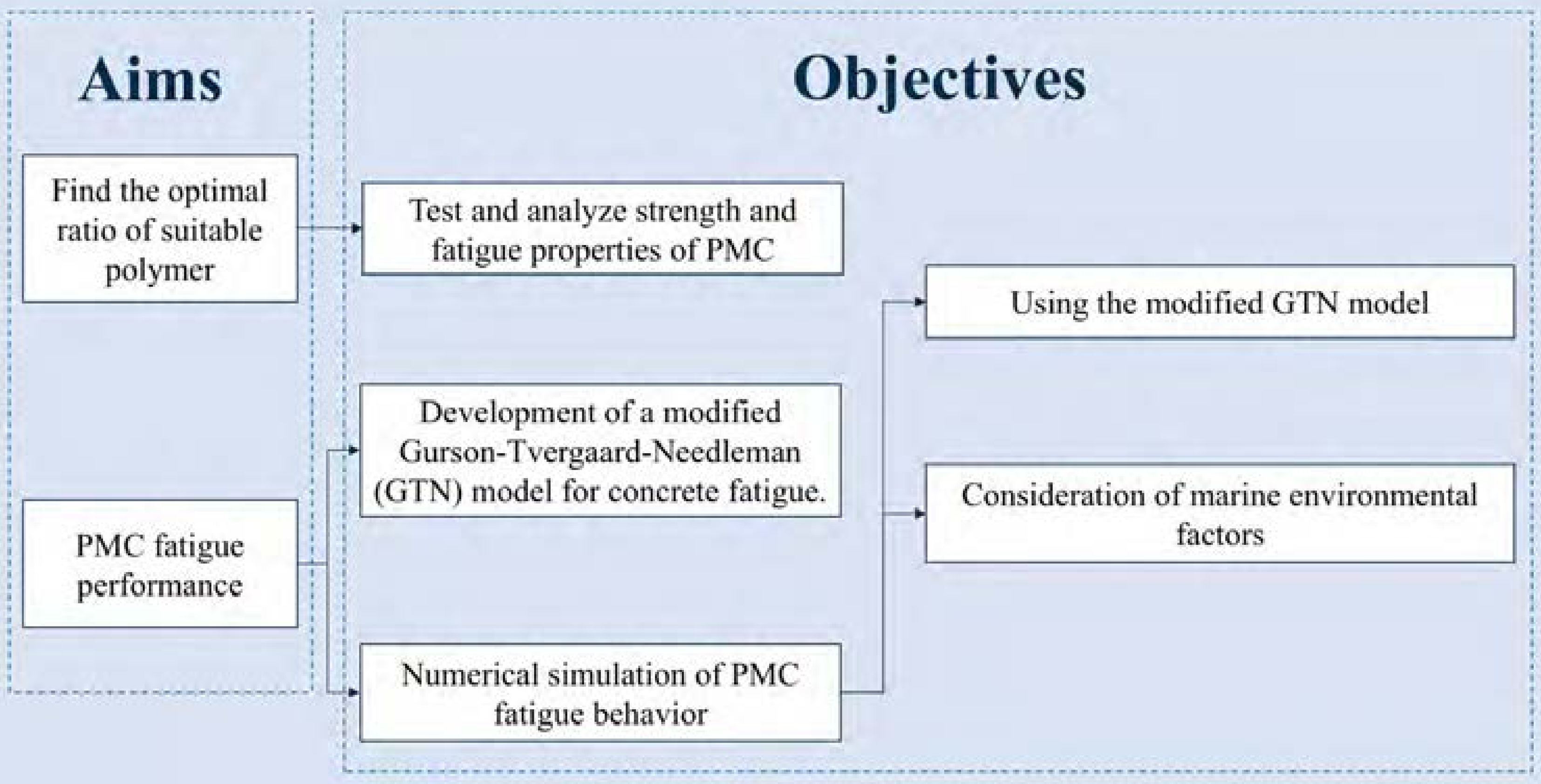

Current test result (7 days)

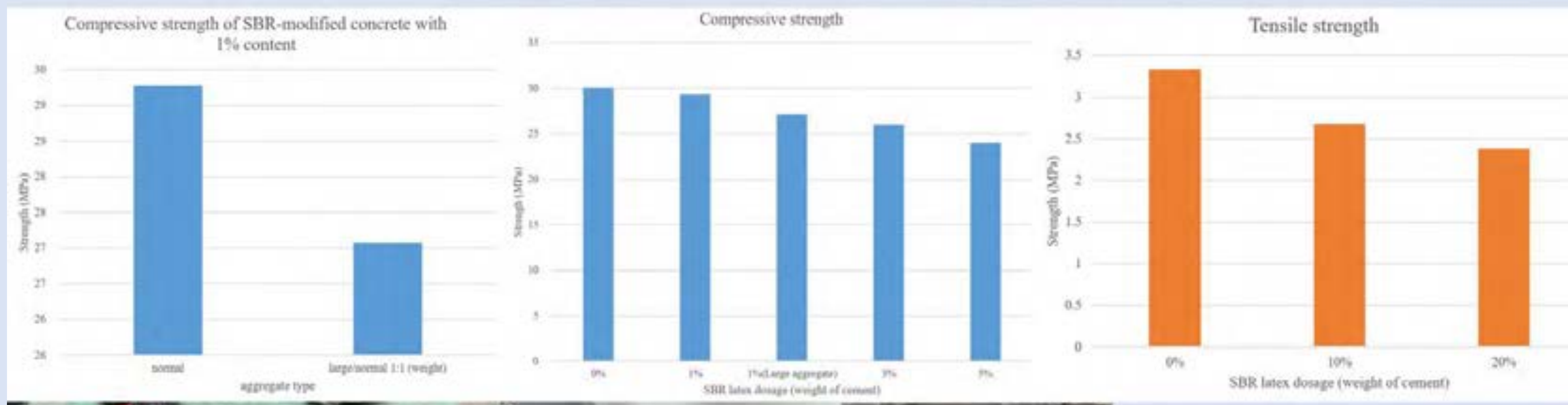

The results do not match some of the literature and more experiments are needed

Future fatigue test with wet/dry circle

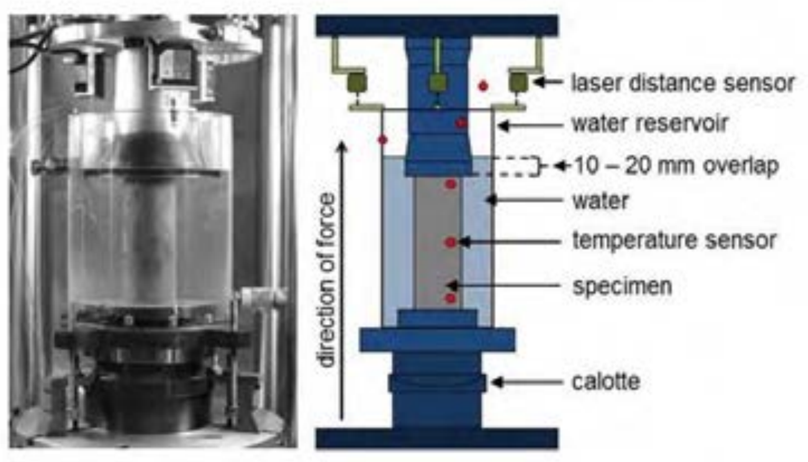

	Wetting	Drying
Time	8 hours	4 hours
Equipment	Water tank	Fan (AD) (8.5knots)

Numerical simulations on meso-structure of PMC under fatigue

Random Aggregate Modeling based on Monte Carlo method

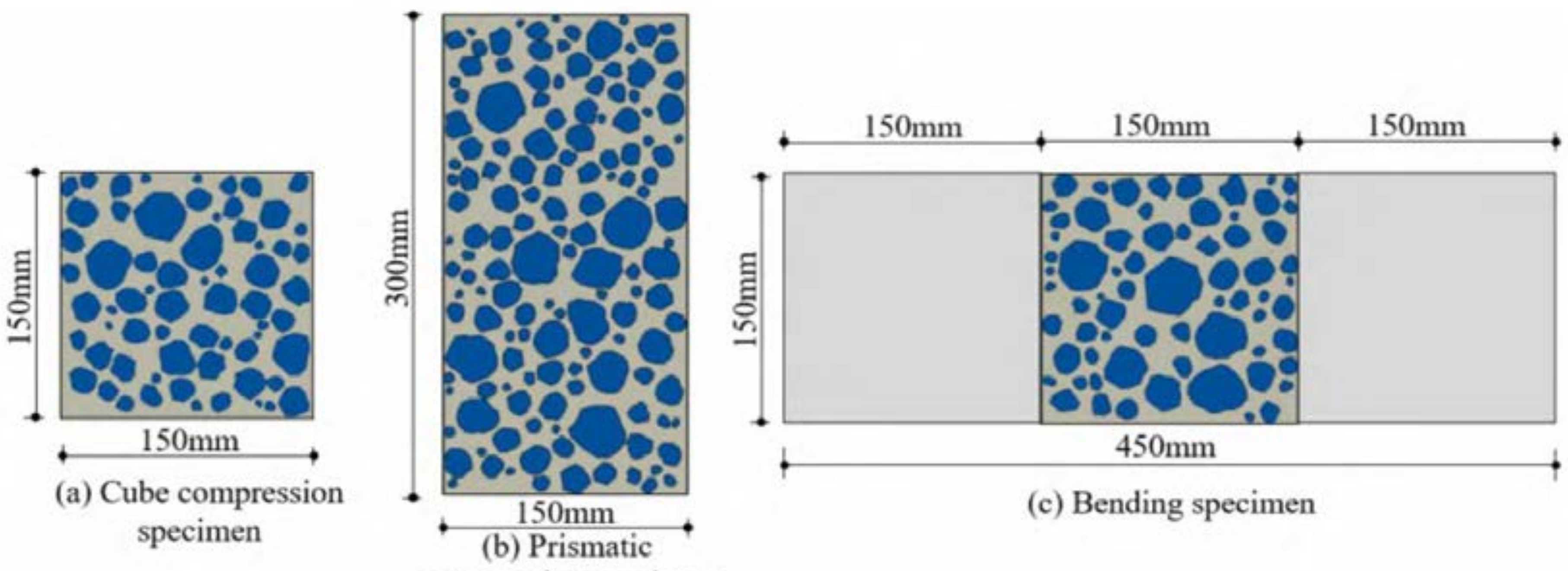

(a) Cube compression specimen

(b) Prismatic compression specimen

(c) Bending specimen

Numerical simulations on meso-structure of PMC

Gurson-Tvergaard-Needleman (GTN) model

Yield function of the GTN model

- $\Phi = \frac{q^2}{\sigma_m^2} + 2q_1 f^* \cosh\left(\frac{-3q_2\sigma_h}{2\sigma_m}\right) - (1 + q_3 f^{*2}) = 0$
- q – Macroscopic von Mises equivalent stresses
- σ_m – Equivalent stress
- q_1, q_2, q_3 – Calibration coefficients, usually q_1=1.5, $q_2 = 1.0$, $q_3 = q_1^2$
- f^* – Equivalent pore porosity
- σ_h – Macroscopic hydrostatic stress

Equivalent pore porosity

$$f^* = \begin{cases} f, & f \le f_c \\ f_c + \frac{f_u^* - f_c}{f_F - f_c}(f - f_c), & f_c < f < f_F \\ f_u^*, & f \ge f_F \end{cases}$$

f – The porosity obtained from the pore evolution model

f_c – The porosity of the material at the time of the start of pore aggregation

f_u^* – Equivalent porosity at the time of occurrence of fracture

f_F – The porosity of the material at the time of occurrence of fracture

Pore nucleation and pore growth

$$\dot{f} = \dot{f}_{growth} + \dot{f}_{nucleation}$$

$$\dot{f}_{growth} = (1 - f)\dot{\varepsilon}_m^p$$

$$\dot{f}_{nucleation} = A\dot{\varepsilon}_m^p$$

$$A = \frac{f_N}{s_N\sqrt{2\pi}} exp\left[-\frac{1}{2}\left(\frac{\varepsilon_m^p - \varepsilon_N}{s_N}\right)^2\right]$$

f_{growth} – The porosity increment due to pore growth

$f_{nucleaton}$ – The porosity increment due to pore nucleation

$\dot{\varepsilon}_m^p = (\dot{\varepsilon}_{11}^p + \dot{\varepsilon}_{22}^p + \dot{\varepsilon}_{33}^p)/3$ The mean plastic strain increment of the material

A – The rate of pore nucleation

f_N – The volume fraction of the nucleated particle

s_N – Nucleation strain standard deviation

ε_N – The average strain of the pore nucleation

Damage factor calculation with asymptotic homogenization method

Lemaitre model

$$\tilde{\sigma} = \frac{\sigma}{1-D}$$

$\tilde{\sigma}$ – The effective stress tensor

σ – The non-destructive stress tensor

D – The damage factor

$$\varepsilon = \frac{\sigma}{\tilde{E}} = \frac{\tilde{\sigma}}{E} = \frac{\sigma}{(1-D)E}$$

$$D = 1 - \frac{\tilde{E}}{E}$$

$$\tilde{E} = (1 - D)E$$

E – The damage-free elastic modulus

$\tilde{E}$ – The effective elastic modulus

(1) Idrees, M., Akbar, A., Saeed, F., Saleem, H., Hussian, T., & Vatin, N. I. (2022). Improvement in durability and mechanical performance of concrete exposed to aggressive environments by using polymer. Materials, 15(11), 3751

(2) Aggarwal, L. K., Thapliyal, P. C., & Karade, S. R. (2007). Properties of polymer-modified mortars using epoxy and acrylic emulsions. Construction and Building Materials, 21(2), 379-383.

(3) Oneschkow, N., Huemme, J., & Lohaus, L. (2020). Compressive fatigue behaviour of high-strength concrete in a dry and wet environment. Construction and Building Materials, 262, 119700.

(4) A.Demayo. (1985).Elements in sea water. CRC handbook of chemistry and physics.

(5) Numerical analysis of mesoscale fatigue cracking behavior in concrete based on cohesive zone model

Email: zhenyi.yan@plymouth.ac.uk

LinkedIn: Zhenyi Yan

Impact of support structure modelling methods in actuator line method large eddy simulations of wind turbine wakes

Markella Zormpa, Christopher R. Vogel, Richard H.J. Willden
Department of Engineering Science, University of Oxford
markella.zormpa@eng.ox.ac.uk

Influence of nacelle and tower on wind energy aerodynamics

Rotor Loads

Tower shadow;
Instantaneous decrease in aerofoil performance.

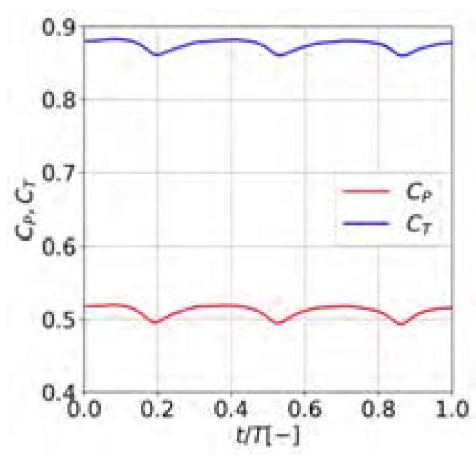

Near wake

Coherent structures;
Breakdown of tip vortices;
Hub vortex [2].

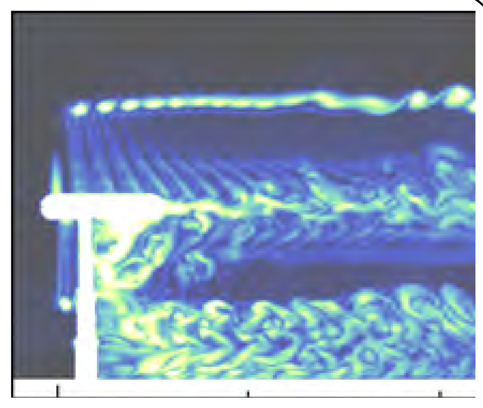

Far wake

Far wake asymmetry [1];
Increased turbulence.

Farm Scale

Wake meandering [2];
Influence on the farm resistance [3].

? *How should we numerically model the support structure in actuator line method large eddy simulations?*

Meshed representation

20<y+<300;
Analytical wall function

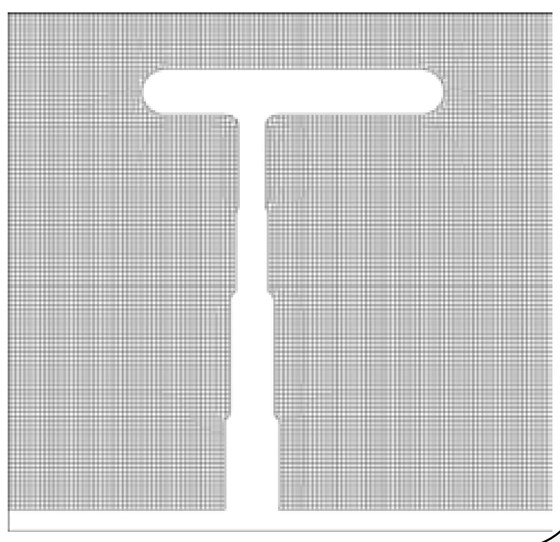

Cell blocking method

Momentum source;
No penetration condition;
Meshless method;
[4].

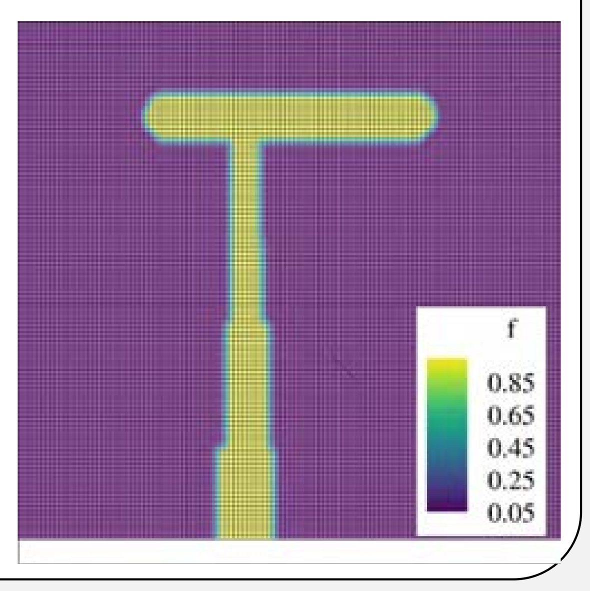

Actuator Line/Disc Method

Actuator disc nacelle, $Cd = 0.3$;

Actuator line tower, $Cd = 1.2$; $St = 0.2$. [5]

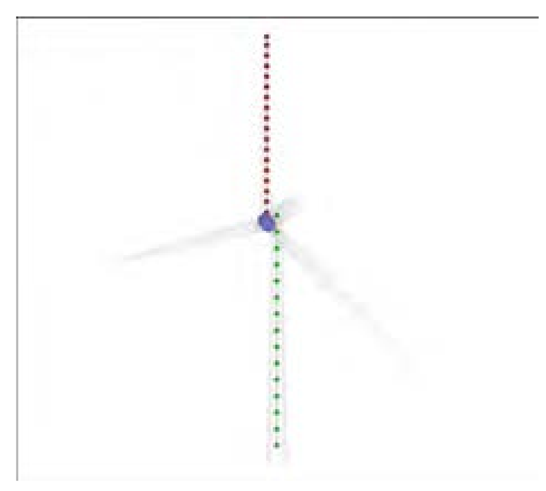

Mean flow, near wake, $x/D = 1$

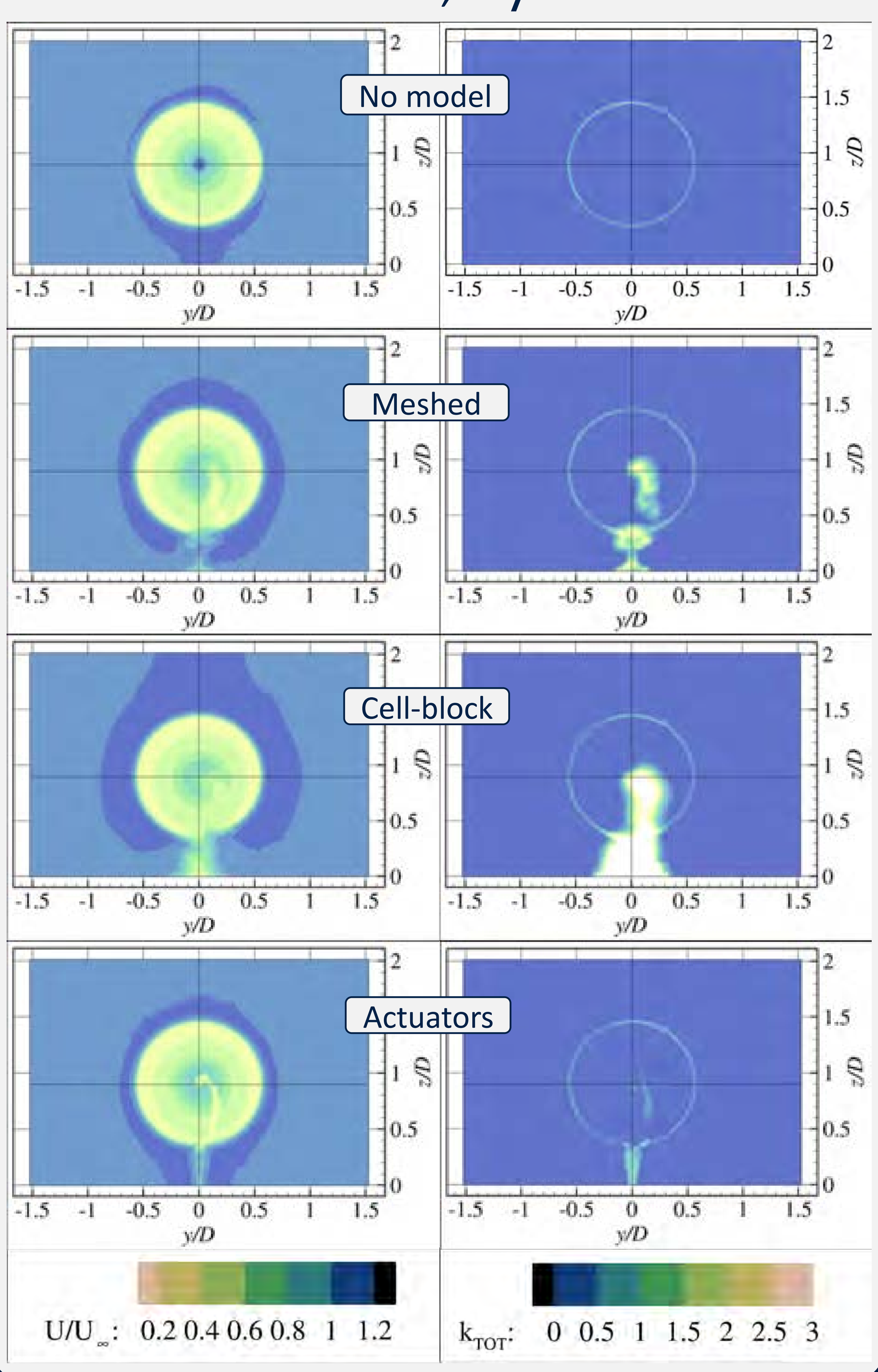

Instantaneous Flow

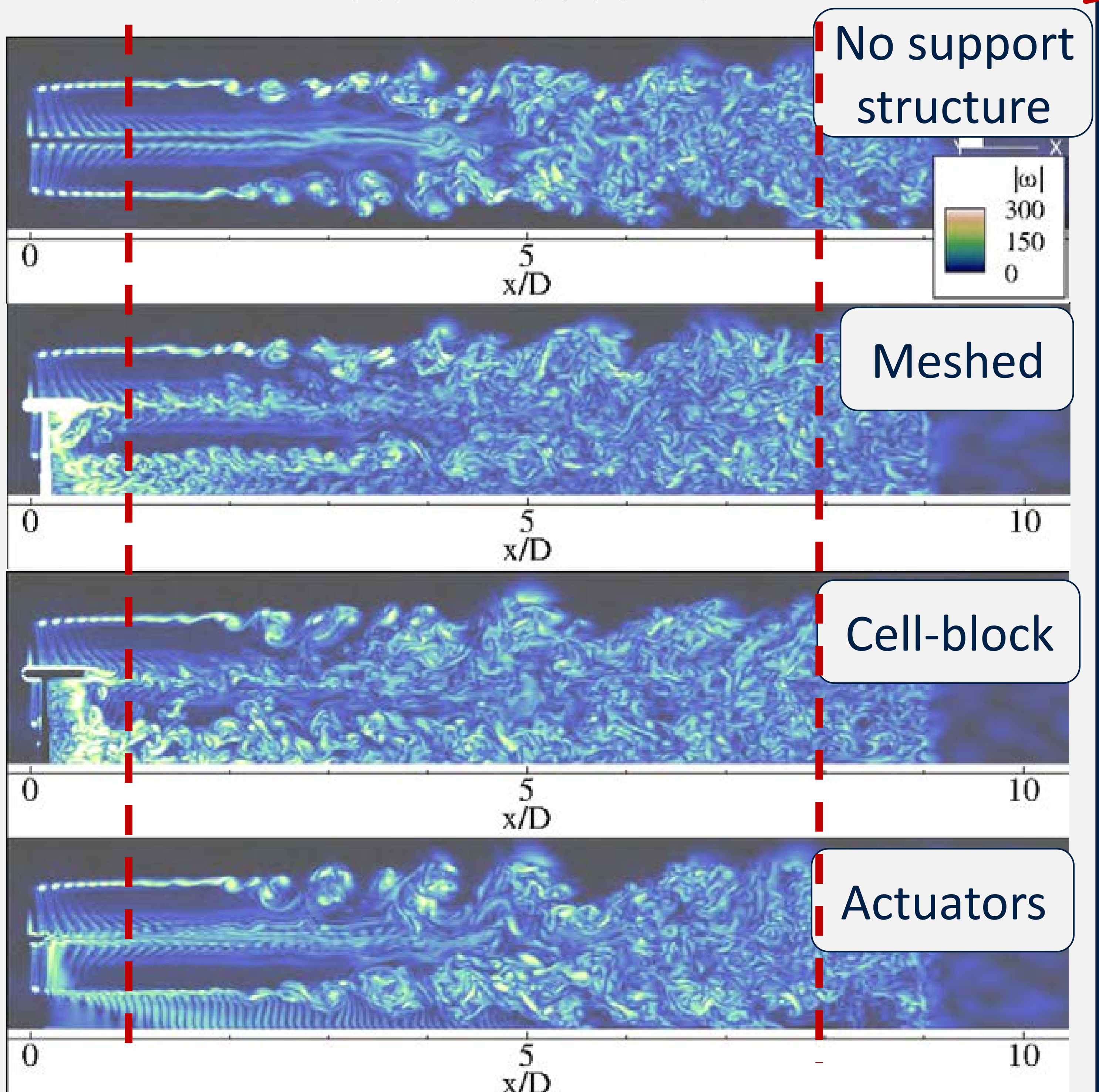

Method	Rotor Thrust [N]	Support Structure Drag [N]
No support structure	33.59	0
Mesh	33.59	1.59
Cell-block	33.43	3.45
Actuators	33.55	1.19

Mean flow, far wake, $x/D = 8$

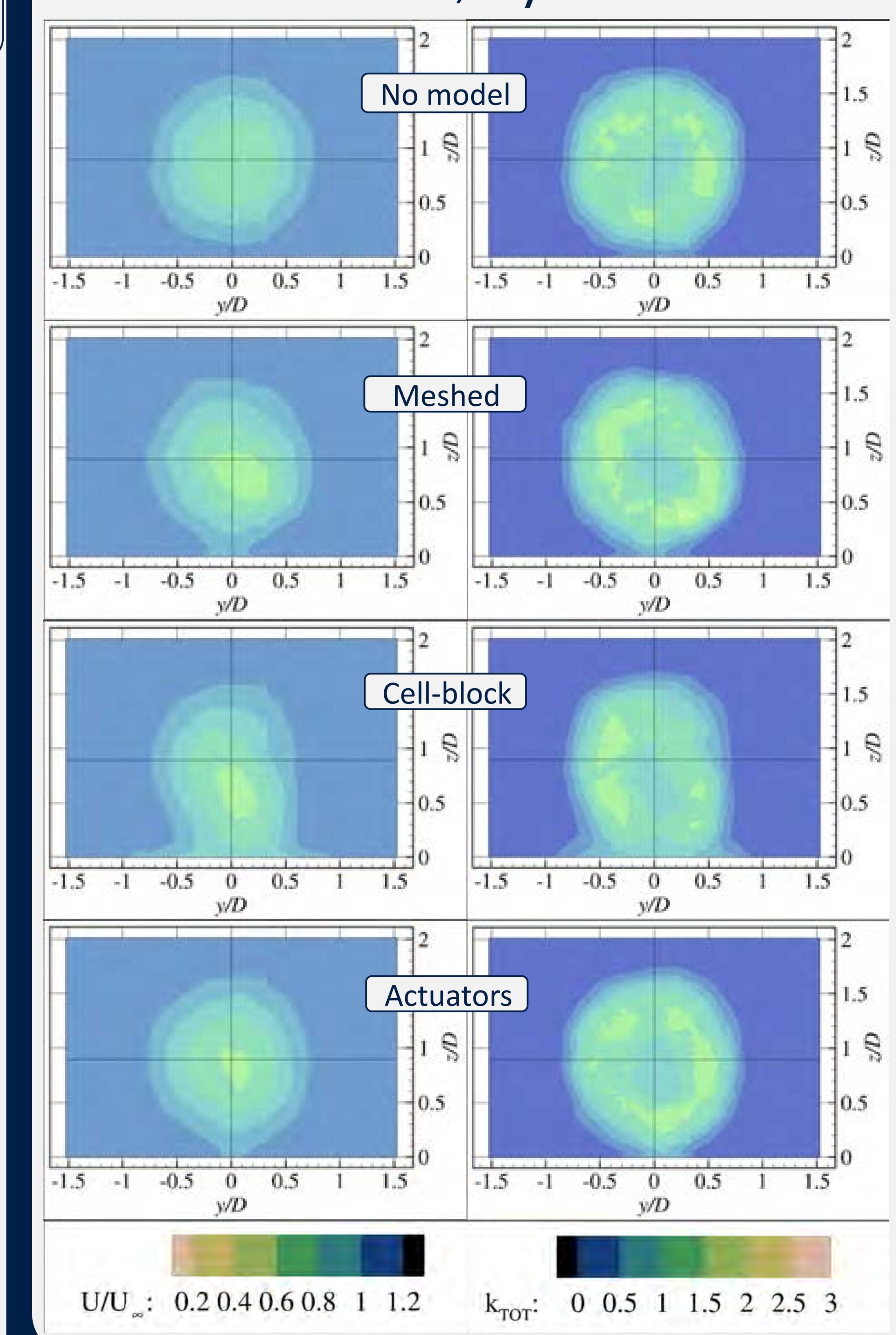

Comparison With Experiments

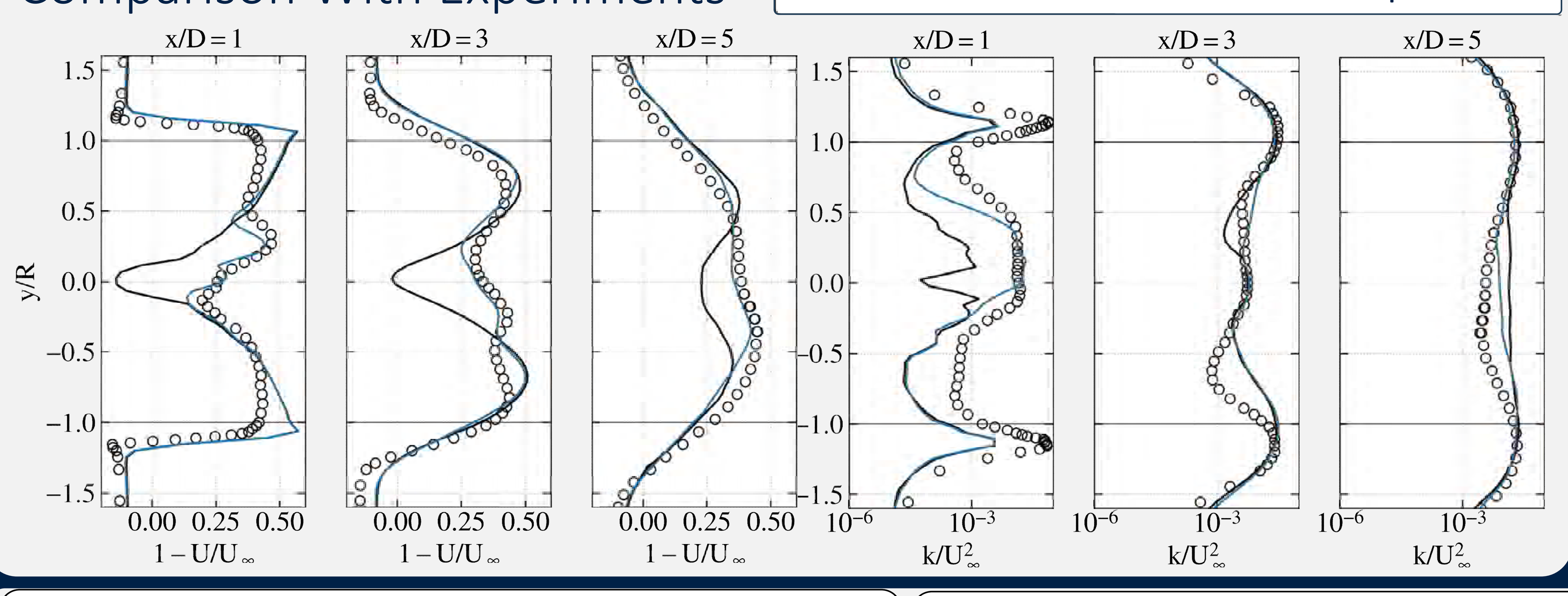

Conclusion

Three support structure modelling methods were tested for the NTNU lab-scale rotor [1] with diameter $D = 1\,m$ using actuator line method large eddy simulations.

The meshed representation provides the best agreement with experiments, capturing both flow behaviour and magnitude.

The cell-blocking method reproduces asymmetric behaviour but overstates TKE production at the near wake.

The actuator method understates the effect of the support structure and therefore does not induce far wake asymmetries.

Having tested the methods for a lab-scale rotor for which experimental data are available, future work will aim to assess the impact of the support structure in the utility scale.

References: [1] Pierella and Sætran 2017 Wind Energy 20,1753-1769.
[2] Yang and Sotiropoulos 2019 Energies 12(24), 4725.
[3] Ma et al. 2022 Wind 2, 51-67.
[4] Apsley et al. 2018 Journal of Ocean Engineering and Marine Energy 4, 259-271.
[5] Sarlak et al. 2015 Renewable Energy 77, 386-399.

Acknowledgements: The authors would like to acknowledge the use of the University of Oxford Advanced Research Computing (ARC) facility in carrying out this work http://dx.doi.org/10.5281/zenodo.22558. We also acknowledge Dr David D. Apsley for his discussions and insights into the cell-blocking method. MZ would like to acknowledge the support of RWE Renewables and the Department of Engineering Science of the University of Oxford. CRV acknowledges the support of the UKRI through his Future Leaders Fellowship MR/V02504X/1. RHJW would like to acknowledge EPSRC who support his fellowship through grant number EP/R007322/1.